DEVELOPMENT OF A CONCEPTUAL MODEL FOR ASH DUMP SYSTEM USING HYDRAULIC AND TRACER TEST TECHNIQUES

By

October Adolf Gerswin

A Thesis Submitted in fulfillment of the requirements for the degree of Master of Science

In the
Department of Earth Sciences
Faculty of Natural Sciences
University of the Western Cape

Supervisor Mr.: Jaco Nel
Co-supervisor Prof: Yongxin Xu

April 2011

DECLARATION

I declare that **DEVELOPMENT OF A CONCEPTUAL MODEL FOR ASH DUMP SYSTEMS USING HYDRAULIC AND TRACER TEST TECHNIQUES** is my own work, that it has not been submitted for any degree or examination in any other tertiary institution, and that all the sources I have used or quoted have been indicated and acknowledged by complete references.

NAME: Adolf Gerswin October

SIGNED: 

DATE: April 2011

Abstract

Development of a Conceptual Model for Ash Dump System using Hydraulic and Tracer Test Techniques

Key words: Ash dump system, conceptual model, hydraulic techniques, tracer techniques, hydraulic properties, transports properties,

Coal provides for 77% of South Africa's primary energy needs and is therefore a major resource that supports the socio-economic needs of South African citizens. Power stations are the major consumers of coal in South Africa and produces electricity from burned coal. The burning of coal produces a large volume of ash that is disposed in the form of ash dump systems.

The ash dump system is treated with high salinity process water from the power station for dust suppression. The process water contains salts due to evaporation processes from the recirculation of water in the cooling water system. Various studies to evaluate the sustainability of the ash dump system as a sustainable salt sink were therefore conducted. This study aimed to develop a conceptual model for the ash dump system by evaluating the movement of the process water trough the ash dump and the impacts it might have on the underlying weathered dolerite aquifer. This was achieved by evaluating the hydraulic and transport properties of the ash dump system. An initial site conceptual model was first established prior to the application of the hydraulic and transport methods. The initial conceptual model was based on the literature, previous reports and an initial site walk over.

Known and tested hydraulic and transport methods were applied on bo.th field and laboratory scale for the saturated part of the ash dump system. The laboratory experiments comprised of column and core experiments. These methods assisted in parameter estimation of hydraulic and transport properties and also assisted in the planning of the field experiments. The field experiments were conducted in the form of slug tests, tracer dilution and natural gradient divergent tracer test experiments. The combined laboratory and field experiments provided statistically significant values that were then used as inputs into the conceptual model. Field

experiments were also applied to a surrogate aquifer that represented the underlying shallow weathered dolerite aquifer of the ash dump system.

The components of the updated conceptual model identified and investigated include the physical environment, the calculated hydraulic and transport properties.

The ash dump can be conceptualized as a 20 to 30 meter high heap of consolidated clay size ash particles built on top of an underlying shallow weathered dolerite aquifer. The ash dup is directly connected to the underlying weathered dolerite aquifer. The saline water within the saturated zone has the ability to move through the ash dump system with hydraulic conductivities ranging between 10^{-1}-10^{-2} m/day, with flow velocities of 7-8m/day and effective porosities of 1%-2%. The hydraulic properties of the ash dump are, amongst others, controlled by the ash geology, contact time of the process water with the ash and show a significant reduction in hydraulic conductivity over time, before reaching a steady state. The transport properties are controlled by advection and spreading in available pathways. Results for the surrogate underlying fractured rock aquifer show flow velocities of 31m/day and an effective porosity of 1%.This suggests that the underlying weathered dolerite aquifer is vulnerable to process water contamination from the ash dump system.

The study illustrates the importance of a site conceptual model before the application of investigative methods. Hence having a site conceptual model provides an excellent platform for hydraulic and transport estimation. The development of a site conceptual model enhanced the understanding of flow and transport movement of the processed water trough the ash dump, it also assisted as a beneficial tool to enhance ash dump management.

Acknowledgements

- I give to God all the praise, the glory and adoration. I thank Him for giving me the precious gift of life and also blessing me with amazing people. These amazing people are:

- My supervisor, mentor, and friend Jaco Nel that really guided me in my scientific thinking ("jy dink nie reg nie, dink soos die water druppel") throughout this project. If it was not for his guidance and "braai" it would have been impossible to finish this thesis.

- My co-supervisor Prof Xu for his scientific guidance throughout the project

- ESKOM for funding this project and making it possible for me to study. A special word of thanks to Kelley Reynolds for her assistance and support throughout this project words can't express my gratitude. You are amazing.

- The Department of Earth Sciences for there contribution towards building my capacity as a student and making the necessary facilities and structures available that contributed towards finishing this project.

- Marlese Nel, for her patience in editing the thesis and doing it with a smile. Dankie Marlese.

- My postgraduate comrades (too many names), for their support through the years. LAB 60 will never be forgotten.

- My campus friends, His People campus ministries, Visionary Student Youth, Dos Santos Residence, thanks for your friendship and support through the years

- Shamiel Davids for his technical expertise and great conversations.

- Caroline Barnard for being an inspiration and her administrative assistance.

- Ds. Dawid Botha, Ps. Carlton Julies and Me. Ronelle Temmers for there spiritual guidance and leadership that molded me into the person I am today. Thank you.

- Finally the people that has known me from my infant days, my **Beautiful Mother (Diane**), **my Incredible Dad (Adolf Snr.) and Amazing Sister (Adri)**, thank you for your love, support, guidance and inspiration trough the years. I love you guys very much. Also to my extended family, thank you for your support through the years.

Table of Contents

LIST OF FIGURES

LIST OF TABLES

LIST OF SYMBOLS

A	=	cross sectional area
C	=	concentration flux
Ce	=	equilibrium concentration.
C_0	=	tracer concentration at where t =0
D	=	dispersion
d_L	=	flow path length through
D_L	=	Longitudinal Dispersion coeff.
g	=	gravity
I	=	Hydraulic gradient
K	=	Hydraulic Conductivity
K_d	=	straight line distribution coefficient
L_e	=	open or screen portion of the borehole
M	=	injected mass
n_e	=	effective porosity
q	=	amount of contaminant/solute used adsorbs
Q	=	volumetric flow rate
r	=	radial distance
r_w	=	the adjusted value for the porosity packing around the open or screen
t	=	time
t_m	=	arrival time
V	=	seepage velocity
W	=	volume of fluid contained in the test section

y_0/y_t = water level rise

LIST OF GREEK SYMBOLS

α = borehole distortion factor

α_L = longitudinal dispersivity

ρ = liquid density

μ = viscosity

CHAPTER 1: INTRODUCTION

1.1 Background of Study

Eskom and Sasol Power Plants are large consumers of coal that result in large disposal quantities of ash containing high salinity process water (brine). These two organizations have come together through a joint initiative to address best practice methods for the disposal of brines in conjunction with ash. The overall aim of the project is to work towards the development of sustainable salt sinks by investigating the co-disposal of brines within inland ash dumps. In order to solve this complex environmental problem a thorough knowledge and conceptual understanding of the high salinity process water movement within the ash dump environment must be obtained. This can then be applied in the overall project to assess the potential environmental hazards and risks related to the current practices. Future maintenance and monitoring of management practices can then also be optimized with this knowledge.

1.2 Problem Statement

Coal provides for 77% of South Africa's primary energy needs providing a major resource for the socio-economic requirements of South African citizens. Power stations are the major consumers of coal in South Africa and produces electricity off burned coal (Eskom, 2009). The burning of coal produces a large volume of ash that is disposed in the form of ash dumps. High temperature water for steam production at the power station is cooled down by evaporative cooling towers. During this process a build of salts are produced within the cooled water producing high saline water that are irrigated onto the ash dump. The high salinity processed water has the possibility to move through the ash dump, posing potential problems such as groundwater pollution into the underlying aquifer. The literature shows that the hydraulic properties of ash have been studied globally through a number of experiments. These experiments include: hydrodynamic columns fly ash amendment, hydraulic barrier and the physical and chemical properties of ash (Pathan; 2002; O'Nell et al, 2003; Sivapullaiah and Lakshmikantha, 2004; Kostas, 2005; Boel, 2006). The experiments were primarily performed for ash utilization in agriculture. In South Africa the hydraulic properties of ash dumps has been primarily studied for geotechnical purposes (Geo Hydro Technologies, 1998). The need to assess

ash dumps from a hydrogeological perspective is therefore important to understand the high salinity process water movement through the ash dump and the possible impact it may have on the underlying aquifer. To achieve this understanding, it is necessary to develop a conceptual model in order to describe the process water movement through the ash dump.

1.3 Aims and Objectives

The overall aim is to establish an ash dump conceptual model describing the process water movement through the Tutuka ash dump system. The objectives of the study therefore are to:

- Conduct a literature review of published information of the components of a conceptual model and methods to investigate the components.
- Describe the physical environment component of the conceptual model for the ash dump system to establish an initial conceptual model of the site.
- The application of hydraulic and tracer tests on both laboratory and field scale to estimate hydraulic and transport parameters of the ash dump system.
- The application of hydraulic and tracer tests to determine the hydraulic and transport properties on a surrogate fractured rock aquifer representing the aquifer underlying the ash dump.
- Describe the conceptual model and the benefit for management of the ash dump system.

1.4 Thesis Structure

Chapter 2 includes a desktop study analysing the relevant literature on the different components of a conceptual model and the methods to evaluate these components. Discussions with stakeholders, the relevant reports and site visits also contributed to the relevant information. Subsequent to the desktop study Chapter 3 identifies the physical environment of the investigated study areas of the ash dump system and underlying fractured rock aquifer. A fractured shale aquifer at the UWC campus research site was used as a surrogate aquifer to represent the underlying weathered dolerite aquifer of the ash dump system an initial conceptual model is established in the chapter to provide a platform for the quantitative analysis. In Chapter 4 the relevant laboratory work was completed to estimate the hydraulic and transport parameters and prepare for field scale tests. Chapter 5 contains the field scale studies that were completed to

obtain the flow and transport parameters. In Chapter 6 the combination of the physical environment, laboratory and field testing information are used to develop a newly updated conceptual model for the ash dump system. The implications to managing the ash dump system are included in Chapter 6. Conclusions of the study and further recommendations are made in Chapter 7.

CHAPTER 2: LITERATURE REVIEW

2.1 Introduction

Conceptual models are important tools for the evaluation of groundwater resources. In the event of interpreting pumping test data for example, it is of utmost importance to have a conceptual model of the geology and aquifer type (Rushton, 2003). Understanding these factors enables practitioners to apply the appropriate groundwater flow equation while an absence of the conceptual model might lead to inappropriate interpretation of the system. This applies for all groundwater evaluation methods, where the conceptual model for aquifer systems is of utmost importance, in both applying the appropriate investigative method and also enhancing the understanding of the aquifer system (Rushton, 2003). The chapter intends to discuss the components building the understanding associated with conceptual models. Relevant existing literature of the hydraulic and tracer test methods is also presented.

2.2 Conceptual Model

A conceptual model can be defined as a set of rigorously justified assumptions that represent a simplified perception of a real system (Younger, 2007). The conceptual model can be represented by a description of an aquifer system and its inflow and outflow components. Conceptual models can initially start with a sketch and later develop into a detailed three dimensional diagram. The geological framework in the form of cross sections are most probably the first attempts of conceptualizing aquifer systems and as more information are contributed the complexity of the conceptual model increases. The conceptual model must present the flow, transport processes and estimates of the magnitudes of all the relevant parameters. (Rushton, 2003).

Numerous processes of groundwater flow and transport occur in aquifer systems. The inflow of groundwater generally occurs via recharge resulting from rainfall and irrigation, whereas discharge occurs through springs, seeps and abstraction boreholes. Flow and transport processes can even get more complicated if discharge occurs from multiple layers within the aquifer system and also when the vertical and horizontal flow components are taken into consideration. Measuring flow and transport parameters can be very complicated considering the uncertainties of the controlling processes. Recognising and understanding these processes are important in

developing a conceptual model (Rushton, 2003). It is therefore imperative to understand all the different components of a conceptual model. Typical components of a conceptual model are the physical environment, hydraulic properties and transport properties.

2.3 Components of Conceptual Model

2.3.1 The Physical Environment

The physical environment of the groundwater system can be described in terms of voids formed by interstices between individual grains or aggregates of grains, in terms of channels or from unconnected voids, or for fractures or other openings. When these voids, channels and fractures are connected, groundwater can be transmitted from areas of recharge to areas of discharge (McWorther and Sunada, 1977). Within the physical groundwater system different hydrostratigraphic units is present and can be classified as aquifers, aquitards or aquicludes which are defined by the rock type present. Flow and transport occurs differently for each of these hydrostratigraphic units. It is therefore important to describe the physical environment in terms of the boundary conditions, saturated thickness; bedrock position; vertical thickness and horizontal thickness of the hydrostratigraphy (Younger, 2007). The quantification of parameters is generally dependant on the measurement of flow and transport properties. The flow of water can be associated with the hydraulic properties of an aquifer whereas the movement of salts are associated with the solute transport properties (Konikow, 1996).

2.3.2 Hydraulic Properties

According to Fetter (1994) the hydraulic property of general concern is the hydraulic conductivity, that can be defined as the rate at which a geological material will transmit a liquid under unit gradient The parameter for hydraulic conductivity is expressed as K and the units are expressed in length over time (L/T) or in the SI units meters per day (m/d) (Figure 2.1). When considering a velocity an object is always moving. In the case of groundwater the sediments remain stationary while groundwater moves through the geological material. Hydraulic conductivity is not only dependent on the physical material but also the fluid that flows through the medium. When fluids with different densities and viscosities are present within the flow regime, the hydraulic conductivity can be affected (Freeze and Cherry, 1979). Hence it is important to search for a parameter that can describe the conductive properties of a porous media

independently from a fluid flowing trough it. The parameter k is known as the intrinsic permeability and is a function only of the medium. The term is widely used in the petroleum industry, where the existence of gas, oil and water in multiphase flow makes the use of fluid-free conductance parameter attractive. When measured in meters squared or centimetre square, k is very small and it is therefore defined as a Darcy unit of permeability (Freeze and Cherry, 1979).

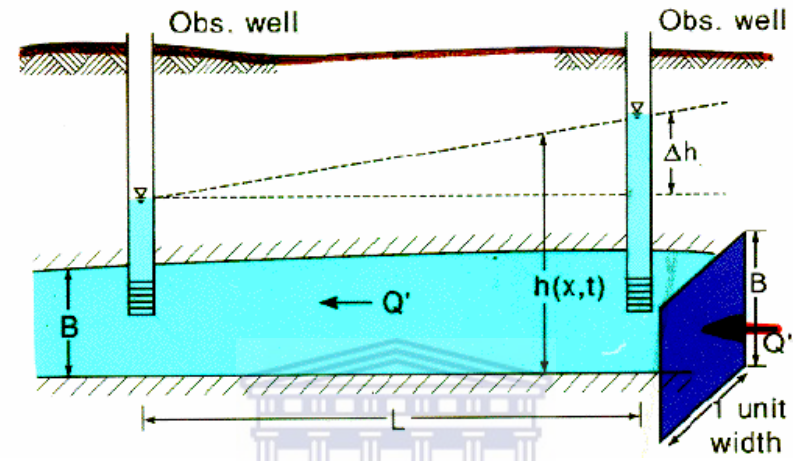

Figure 2.1 Parameters to determine the hydraulic conductivity (Bear, 2008).

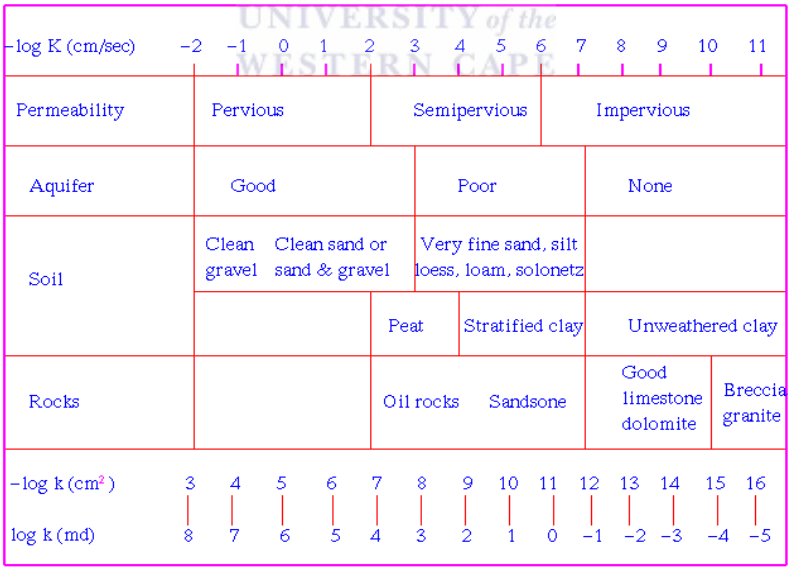

Figure 2.2 The variation in hydraulic conductivity for different rock types (Bear, 2008).

2.3.3 Transport Properties

When looking at transport processes the common starting point would be to look at the movement of solutes into and out of the flow domain. Dissolved substances such as natural constituents, artificial tracers or contaminants are known as solutes (Kruseman and De Ridder, 1994). Solute transport properties are associated with the calculation of the concentration of a dissolved chemical species in an aquifer over a time period and a known distance (Domenico and Swartz, 1998). Solutes have the ability to affect the transport properties depending on the properties of the solute and its behaviour in the environment. The major components controlling solute movement are advection, dispersion and chemical adsorption (Domenico and Swartz, 1998). The advection is the component of transport that moves with the average velocity of the groundwater, hence the movement of the solute is with the groundwater flow. As the solute moves along with the groundwater, it tends to spread out and reduce in concentration. This is known as dispersion and even though the concentration of the solute decreases, more spreading of the solute takes place within the groundwater. Solutes can also attach themselves to the particles of the aquifer and slow down the movement of the solute; this is known as adsorption. All these components are important to consider in the interpretation of transport parameters.

Interconnectedness of void spaces are also of utmost importance since it controls the flow and transport of water through the material (Figure 2.3). Pore spaces of a material that are interconnected can be defined as the effective porosity (n_e). The effective porosity applies for all rock types acting as a natural pipeline through which groundwater can move. Different properties of pores will directly affect the transport of contaminants (Fetter, 1994).

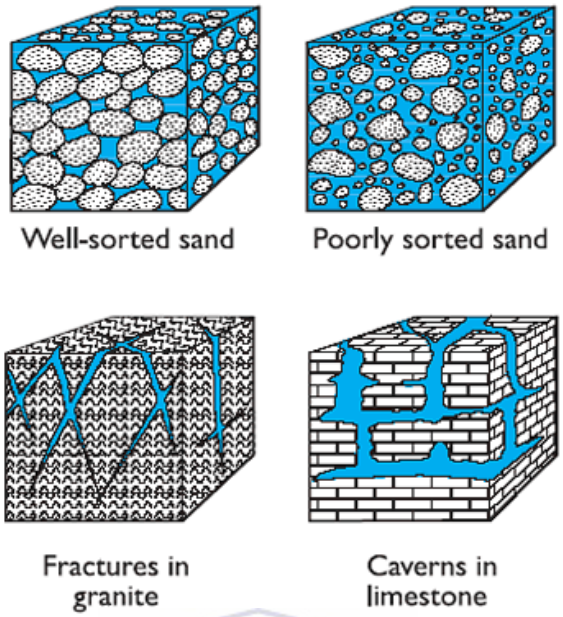

Figure 2.3 Different types of effective porosity exist, dependent on the geological material (Johnson, 2003).

2.3.4 Hydraulic and Transport Flow Conditions

It is important to note that the hydraulic and transport properties exist under different natural conditions. The flow conditions can be distinguished between saturated and unsaturated flow and are associated with different processes, controlling hydraulic and transport properties in the subsurface. The following table displays the distinguishing factors between saturated and unsaturated flow conditions.

Table 1 Distinguishing factors of saturated and unsaturated flow conditions.

Saturated Flow Conditions	Unsaturated Flow Conditions
It occurs below the water table	It occurs above the water table and above the cappilary fringe.
The soil pores are filled with water and the moisture content equals the porosity.	The soil pores are only partially filled with water, the moisture content is less than the porosity .
The fluid pressure is greater than atmospheric pressure hence the pressure head is greater than zero.	The fluid pressure is less than atmospheric pressure hence the pressure head is less than zero.
The hydraulic head must be measured with a piezometer.	The hydraulic head must be measured with a tensiometer.
The hydraulic conductivity K is a constant it is not a function of the pressure head.	The hydraulic conductiivty K and the moisture content are both functions of the pressure head.

2.4 Laboratory Component

Two methods are commonly used in the laboratory to determine saturated hydraulic properties, namely the falling head test and the constant head method (Stephens, 1996). Tracer tests are also often used to determine the transport properties in the laboratory. The constant head method was used in the study to determine the hydraulic properties and laboratory tracer tests were used for the determination of transport properties.

2.4.1 Constant Head Hydraulic Tests

Darcy's law is commonly applied in laboratory experiments to determine the saturated hydraulic conductivity coefficient using constant head hydraulic test data. (Equation 2.2) (Darcy, 1856). Darcy's law can be described as a simple proportional relationship between the instantaneous discharge rate through a porous medium, hydraulic conductivity (K), hydraulic gradient (I) and cross sectional area (A)

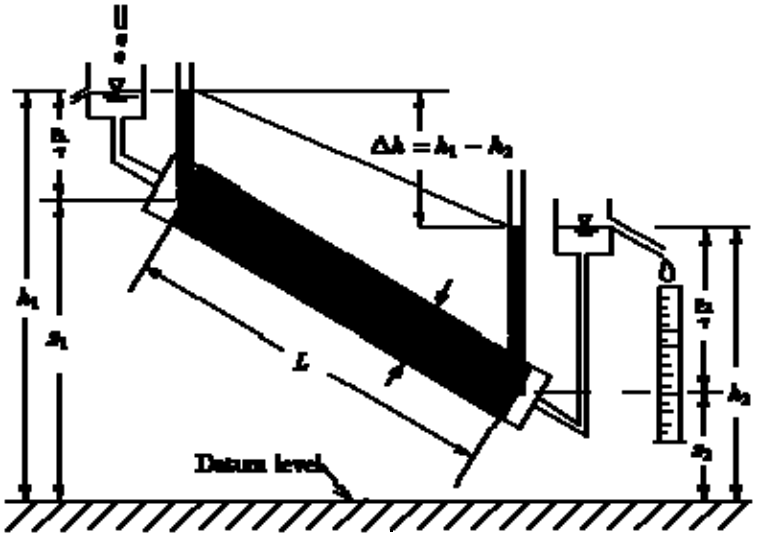

Figure 2.4 Darcy experimental setup and the parameters that controls the flow

$$Q = KIA \qquad \textbf{Equation 2.1}$$

Carter and Gregorich (2008) performed the constant head hydraulic test on the principles of Darcy's law. The test is performed by introducing water to a sand sample by maintaining inflow and outflow reservoirs at constant positions relative to the sample. The water passes from the bottom of the sample, upwards trough a screen plate. Hence the distribution of the water spreads evenly trough the samples, to ensure that the sample is fully saturated. The necessary parameters such as the discharge, gradient and cross sectional area are than measured. The range of saturated hydraulic conductivity that can be conveniently measured with this method is $1\text{-}10^{-5}$ m/day.

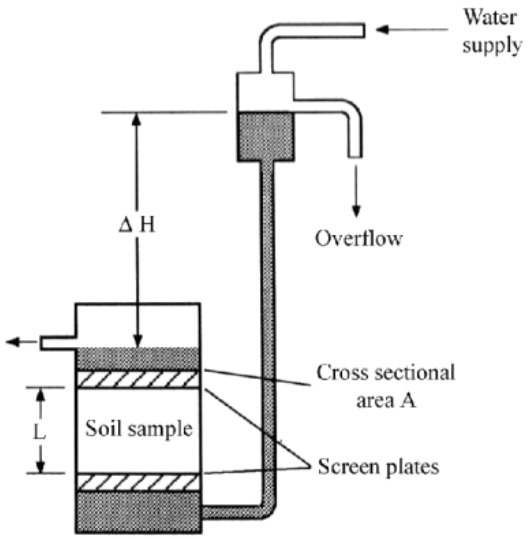

Figure 2.5 Schematic depictions of the Constant Head Method (Fetter, 1994).

The permeability (Freeze and Cherry, 1979) can also be interpreted for the experiments but are dependent on other properties, including the hydraulic conductivity (K), fluid properties such as viscosity (μ), liquid density (ρ) and gravity (g) as expressed in (Equation 2.3).

$$k = \frac{K\mu}{\rho g}$$ **Equation 2.2**

Hydraulic methods in the laboratory are commonly applied and has got both advantages and disadvantages in its application (Table 2.2)

Table 2.2 Advantages and disadvantages of laboratory hydraulic tests (James and Butler, 1998).

ADVANTAGES	DISADVANTAGES
Water flow boundaries and flow fields are well defined (ex. Constant head and one dimensional rectilinear	Small sample sizes that might not be representative of in situ medium
The flow environment can be specified and maintained (ex. Constant pressure, temperature and water chemistry).	Loss of hydraulic contact from which the sample was collected.
Saturated hydraulic conductivity can be determined using equation by which is being defined	Imposed flow field that may be unrealistic or inappropriate
Absence of Sampling disturbance during data collection	

2.4.2 Laboratory Tracer Tests

The most common approach to evaluate transport parameters is by conducting a tracer test (Kass, 1998). Tracer test in the laboratory is achieved by the introduction of a substance (tracer) into a material and monitoring the transport of the substance through the aquifer. The first step in conducting a tracer tests is the selection of an appropriate tracer. The tracer being introduced in the aquifer should generally be ideal, meaning that the tracer is conservative, dissolves in water, moves at the same rate and that no adsorption of the substance to a material takes place (Kass, 1998).

2.4.3 Adsorption Tests

Adsorption tests are often applied with column experiments to identify the adsorption or removal of salts in a system to identify possible appropriate conservative tracers (Leitao et al., 1996; 2000). According to Taha and Debnath (1999) adsorption is a phenomenon whereby a solute attaches itself to the surface of a solid material. It may be either physical or chemical (chemisorption) depending on the type of forces involved. In physical adsorption, the electron cloud of the substance adsorbed interacts as a whole with the adsorbent. On the other hand, in chemisorption, electron transfer and sharing of electrons takes place between the adsorbate and the adsorbent.

The result of batch adsorption experiments are usually analyzed with respect to adsorption isotherms. The parameters used are the amount of contaminant/solute used adsorbs (q) and the equilibrium concentration, (Ce). When the linear relationship between (q) and (Ce) can be approximated, a straight line distribution coefficient K_d can be calculated (Equation 2.4).

$$q = K_d C_e$$ **Equation 2.3**

There are a number of adsorption isotherms, such as Freundlich, BET, Gibbs equation, Fowler-Frumkin's equation, Hill-de Boer, Volmer, Temkin, etc. The most common adsorption isotherms used are the Langmuir isotherm. The Langmuir adsorption isotherm is based on the concept that solid surfaces have finite adsorption sites. When all the adsorption sites are filled, the surface will no longer be able to adsorb solute from solution. Therefore, this isotherm offers an advantage over the other previously mentioned isotherms in that it puts a threshold on the amount of chemical species the soil can adsorb. Thus the maximum amount of solute adsorbed in a particular soil chemical interaction system can be estimated. Analytically, the isotherm (also an L-type) may be written as (Veith and Sposito, 1977), (Equation 2.5):

$$q = \frac{\alpha\beta C_e}{1 + \alpha C_e}$$ **Equation 2.4**

Where alpha is an adsorption constant related to the binding energy or the affinity parameter and betha is the maximum amount of solute that can be adsorbed by the soil. These parameters can be easily obtained from its linearized form:

$$\frac{1}{q} = \frac{1}{\alpha\beta}\frac{1}{C_e} + \frac{1}{\beta}$$ **Equation 2.5**

2.4.4 Tracer Test Application

Laboratory tracer tests are not so popular because it often does not represent the aquifer in terms of scale. Despite this, laboratory tracer tests still provide estimates of transport parameters and assists in planning field tracer tests (Stephens et al., 1998). Laboratory tracer tests are often performed in column experiments of different homogeneous material with different lengths and diameters (Klotz et al., 1980; Khan and Jury, 1990; Huang et al., 1995; Irwin et al., 1996; Rashidi et al., 1996; Sternberg, 1996; Watson, 2002) and also different heterogeneous environments (Danquicney et al., 2004, Gierczak et al., 2005).

The effective porosity is commonly quantified in the laboratory. Effective porosity on the laboratory scale has a small variability compared with hydraulic conductivity and dispersivity and is an excellent simulator for groundwater pollution in the context of drainage and capillary processes. In the experiment a conservative tracer of a specific concentration is introduced into the steady state flow conditions of a column packed full of the material under investigation. The background tracer concentration prior to injection is measured and injected by a pulse release into the flow path of the experiment. The tracer is collected at the point of outflow of the column over time and can then be expressed as concentration over time. This is then graphically presented by means of a breakthrough curve.

Breakthrough curves are interpreted on the basis of their arrival times and shape. The arrival times for breakthrough curves can be estimated by calculating the center of mass for the breakthrough curve, from this information the seepage velocity (v) can be calculated by dividing flow path length (d_L) through the arrival time (t_m) (Equation 2.7). The shape of breakthrough curves can be matrix like, forward tail, bi-modal and backward tail and are dependent on the dominant transport process (Shapiro, 2001).

$$v = \frac{d_L}{t_m}$$ **Equation 2.6**

The effective porosity (n_e) can be calculated from the breakthrough curve as the ratio between Darcy flux and seepage velocity, where q is experimental Darcy flux and v is seepage velocity (Darcy, 1856) (Equation.2.8).

$$n_e = \frac{q}{v}$$ **Equation 2.7**

From this graph the Darcy velocity can also be calculated and analysed (Equation.2.8).

$$v = \frac{Q}{A}$$ **Equation 2.8**

2.5 Field Component

2.5.1 Slug Test Hydraulic Method

Slug tests are frequently used to estimate hydraulic conductivity in an area close to a borehole and can be classified as small scale in situ field hydraulic tests (Hiscock, 2005). Tests are carried out by either creating a sudden change in the water level in a borehole through the rapid introduction in the form of a slug or the rapid removal in the form of a bail-down test of a known volume of water (James and Butler, 1998).

Prior to performing a slug test, it is necessary to have information about the borehole construction of the investigated site. The design process (James and Butler, 1998) of a slug test is highly dependent on borehole construction, borehole development and applicability of conventional theory. Two critical considerations need to be addressed when performing slug tests: the formation response to the initial injection of the slug and the estimate of the initial change in hydraulic head when injecting a slug. The method being used to perform a slug test is highly dependent on the seep with which the formation response as well as the changes in head (James and Butler, 1998).

The bail-down method is one of the most common methods used in slug testing. The removal of water from the aquifer via a bailer is referred to as a bail down test (Figure 2.6). When conducting a bail-down test, the pre-test water-level is measured and noted. The same water-level reference measuring point should be used throughout testing. A bailer is then used to rapidly lower the water-level in the well for a period of one or more minutes. The exact time

when bailing is stopped should then be noted and periodic water-level measurements collected to track the rate of water-level recovery. An electric tape measuring device generally provides the best and most rapid measurements. The first measurement should be made as soon after bailing is stopped as possible. Subsequent measurements should be made at frequent intervals initially, and less frequent intervals as water level recovery slows sufficient to define the recovery trend. Recovery measurements should be continued until a good percentage of total recovery is attained. If feasible, at least 75% of full recovery should be attempted (James and Butler, 1998).

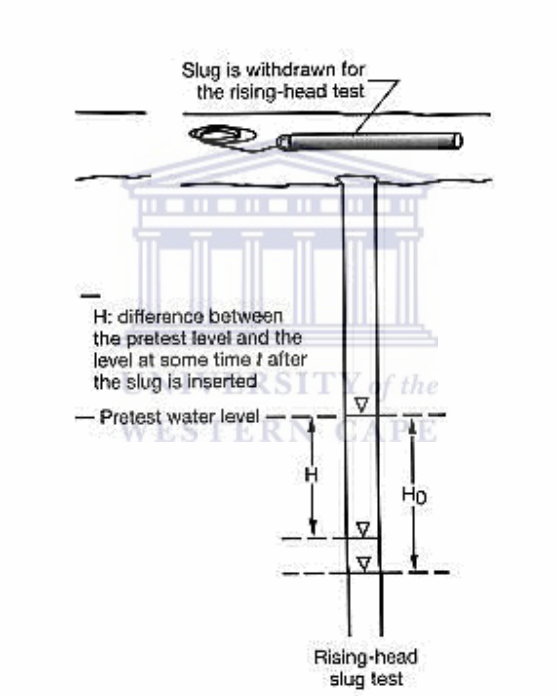

Figure 2.6 Diagram displaying the bail-down slug test.

The first step succeeding the application of a slug test is the identification of the appropriate analysis method for the data being collected which is dependent on the hydrological setting of the series of tests performed (James and Butler, 1998). Slug test data are generally analyzed using relatively standard analytical solutions to the equations which govern groundwater flow. Homogeneity and constant aquifer thickness are common assumptions for conditions within the

area of influence of the test. In practice, these are usually met because the radius of influence of most slug tests is fairly small (Bouwer and Rice, 1976).

The commonly applied slug test analysis method is the Bouwer and Rice slug analysis (Bouwer and Rice, 1976). The method is used because it produces consistent results compared to other methods (Summers, 1983; Melby, 1989) and it estimates the hydraulic conductivity of a material surrounding a borehole. The design of the method specifically accommodates partially penetrating and fully penetrating boreholes of unconfined aquifers. It is assumed if the water level rises (y_0/y_t) within an open or screen portion of the borehole (L_e), the adjusted value for the porosity packing (r_w) around the open or screen needs to be accounted. The hydraulic conductivity can be calculated by (Bouwer, 1978) (Equation 2.9).

$$K = \frac{r_c^2 \mathrm{Ln}(R_e / r_w)}{2L_e} \frac{1}{t} \mathrm{Ln} \frac{y_0}{y_t}$$

Equation 2.9

2.5.2 Pumping Test Hydraulic Method

A pumping test (Kruseman and de Ridder, 1994) is a hydraulic method that has been applied for many years to predict hydraulic-head drawdown in aquifers under proposed pumping. Pump tests are generally applied for parameter estimation of larger aquifer area and are more expansive than slug tests to provide measurements of aquifer transmissivity and storativity. Water is pumped from a borehole, creating a localized hydraulic gradient, which causes water to flow from the surrounding aquifer. During pumping a cone of depression expands outwards from the borehole, due to a reduction of hydraulic head within the aquifer. The shape and extent of the cone of depression is dictated by the rate of pumping and the hydraulic properties of the aquifer. By monitoring the pumping borehole and observation boreholes it is possible to observe the cone of depression and determine aquifer properties. Different types of pumping tests can be executed, of which the step drawdown and constant rate discharge tests are used most commonly. A pumping test is often conducted simultaneously with tracer test (Yong Lee et al., 2003; Dann et al., 2008) and contributes to hydraulic and transport parameter estimation.

2.5.3 Tracer Tests

Different types of tracer tests exist for the field and depend on the specific objective that needs to be achieved. These tracer tests can be analyzed either qualitatively or quantitatively. The aim of qualitative tracer tests is focused on visually interpreting the tracer breakthrough, proving connectivity between boreholes or movement of water through the unsaturated zones. The aim of quantitative tracer tests is to calculate the aquifer properties. Tracer tests are conducted in two types of conditions, either natural gradient or forced gradient conditions. The natural gradient tracer test occurs under the natural flow conditions of the aquifer, whereas the force gradient tracer test is conditioned by pumping the aquifer (Kass, 1998).

2.5.4 Natural Gradient Radial Divergent

The natural gradient tracer test (Figure 2.7) is a type of tracer test where an amount of tracer is injected into the natural gradient flow field and detected at many observation boreholes. Natural gradient tracer tests are applied mainly in porous media such as unconsolidated sands (Yang et al., 2001, Le Blanc et al., 1991, Davis et al., 2001), karstic aquifers (Goldscheider, 2008); mine dumps (Wolkersdorfer and Hasche, 2001) and are rarely used in fractured aquifers due to heterogeneity (Maloszweski, 1993; Shapiro, 2001).

The most common interpretation method used is the instantaneous injection method (Maloszwenski, 1990). Field data is normally interpreted by using tracer breakthrough curves whereby the arrival time and breakthrough curve shape is interpreted.

Aquifer parameters can also be obtained by using traditional solute transport modeling. Transport parameters can be obtained by using the advection dispersion equation, where (C) represents the concentration flux, (M) the injected mass, (Q) the volumetric flow rate, the time variable and (D) the dispersion (Equation 2.11). Each tracer test is unique and has its advantages and disadvantages, this also account for the natural gradient radial divergent tracer test (Table 2.3).

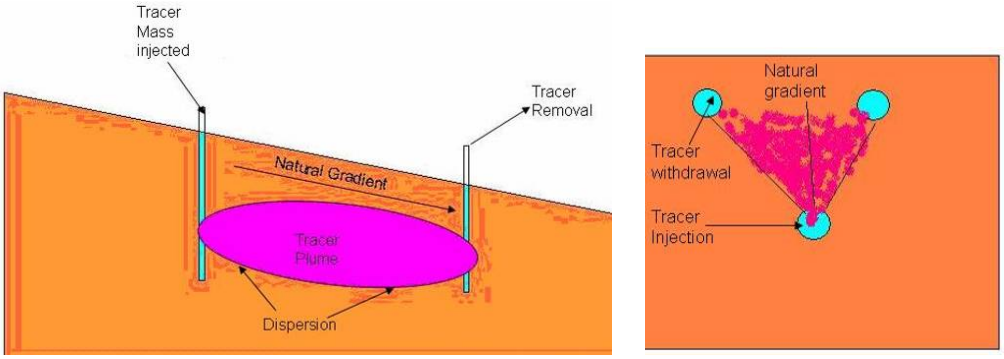

Figure 2.7 Natural gradient radial divergent tracer test cross sectional and plan view.

$$C = \frac{M}{2Q\sqrt{\pi * \alpha_L * vt^3}} \exp\left[\frac{(r - vt)^2}{4D_L t}\right]$$

Equation 2.10

Table 2.3 Advantages and disadvantages of natural gradient radial divergent tracer test. (Kass, 1998).

ADVANTAGES	DISADVANTAGES
Generally provide the most complete and best quality information provided a sufficient number of	Requires many wells (multi well) quality of information proportional to number of wells
Generally provide the most complete and best quality information provided a sufficient number of well exist	High risk no guarantee of tracer recovery, test durations can be very long
Best suited for environmental tracers and contaminant plume monitoring	Can be sensitive to well completions and drilling

2.5.5 Single Well Tracer Dilution

The singe well tracer dilution test (Figure 2.8) aims to relate the observed rate of a tracer dilution in a borehole to the average groundwater velocity in the aquifer (Guven, 1985; Wolkersdorfer and Hasche, 2001, Yang, 2001, Xu et al., 1997; Rieman et al., 2003; Van Wyk, 2001). This is achieved by obtaining a dilution curve from the tracer that was injected into a borehole. From the dilution curve the volumetric flow rate through the borehole can then be calculated. The flow velocity can be interpreted with the concentration of data at that point where consistency in the tracer concentration is achieved. With conditions of steady state and thorough mixing of the tracer in the borehole, the Darcy velocity is computed from a dilution test and can be defined as the volume of water flowing through a unit cross section area normal to the direction of flow $q = -\frac{W}{\alpha t}\ln\left(\frac{C_0}{C}\right)$

Equation **2.11**) (Van Wyk, 2001). A single well tracer test has its advantages and disadvantages (Table 2.3).

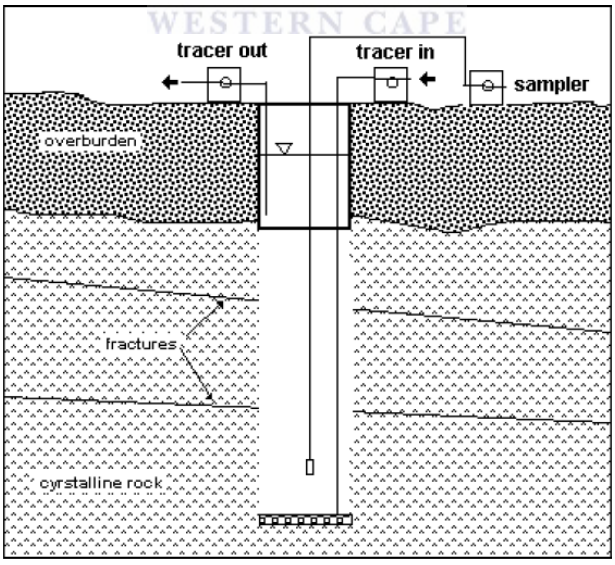

Figure 2.8 Tracer dilution method performed in a fractured aquifer.

$$q = -\frac{W}{\alpha t}\ln\left(\frac{C_0}{C}\right)$$ **Equation 2.11**

Table 2.4 Advantages and Disadvantages Single well Tracer Test (Kass, 1998).

ADVANTAGES	DISADVANTAGES
Requires only one well, many often exist	Generally interrogates smaller volume of aquifer
Relatively short, controllable duration	More complicated requirements
Tend to be easier to permit, low tracer masses, high tracer recoveries, smaller discharge volumes	Can be influenced by well completions or drilling damage.
Provides estimates of groundwater velocity if multiple tests conducted	Poor, unconstrained estimates of flow porosity, dispersion and solute retardation factors

2.5.6 Forced Gradient Radial Divergent

A radial divergent (Figure 2.9) tracer test is conducted, by pumping a borehole to steady state and effectively creating a radial divergent flow field (Vandenbohede et.al 2005; Sauty et al., 1980; Van Wyk et al., 2001). Subsequent to creating the appropriate condition in the aquifer a tracer is injected in the injection borehole, while the tracer breakthrough curve is monitored at the pumping borehole. The analysis (Sauty et al., 1980) of the breakthrough curve yields estimates of kinimetic porosity, aquifer dispersivity and groundwater velocity. The concentration distribution with time for a one dimensional uniform flow is given by (Equation 2.13). The forced gradient radial divergent tracer test is a very effective method and has its advantages and disadvantages. (Table 2.5)

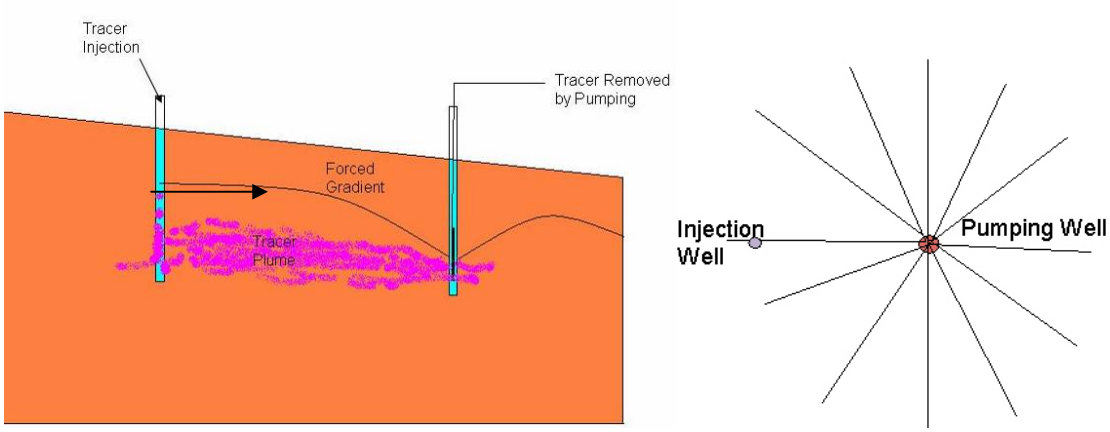

Figure 2.9 Radial convergent flow field cross sectional and plan view.

$$C = \frac{M}{2Q\sqrt{\pi * \alpha_L * vt^3}} \exp\left[-\frac{(r - vt)^2}{4D_L t} \right]$$

Equation 2.12

Table 2.5 Advantages and Disadvantages radial divergent tracer test (Kass, 1998).

ADVANTAGES	DISADVANTAGES
Interrogates larger volume of aquifer	Requires multiple wellls
Yields estimates of more parameters than the singe well	Relatively long and uncontrolled duration
	Difficult to permit high tracer recoveries

CHAPTER 3: TUTUKA ASH DUMP PHYSICAL ENVIRONMENT

3.1 Introduction

The ash dump is situated in the Mpumalanga province 25 kilometers away from Standerton. A description of the physical environment where the hydrology, groundwater flow and transport occurs is an important component of any conceptual model. In this section the physical environment will be described using the existing information available of the site as well as information obtained during site investigations.

3.2 Site Hydrology

The site lies in a summer rainfall region. According to the Köppen classification (Viterito, 1987), the climate of the area under investigation is classified as Highveld, which is defined as a climate with a temperate to warm temperature and summer rain. It is also a climate in which the potential to evaporate water exceeds the precipitation. The winds in the region are usually north-westerly and reach their maximum speed in the afternoon. During thunderstorms, strong and gusty south-westerly winds are common. The duration of these winds, however, is very short. During prolonged drought, dust-storms may be frequent. Temperatures show large daily and seasonal variations.

Mean temperatures reach a maximum in December/January and a minimum June/July. The period during which frost can be expected lasts for about 150 days (May to September). Local thunderstorms and showers are responsible for most of the precipitation during the summer, from October to March and peaking in January. Hail is sometimes associated with the thunderstorms and mainly occurs from October to December and in March. Fog occurs frequently throughout the year with its highest occurrence from March to August. The mean annual precipitation for the region, calculated from these stations, is 737 mm per year. Precipitation occurs predominantly as thunder showers with the peak period of occurrence during the months November, December and January (Eskom, 1993).

The significance of rainfall with reference to water quality aspects at the ashing operation is three-fold. Precipitation is the main source of fresh water recharge to the ground water system.

Heavy rainfall periods may cause problems with storage capacity of effluent. Heavy rainfall periods may cause direct infiltration, percolation and leachate formation. According to Monteith (1985) the difference between rainfall and run-off is largely explained by total evaporation and infiltration. The annual amount of water leaving an area as run-off can be as little as 10% of the yearly precipitation.

3.3 Site Geology

The geology of the site consists of dolerite and shale which serves as a natural bedrock. The age of the rock type extends from late Triassic to early Cretaceous volcanic rocks. The rock types appear as fresh rock with occasional weathered zones. The dolerites on the site generally weather to clay (Eskom, 2007).

3.4 Site Geohydrology

The upper aquifer is associated with a weathered dolerite sill. Water is found a few meters below the surface. This aquifer is fed by rainfall and seepage from the ash dump, infiltrating the weathered material, it is eventually stopped by impermeable, unweathered dolerite. Ground water movement (laterally) follows the direction of the surface slope; this water re-appears on surface at the toe of the standby area of the ash dump. This usually happens when the path of the ground water is obstructed by some barrier or where the surface topography cuts into the water table, such as at a stream. The deeper aquifer lies within the consolidated rocks, below the weathered zone. Ground water is contained in fractures, cracks and joints within these rocks (Eskom,1993).

3.5 Ash Dump Formation

When coal is burned at very high temperatures ash is produced as a by-product. The ash is then removed via a conveyer belt (

Figure 3.1) and disposed on a dump with 10% moisture content. The ash is typically dumped over the edge of the ash dump and leveled by a bulldozer after dumping at a height of between 20 to 30 meters. Brine water is used for dust suppression until rehabilitation of the site occurs. The major composition of the brine consists of (Na; Cl; SO_4; Ca; K; F; CO3 and F), where, Na; Cl and SO4 are the dominant elements. The deposition of ash over time results in the process of burial, which causes the ash to undergo hardening and as a result transforming into hard core ash (Figure 3.2). Rehabilitation is done by placing topsoil, which is removed from the natural soil at the foot of the progressing ash dump, and then placed on top of the dump. The soil layer is then fertilized and planted with grass that can be used for livestock feeding.

Figure 3.1 **Arial view of the Tutuka Ash dump, ash transported via conveyer belt to the ash dump. Rehabilitated parts of the ash dump can be observed and also freshly dumped ash.**

Figure 3.2 **Ash dump system formation showing power station where coal is burned, the by product of burned coal ash transported via conveyer belt onto the ash dump, compacting the ash by compaction and suppressing the ash by irrigation and then irrigating the ash for dust suppression ,rehabilitation of ash dump.**

3.5.1 Site Description

Detailed site descriptions (Figure 3.3) completed on the ash dump indicate steep slopes on the ash dump system. Inflow to the ash dump system occurs on the top of the ash dump and the outflow point of the water is at the bottom of the ash dump where it discharges into a tow drain. At the bottom of the ash dump water levels and the leaching of salts can be observed. The ash displays a fine to medium to coarse grain size and takes up silt to sandy appearance observed in ash cores. Variable hydraulic conductivities and porosities can thus be expected from the ash.

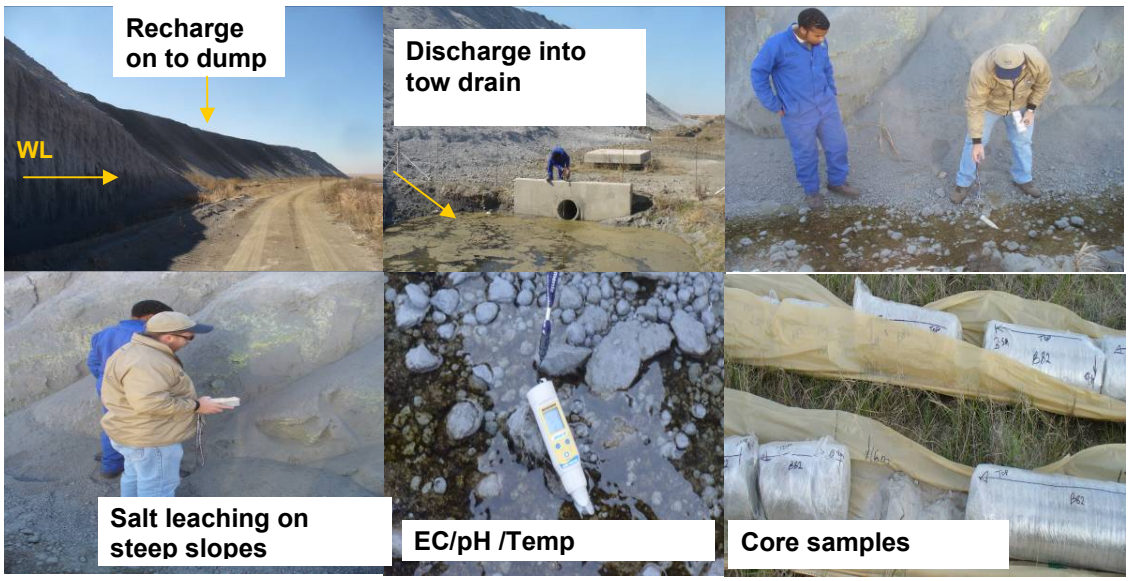

Figure 3.3 Formulation of a site description of the ash dump system.

Five boreholes have been installed on the study site (Figure 3.4). They were sited from interpreted geophysical data in areas of different ash age and salt content. These boreholes were drilled to different depths to observe and monitor the subsurface geology (Eskom, 2007).

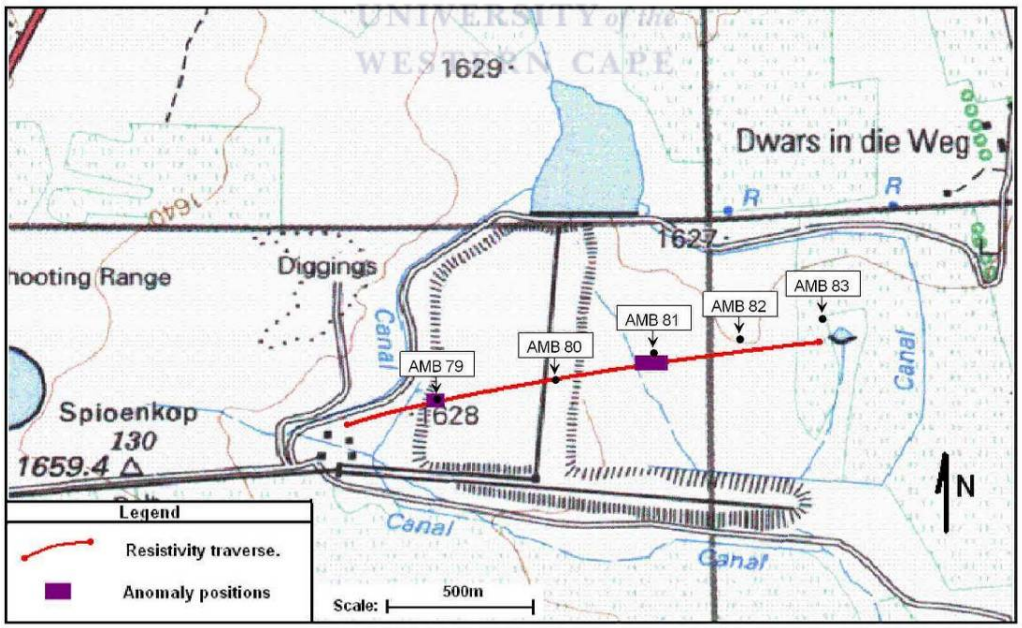

Figure 3.4 Boreholes drilled across the Tutuka ash dump

Electrical resistivity data shows that the depth of the ash dump is about 26m at the experimental sites with high resistivity bedrock underlying the site (Figure 3.5). Drilling showed that the toe drain is underlain by clay from the weathered bedrock.

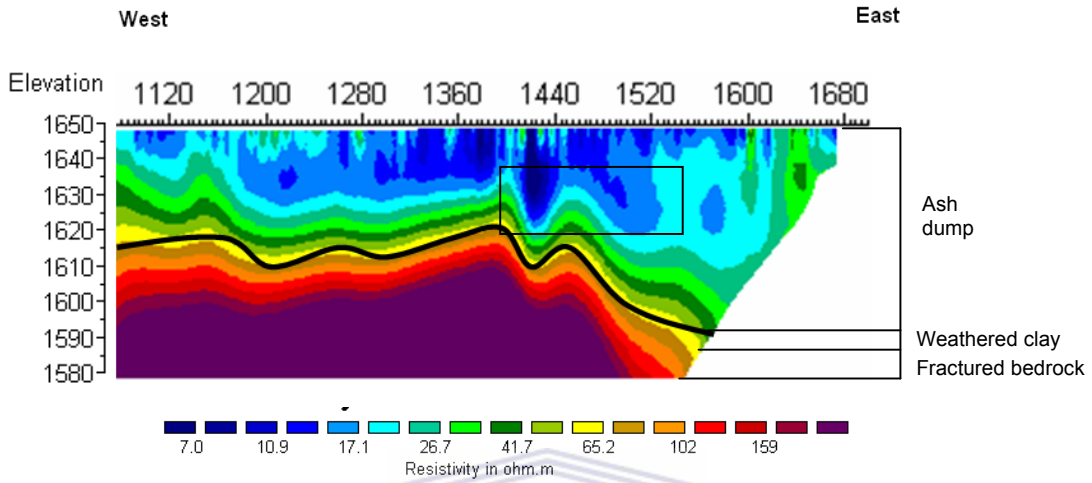

Figure 3.5 **Geophysical Profile west to east from the ash dump, different saturation levels and salt concentration displayed. The experimental site is situated at the bottom of the ash dump.**

Unfortunately the boreholes drilled at the toe of the Tutuka ash dump was destroyed, during the expansion of the ash dump. It was therefore decided to conduct part of the field tests on a surrogate aquifer of similar nature to obtain relative parameters compared to ash.

3.5.2 Surrogate Experimental Fractured Aquifer

The aquifer selected as surrogate fractured aquifer is situated at the University of the Western Cape Bellville Campus and consists of a primary aquifer underlain by fractured shale bedrock. The fractured shale can be compared with the underlying fractured bedrock of the ash dump system that is overlain by the ash dump.

3.5.3 Site Geology

The late-Precambrian age (800 million years) Malmesbury Group is the oldest rock formation in the Western Cape area, comprising of low grade metamorphic rocks such as phyllitic shale's, quartz and sericitic schists, greywacke sandstone and slate. The Malmesbury Group is subdivided by two faults, the Colenso Piketberg and the Worcester Faults and these faults have a

North West trend. The occurrence of this faulting has divided the Malmesbury Group into three geological terrains namely the Tygerberg; Boland and the Swartland Terrain. These terrains display the different formations of the Malmesbury Group (Johnson et.al, 2008). The Late Precambrian Malmesbury forms the basement rock on the campus site and forms part of the Tygerberg Terrain which consists of highly weathered shale and clays. The Malmesbury Formation is unconformably overlain by the tertiary cape flats sand, that primarily consist of argillaceous sand and lenses of clay and peat. Strata presented on the campus site can be divided into 4 different lithological units: shale, clay, peat and sand.

3.5.4 Borehole Field

The campus site consists of both unconfined and semi-confined aquifers that is made up from a primary aquifer (Cape Flats) which is underlain by the secondary Malmesbury aquifer. Six percussion boreholes were sponsored and drilled by the Department of Water Affairs in 2001. Two of the boreholes (UWC6 and UWC5) penetrate into the deeper Malmesbury fractured aquifer at depths of 80m (UWC6) and 100m (UWC5). Construction in both the boreholes consists of solid PVC with screens at the bottom 12m of the boreholes. These screens positions are assumed to correspond with water strikes and corresponding fracture zone, with the possibility of linking the boreholes to allow flow and transport to take place between the screened zones (Figure 3.6).

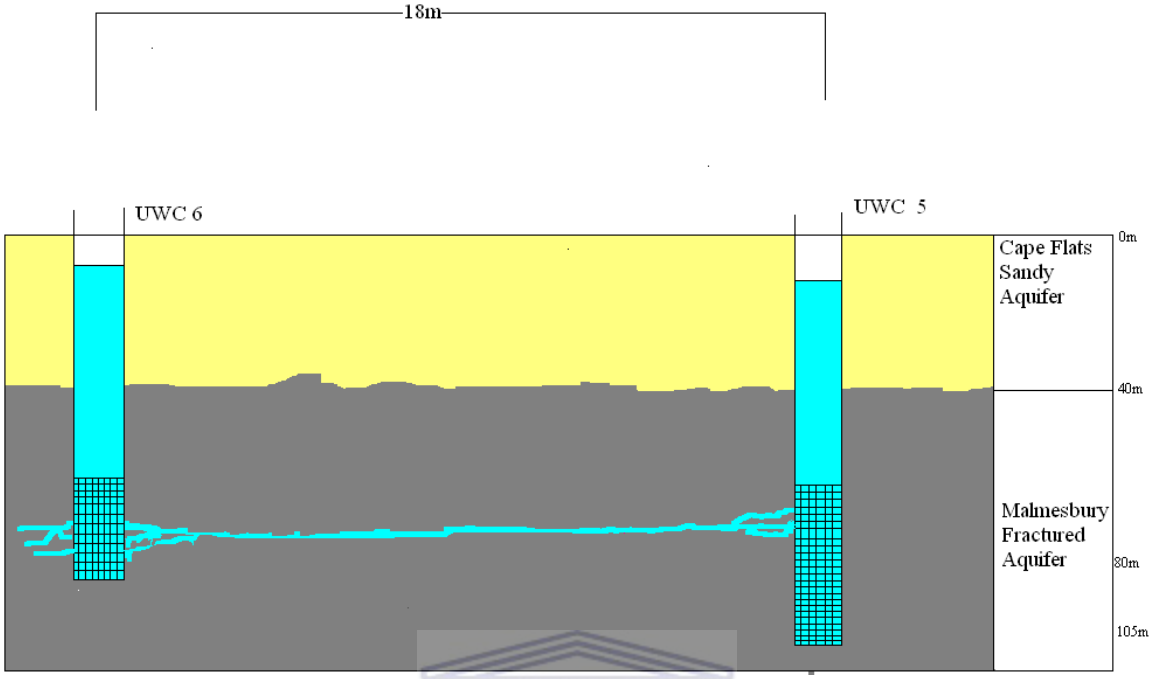

Figure 3.6 **Geological cross section of surrogate fractured aquifer displaying two of the installed boreholes, at different depths.**

3.6 Initial Site Conceptual Model

The ash dump system is recharge by both natural and artificial processes. Natural or fresh recharge occurs by precipitation, whereas artificial or process water (90% NaCl) recharge occurs on a daily basis. The ash dump system can be divided into an upper unsaturated and lower saturated zone. The unsaturated zone exhibit moisture content of between 20-30% and the saturated zone are 2-3 m above the bottom of the ash dump. The ash dump is underline by weathered dolerite. The saline water gradually infiltrates to the bottom of the ash dump where it infiltrates the weathered dolerite. At the bottom of the ash dump water levels and the leaching of salts from the process water can be observed. Discharge of the saline water eventually occurs in a toe drain on the side of the ash dump. There are still some uncertainties regarding the hydraulic and transport properties of the process water through the ash dump system. It is therefore imperative to quantitatively and qualitatively define the various components identified on the ash dump.

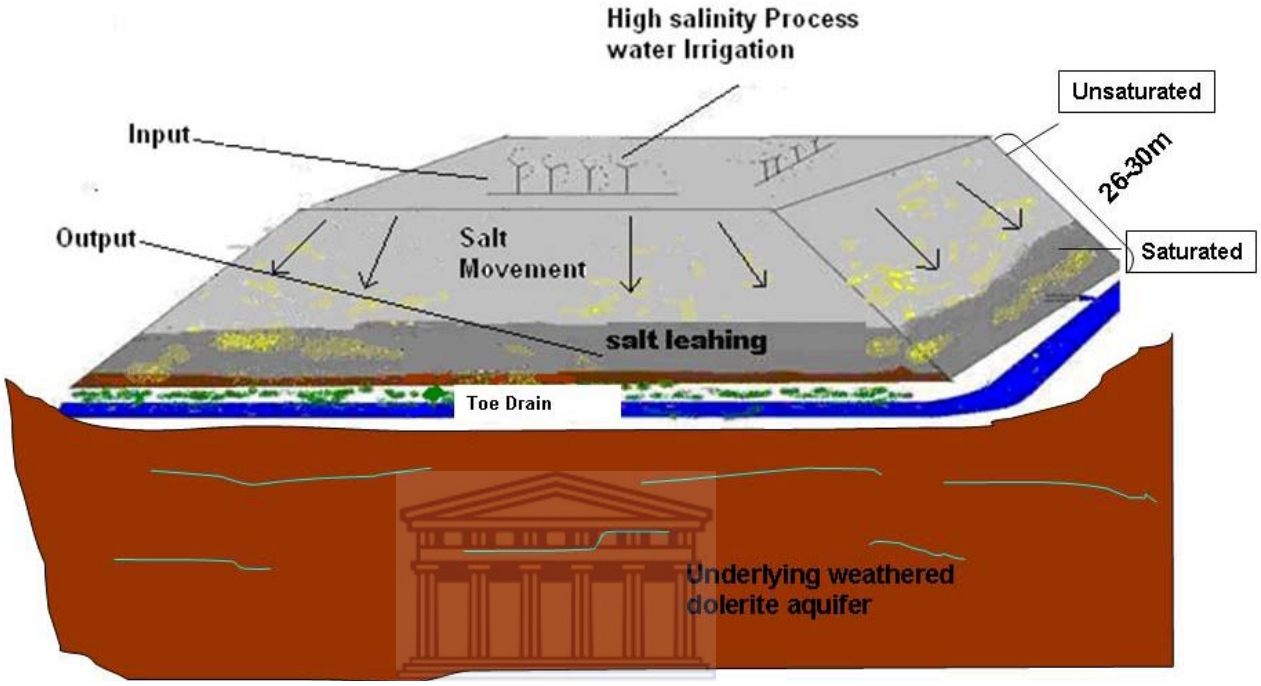

Figure 3.7 The initial site conceptual model of the Tutuka ash dump system

CHAPTER 4: ASH LABORATORY COMPONENT

4.1 INTRODUCTION

Laboratory methods provided an opportunity for parameter estimation under controlling conditions that represented the ash dump. The parameters measured were the temperature, liquid density, liquid viscosity and ash density. Laboratory experiments were conducted to determine saturated hydraulic and transport conditions of the ash. Darcy experiments on both packed column and intact core experiments were conducted in the laboratory. NaCl shakeup experiments were conducted in the lab to determine its suitability as tracer for the ash. Tracer tests were conducted on the ash columns and ash cores.

4.2 Ash Column

4.2.1 Experimental setup

The ash column is prepared by first placing filtering paper at the bottom of the column, to prevent the ash from blocking the piping system and to provide an even distribution of input water through the container. A tracer injection point was inserted into the piping system, 20cm away from where the initial inflow of process water occurs into the ash sample. The tracer injection point was inserted close to the ash sample, so that immediate contact of the tracer and sample could be achieved.

Loose, dry ash from the ash conveyor belt was collected and packed according to the standard leaching packing procedure (ASTM 4874, 2006). The objective of the standard leaching packing is to fill up the column with material in at least 5 consecutive layers. Each of the 5 layers are introduced into three sub layers and levelled. The compaction of the ash material into the column is achieved by using a rammer with a weight of 125g to a fall down along a guide rod onto the compacting disk of 10cm diameter. The rammer is applied three times on the sample layers falling from a height of 20cm. (Figure 4.1).

4.2.2 Experimental Flow Conditions

The flow of the process water is provided at a constant head with water percolating upwards through the ash column of 6.5 cm. This is primarily done to saturate the sample and to prevent air trapping. The constant head is created by using a mariotte bottle (O'Neill, 2003). The compacted column is them immersed into a constant temperature water bath set at 30 degrees Celsius, conditions similar to that of the ash dump (Figure 4.2).

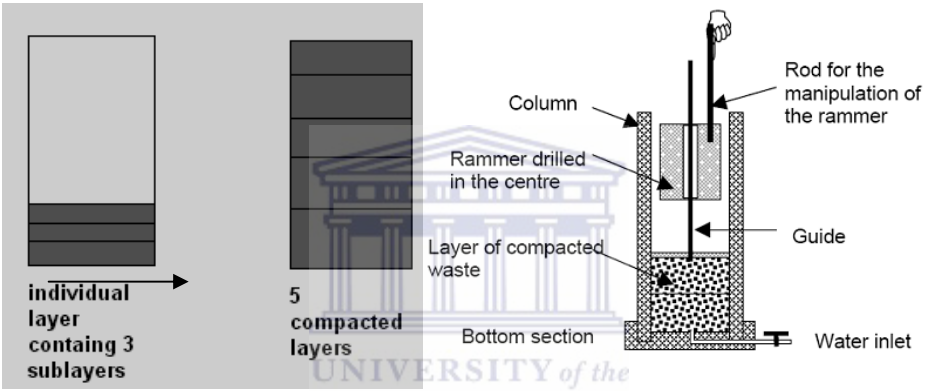

Figure 4.1 **Standard leaching packing method displaying individual layer with sub layer packing and the five compacted layers as well as the different equipment and measuring devices necessary to perform the packing method.**

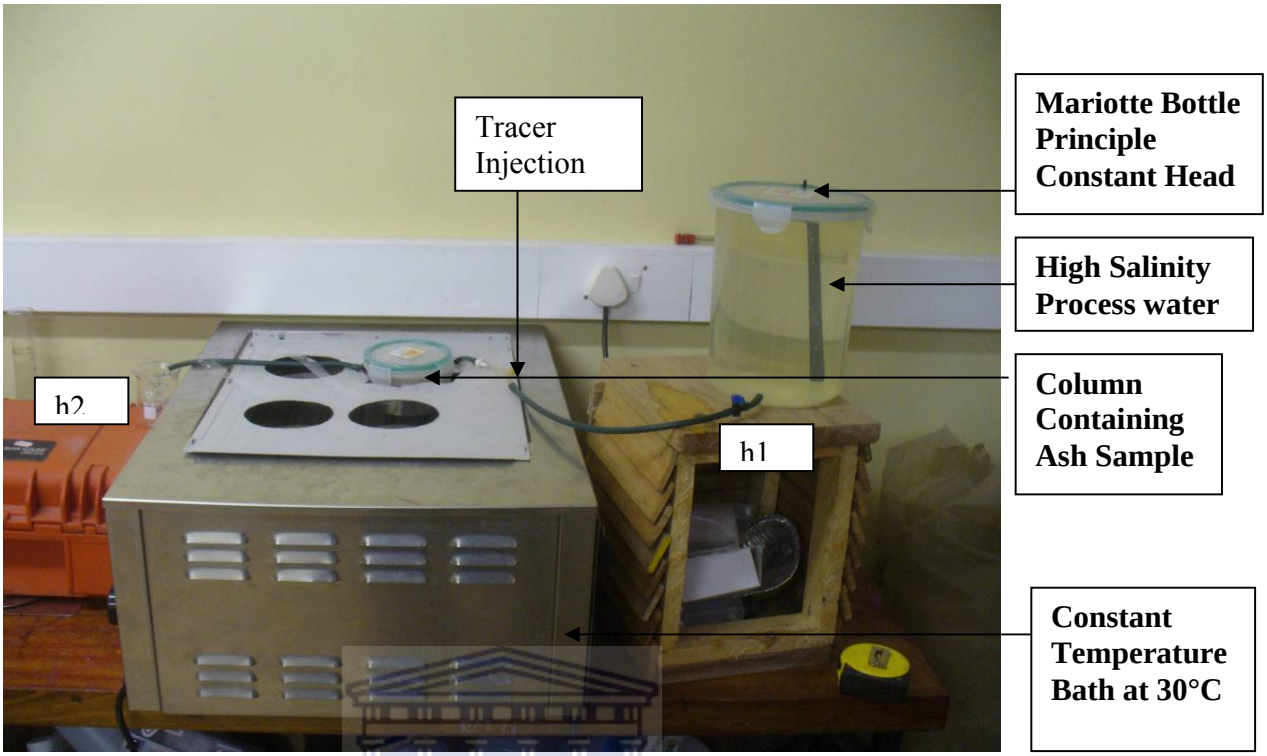

Figure 4.2 **Experimental setup testing column hydraulic properties under a constant temperature of 30ºC. Hydraulic head controlled using a mariotte bottle.**

4.2.3 Hydraulic Parameters Measured

Both outflow and inflow rates of the experiment are measured assuming that when rates are equal, the ash column reached saturation. Discharge was measured by collecting volumetric rates of flow at 5 minute intervals. The Darcy equation (Equation 2.2, section 2.5.1) was used to calculate the hydraulic conductivity measuring the different variables such as hydraulic gradient and area of the sample.

The discharge rate was divided by the area to obtain the Darcy flux over time (Equation 2.9, section 2.5.4. Samples for liquid density and viscosity (Figure 4.3) were analyzed, using Cannon constant temperature bath and Cannon Fenske tubes to obtain the various parameters for the permeability (Equation 2.3, section 2.5.1).

Figure 4.3 Viscosity and Liquid Density measurements performed under constant temperature of 30 degrees.

4.2.4 Adsorption Tests

Adsorption experiments were applied to identify a suitable conservative tracer for the tracer test experiments in the laboratory and field. Considering that 90% of the irrigated process water consists of NaCl it was therefore considered that the ash is already fully adsorbed by NaCl and that NaCl would be conservative when moving through the ash. The maximum adsorption capacity of the ash for NaCl, the maximum adsorption of NaCl on the ash and the affinity the NaCl has to be adsorbed by the ash were therefore assessed. These parameters would determine whether the NaCl would be an appropriate conservative tracer.

A solution of NaCl with a ratio of 50g of NaCl to 500L of water was prepared. Five containers were prepared by mixing 100mL NaCl solution with 10g of ash. All the containers were placed in a shaker where it was continuously shaken until it was removed at different intervals. The first sample was removed after one hour and consecutive samples at one hour intervals. Samples from the shaker were filtered through a 0.45 micron membrane filter paper. The filtering process was accelerated by using a vacuum pump to suck it through a filtering system. The samples were then collected in 60ml sample bottles and the electrical conductivity of the NaCl was measured. The electrical conductivity was measured as an indicator of the salt content in the sample. A linearized Lanqmuir adsorption isotherm was plotted to calculate the adsorption parameters.

4.2.5 Tracer Test

5g of NaCl was thoroughly mixed with 500ml of process water; 5ml of the solution was then injected into the tracer injection system at steady state conditions. The 5ml of NaCl tracer solution was primarily used to create a highly concentrated spike into the flow system to observe a breakthrough curve of the concentration injected.

The electrical conductivity was monitored over time at constant time intervals of 5 minutes. The electrical conductivity over time is plotted to establish a breakthrough curve of the tracer experiment. The tracer breakthrough curve travel time enables the interpretation of a tracer arrival time, to calculate the velocity of the salt tracer through the ash.

4.2.6 Hydraulic Data and Discussion

The comparison of inflow and outflow rates is shown for duplicate experiments (Figure 4.4 and Figure 4.5). Two flow conditions are identified on the graphs, namely steady and unsteady flow. The unsteady flow can be associated with the unsaturated nature of the ash at the initial stages of the experiment. As the saturation of the ash increases due to constant water inflow, steady flow conditions were eventually achieved after 268 minutes (experiment 1) and 345 minutes (experiment 2).

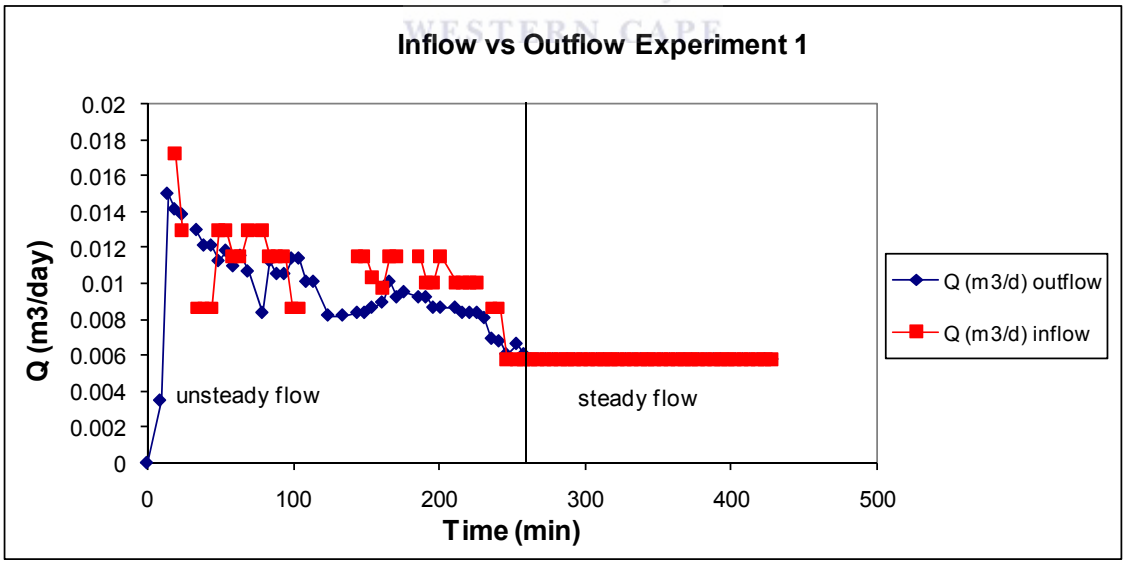

Figure 4.4 Unsteady flow and steady flow conditions identified during ash column experiment 1.

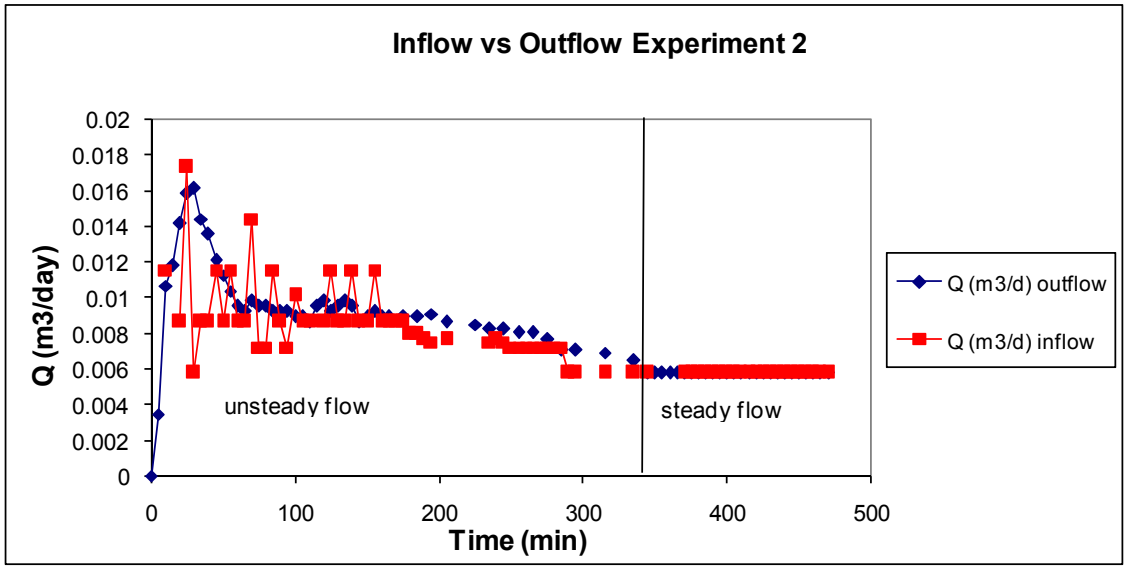

Figure 4.5 Unsteady flow and steady flow conditions identified at column experiment 2.

Hydraulic conductivity over time for the two experiments is presented in

Figure 4.6). An initial high hydraulic conductivity of between 1m/day to 2.6m/day was calculated for the up flow column experiments. Over time the hydraulic conductivities decreased and eventually reached steady state. The saturated hydraulic conductivity at a steady state for both experiments was calculated at 0.92 m/day. The high initial hydraulic conductivity at the initial stages of the experiment under saturated conditions can be as a result of pore scale movement of the process water trough the ash. During the initial stages of the experiment, the primary force of the water movement occurs as a result of the hydraulic head of the incoming water at the pore scale. As the process water moves timely trough the ash it possibly starts to bond with the minerals in the ash, reducing the hydraulic conductivity.

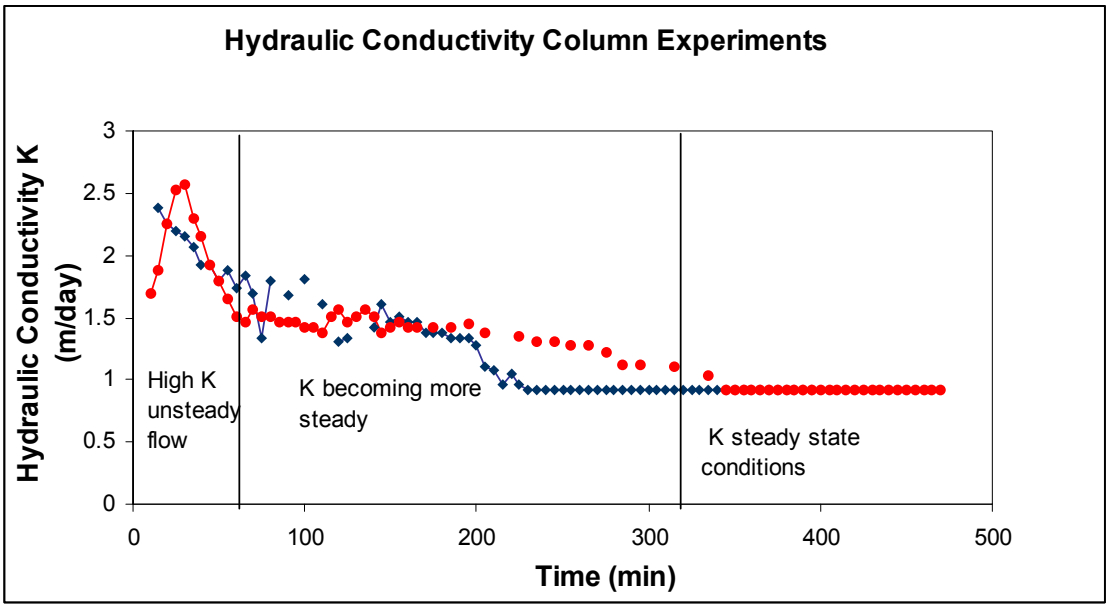

Figure 4.6 Saturated Hydraulic conductivity of column experiments.

The possibility of density driven flow was tested for the columns by measuring viscosity and liquid density. The permeability of the ash columns could therefore be calculated for different times during the experiment. The hydraulic conductivity is plotted against the permeability for the two experiments presented in (

Figure 4.7 and Figure 4.8). The trend of the permeability is similar to that of the hydraulic conductivity. High initial permeability values of between 0.17 m/day to 0.2 m/day were calculated during the permeability experiment. Over time steady state were achieved and a permeability of 0.09 m/day were calculated. It can therefore be concluded that density driven flow does not play a role in the column experiments

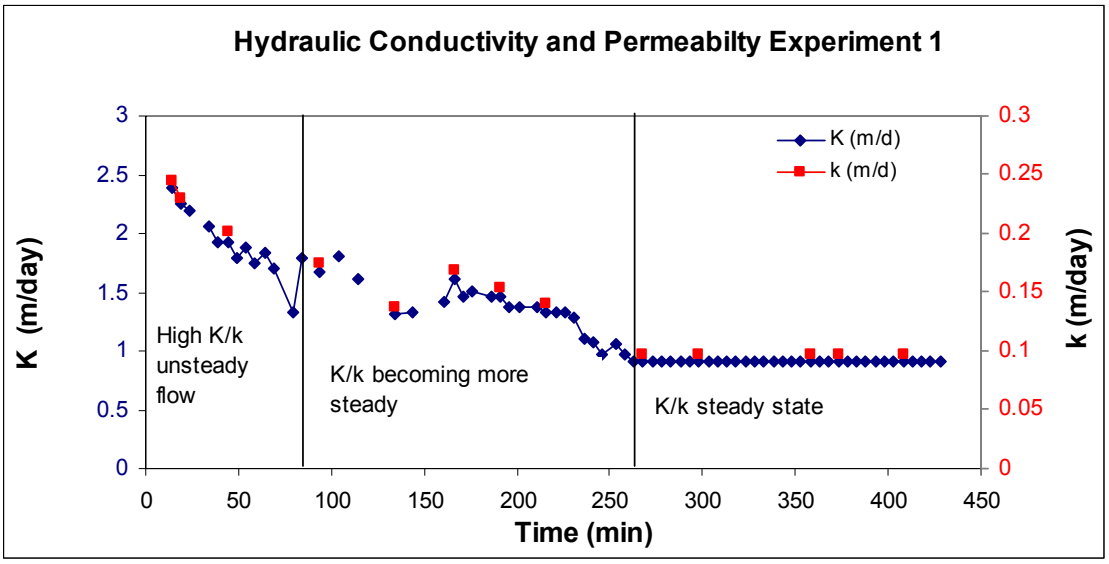

Figure 4.7 Hydraulic conductivity and permeability during column experiment 1.

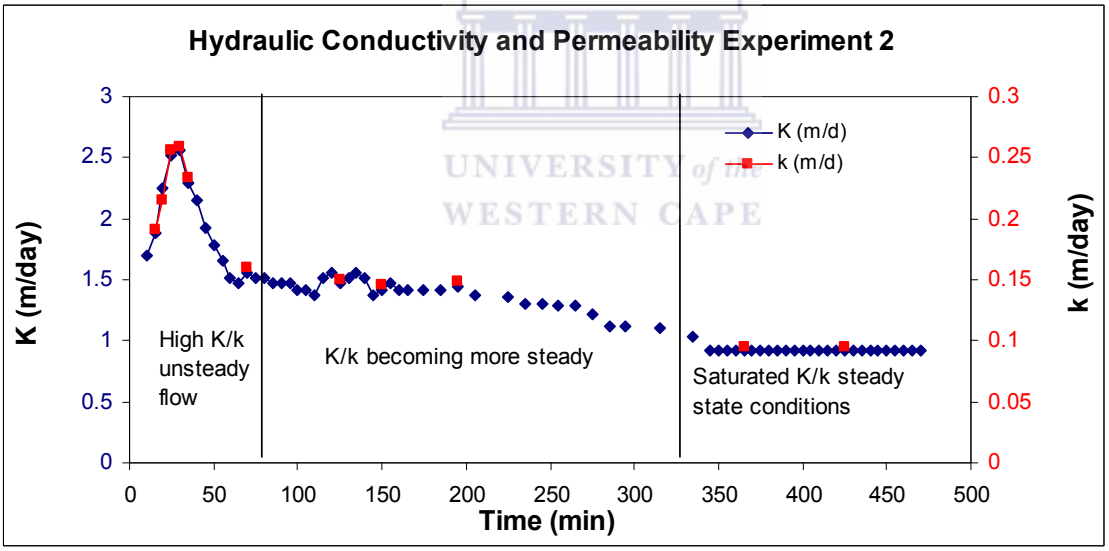

Figure 4.8 Hydraulic conductivity and permeability during column experiment 2.

4.2.7 Adsorption Data and Discussion|

The linearized Langmuir adsorption isotherm (Figure 4.9) displays calculated adsorption parameters of NaCl on the ash. The affinity (alpha) of the ash to adsorb the NaCl is calculated at 0.001L/mg. The intersection of the adsorption isotherm through the y-axis (Beta) is calculated at 0mg/kg, suggesting that NaCl is not being adsorbed. The maximum adsorption capacity of the ash for NaCl was calculated at 9.235mg/kg. The results suggest that NaCl is an excellent conservative tracer seeing that almost no adsorption takes place during interaction with ash.

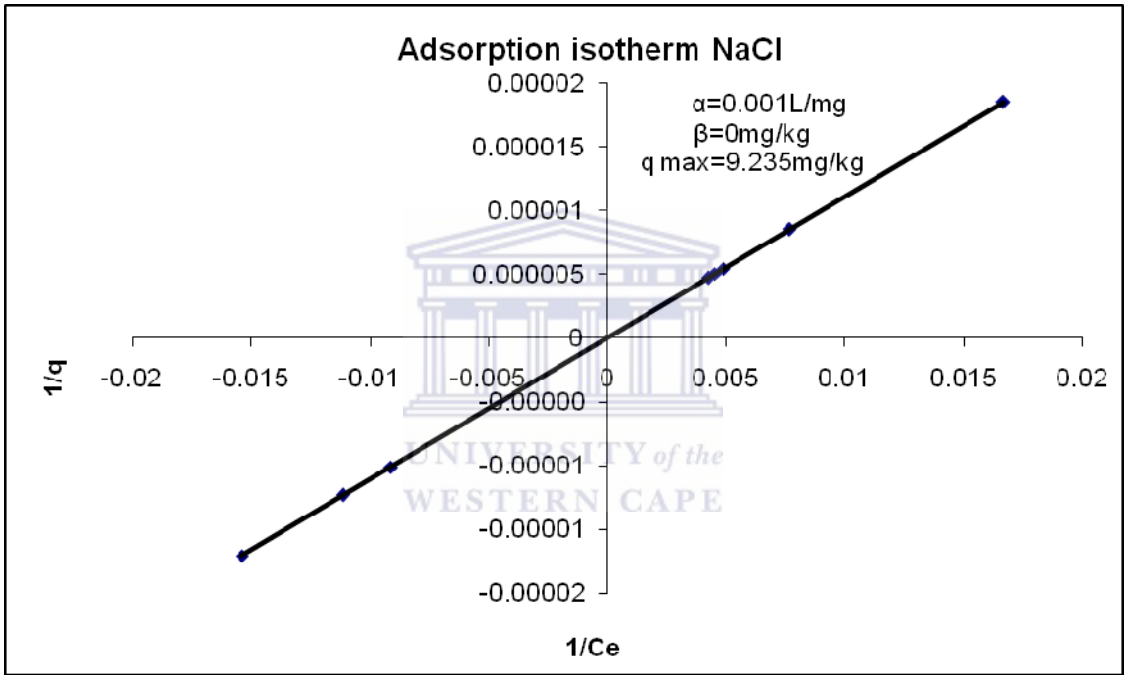

Figure 4.9 Langmuir adsorption isotherm displaying the adsorption behavior of the NaCl on the ash.

4.2.8 Transport Data and Discussion

The breakthrough curves for experiment 1 and experiment 2 display a long increase to a sharp peak with a long tail at the end that suggests a delayed tracer arrival time. The delayed tracer arrival was primarily caused by the uneven distribution of the tracer within the ash column. This means that while some of the tracer arrives at the outflow point, the other part of the tracer are still distributing within the column. The uneven distribution of the tracer results in a delay of the tracer arrival (Figure 4.10).

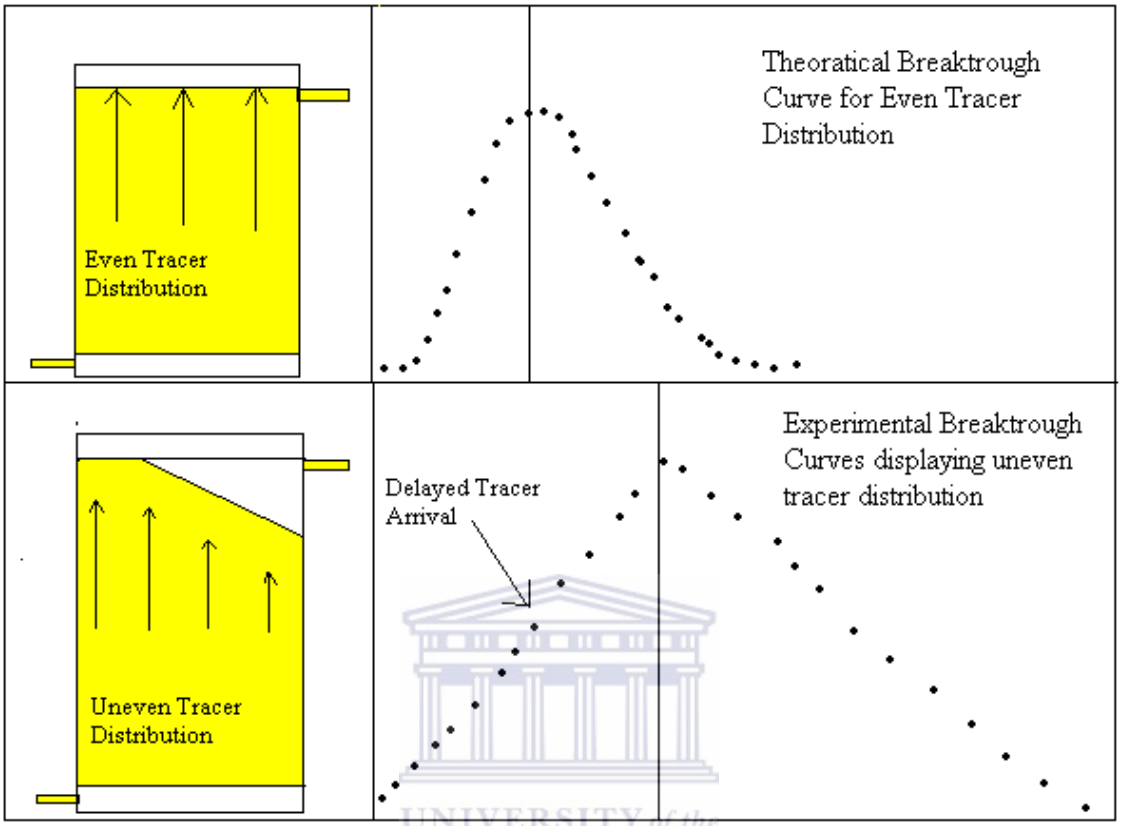

Figure 4.10 Theoretical breakthrough curve (Kass, 1998) for even distribution of a tracer through a medium. The tracer breakthrough curve is generally associated with a steep slope and smooth peak. The tracer experimental breakthrough curve of experiments 1 and 2 suggests an uneven distribution of tracer that delays the tracer arrival time.

It was therefore decided to take the first arrival time of the tracer to determine the velocity (Figure 4.11). The arrival time for the breakthrough curve was 15 minutes and from this information the velocity was calculated at 6.5m/day over a length 0.065m. The Darcy flux was calculated at 0.917m/day, from this information the effective porosity can be calculated using at 13% for the ash column.

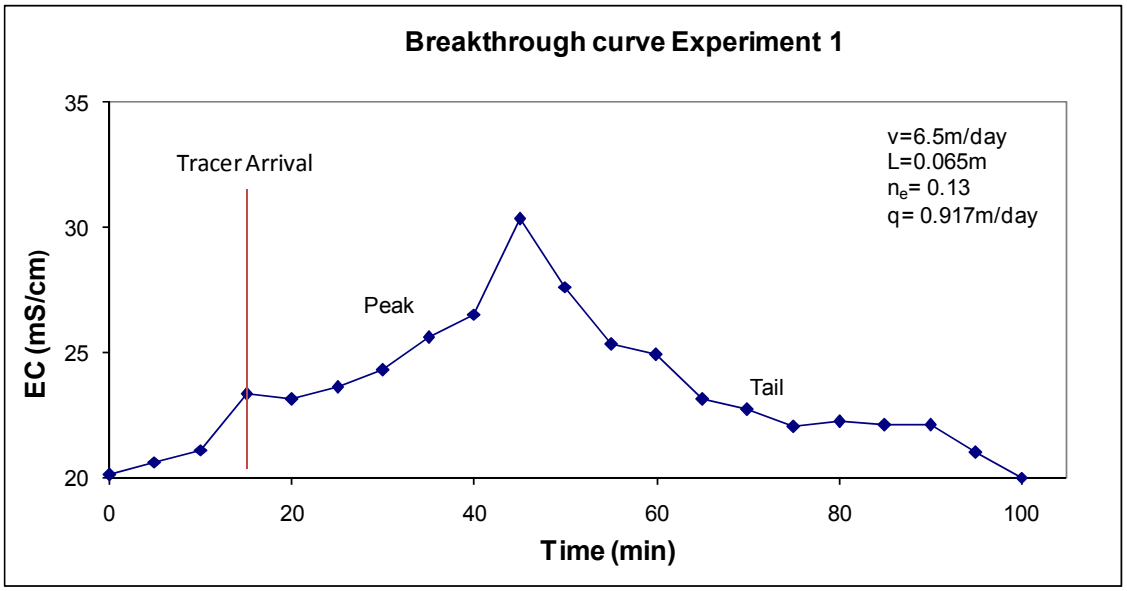

Figure 4.11 Tracer breakthrough curve showing the selected tracer arrival time at 15 minutes and calculated transport parameters.

Similar conditions of steady state were achieved in experiment 2 using NaCl as the tracer. The breakthrough curve display a similar pattern as experiment 1, long rise to sharp peak with a long tail. This can be accounted to the conditions explain previously (Figure 4.12). The arrival time for the tracer was 15 minutes and the velocity was calculated at 6.5m/day with Darcy flux of 0.917 m/day. Effective porosity was calculated using at 13% similar to experiment 1 (Figure 4.14).

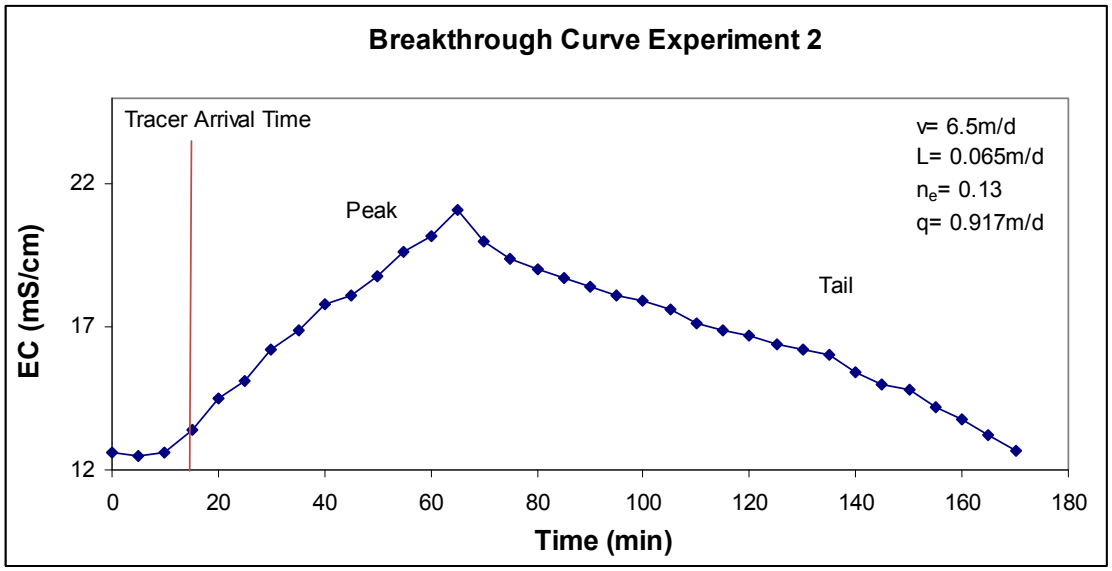

Figure 4.12 Tracer breakthrough curve experiment showing the selected tracer arrival at 15 minutes after injection of the tracer. The long peak is caused by a delay in tracer arrival time.

4.3 Ash Core

4.3.1 Sampling Positions

The laboratory experiments were conducted on the ash core to eliminate uncertainty regarding the packing method. Undisturbed ash core samples were obtained from different depths in the ash dump (Figure 4.13), using air flush coring. The core sample represents the physical properties of the ash in its field condition. Core samples were tested in the laboratory to estimate hydraulic and transport parameters.

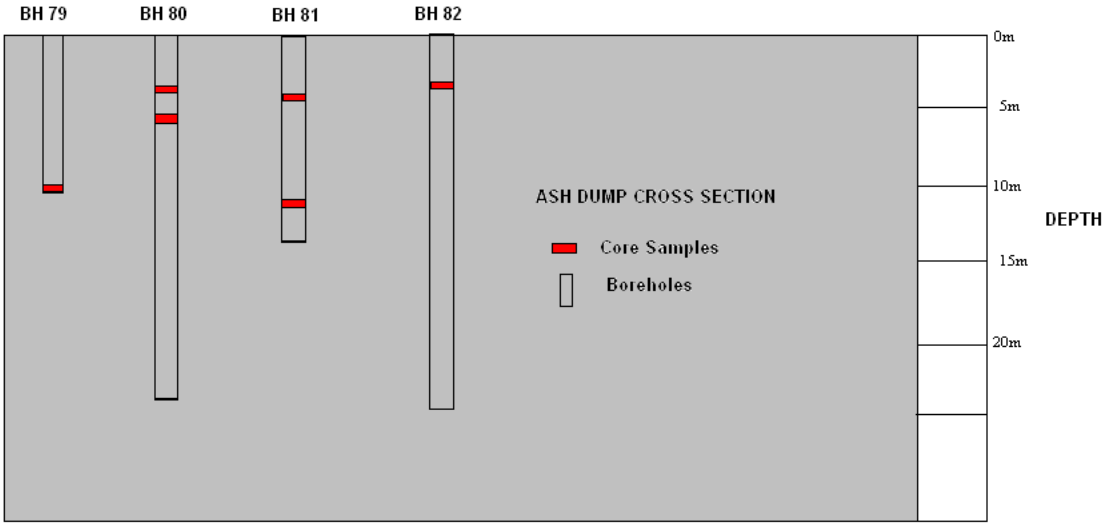

Figure 4.13 Cross sectional view of ash dump indicating the depth of the core samples assessed the laboratory.

4.3.2 Experimental setup

The ash core had to undergo waterproofing prior to predicting any hydraulic and transport parameters. This was completed by applying a double coat (1 mm) of concrete binder paint on the ash core, then a double coating (1mm) of roof water proof paint on to the ash cores. Both inflow and outflow ends of the ash cores were covered with galvanized steel caps. These steel caps were attached to the cores with the aid of expanding foam. It is essential to make the ash cores waterproof and to provide a strong capping both on the inflow and outflow points of the core so that no leaking of water occurs during the experiment (Figure 4.14).

The experimental setup was based on the same principles as Darcy's law whereby a constant head is provided by a pump and over flow setup. The water moves from the constant head (h1) to a lower head (h2) through the ash core (Figure 4.15).

Figure 4.14 Sample preparation of cores for laboratory hydraulic and tracer testing.

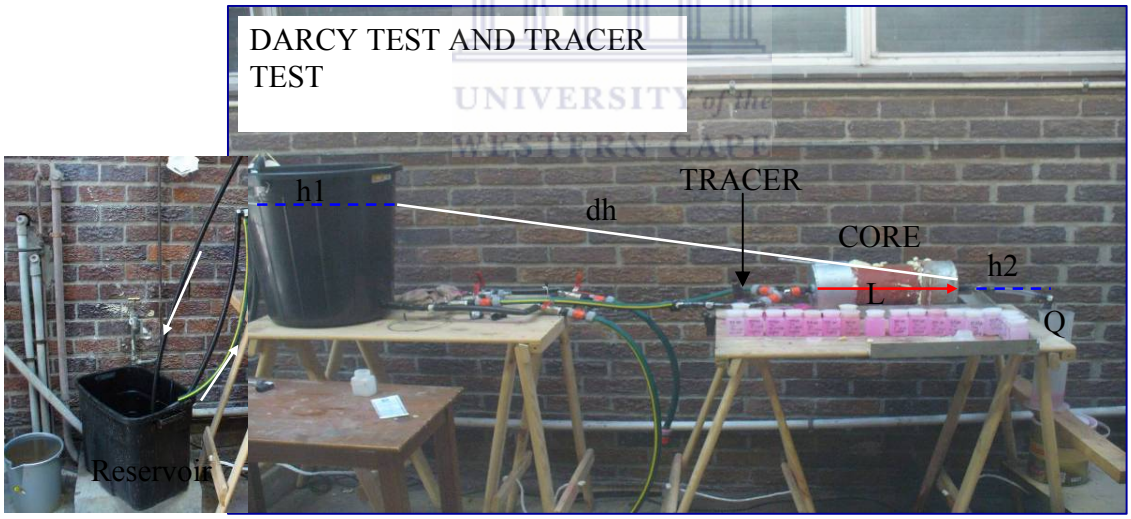

Figure 4.15 Experimental setup for constant head Darcy test on ash core. The tracer injection location is also indicated.

4.3.3 Methods

Full saturation levels for the core were assumed after a steady state was reached. Measurements of the water flowing through the ash core began as soon as the water started discharging from the outflow point (h2). The hydraulic conductivity was calculated using Darcy's law (Equation 2.2, Section 2.5.1)

Tracer testing was performed on the core ash by adding fluorescent dye and NaCl as a tracer into the system (Figure 4.16). Due to the high adsorption ability of the Fluorescent dye on the ash it was primarily used as a qualitative tracer to visually identify the tracer arrival. Tracer samples were collected from the outflow point and were visually interpreted by observing the different contrast in colors of the samples. Samples varied from light to dark resembling the different concentrations at a point in time (Figure 4.17).

Figure 4.16 Dye and NaCl Tracer injected into the tracer injected system, during steady state.

The NaCl was used to quantitatively calculate the parameters from the breakthrough curve. Fluorescent dye concentrate (5ml) and 10g of NaCl were dissolved in 50 ml of water, 10 ml of the tracer concentration was injected. This effectively gave an idea of the tracer arrival time through the ash that was used to calculate the velocity. With the velocity information, the effective porosity could be determined.

Figure 4.17 Qualitative display of tracer breakthrough, lighter colors are observed for the first sample and darker colures are observed with time.

4.3.4 Hydraulic Data and Discussion

The initial hydraulic conductivity for all the cores display high values and achieves a steady state over time, similar to the compacted ash columns due to the physical properties of the ash changing with water contact time (Figure 4.18).

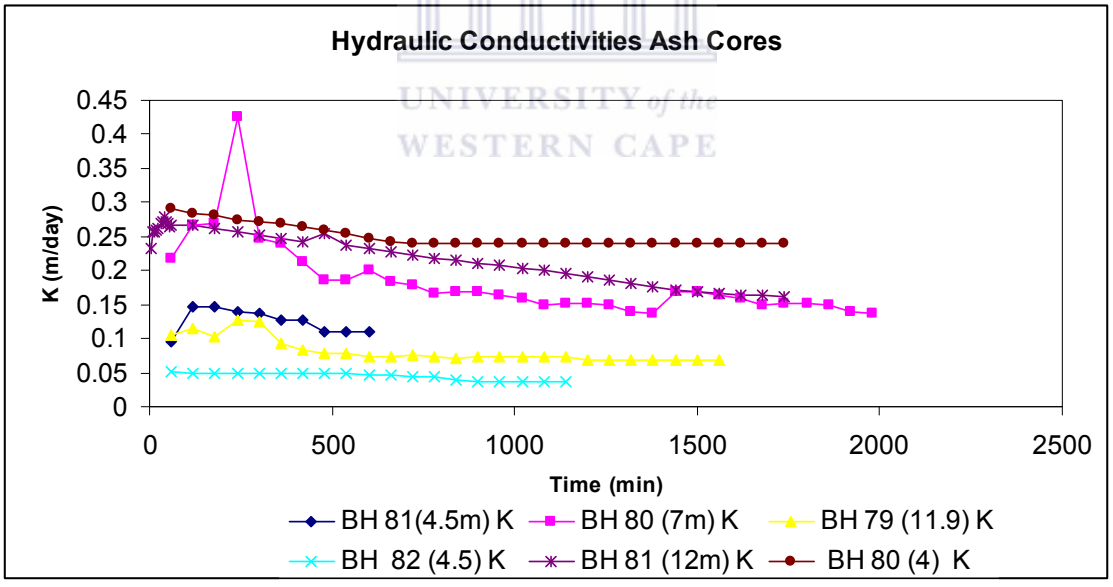

Figure 4.18 Hydraulic conductivity for different cores

The hydraulic conductivities calculated for the initial stages of the experiments ranged between 0.06 m/day and 0.4 m/day and can be accounted to the unsteady flow at the initial stages of the experiment. The hydraulic conductivities at steady state were calculated at minimum of 0.03, mean of 0.12 and a maximum of 0.16 m/day and can be accounted the saturation conditions due to constant water inflow. The hydraulic conductivity values is highly effected by the core texture, hence different ranges for the initial hydraulic conductivity and steady state hydraulic conductivities is obtained as represented in (Table 4.1).

Table 4.1 Hydraulic core texture vs. hydraulic conductivity over initial hydraulic conductivity and steady state hydraulic conductivity.

Core Name	Core Texture	Hydraulic K Initial peak (m/day)	Hydraulic K Steady State (m/day)
BH 81(4.5m)	Fine-Medium	0.15	0.11
BH 80 (7m)	Very Coarse	0.425	0.15
BH 79 (11.9m)	Medium	0.13	0.07
BH 82 (4.5m)	Fine	0.06	0.04
BH 81 (12m)	Coarse	0.27	0.16
BH 80 (4m)	Fine-medium	0.29	0.24

4.3.5 Transport Data and Discussion

The tracer test breakthrough curve for ash the core BH 81 displays a steep initial peak at the first half of the tracer breakthrough curve and a long tail in the second half of the tracer breakthrough curve (Figure 4.19).

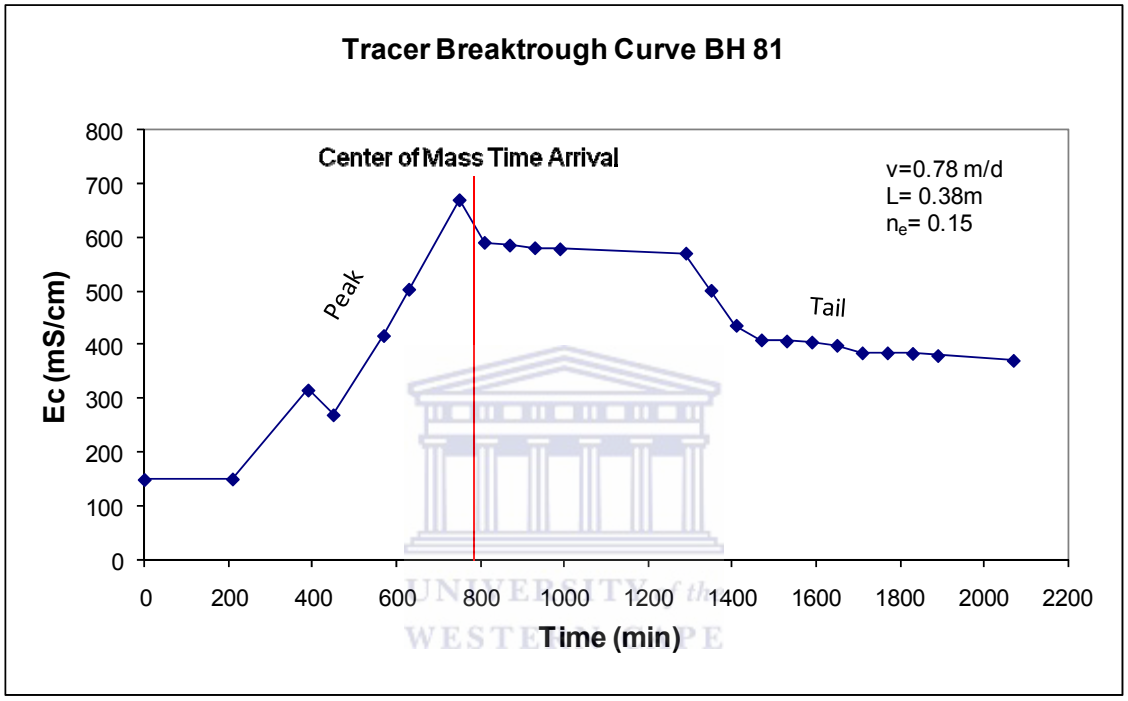

Figure 4.19 Tracer breakthrough curve BH 81, arrival time, breakthrough curve behavior and transport parameters displayed.

The center of mass arrival time for the breakthrough curve was calculated to be at 780 min. The velocity of the tracer breakthrough in the ash was then calculated at 0.78m/day through 0.38m core, using Equation 2.7 (Section 2.5.3). The Darcy flux was estimated at 0.12 m/day (Equation 2.8, section 2.5.3) from this the effective porosity were calculated at 0.15. The effective porosity of the tracer is only 15%.

4.3.6 Laboratory Component Summary

Laboratory experiments were performed on the ash to create conditions similar to that of the ash dump. Both ash column and ash core laboratory data provided quantitative and qualitative estimates of the flow and transport parameters. The ash column laboratory experiments provide excellent controlled conditions that can be used to describe the actual site conditions and also provided initial estimates of hydraulic and transport parameters.

Hydraulic conductivity values calculated for the column experiments ranged between a minimum of 1m/day to a maximum of 2.6 m/day for the unsteady flow conditions.
Hydraulic conductivity values calculated for steady state, saturated conditions were 0.92 m/day. The hydraulic conductivity of the column laboratory experiments suggest that an unsteady state is observed at the early stage of the experiment which than recovers to a steady state. Permeability experiments were performed to observe whether density driven flow contributed to the change in flow properties, this was however not the case as the permeability displayed a similar trend to that of the hydraulic conductivity. Permeability values calculated for the column experiments ranged between a minimum of 0.17 m/day and a maximum of 0.2 m/day for unsteady flow conditions. Permeability for calculated for steady flow and saturated conditions was 0.09 m/day.

The phenomenon of the high initial hydraulic conductivity and permeability at the initial stages can be explained by the duration of the contact time of the process water with the ash. During the initial stage of the experiment more flow paths are available for the process water to flow. As the ash becomes more saturated most of the flow paths are occupied leading to decrease leading to longer flow paths and therefore slower flow.
An uneven tracer distribution was observed in the laboratory tracer experiments displaying long rise, sharp peak and long tails of the break trough curve. This was however corrected and tracer arrival time and velocities were calculated. Darcian velocities were calculated at 0.9 m/day and the center of mass calculated velocities of 6.5 m/day for both the column experiments. The effective porosity was calculated at 13 % for both the column experiments.

The ash core experiments provided more undisturbed samples of the ash to assess the hydraulic conductivity in the laboratory. Hydraulic conductivity values calculated for the ash core

experiments range between a minimum of 0.06 m/day to a maximum of 0.4 m/day for the unsteady flow conditions. Hydraulic conductivity values calculated for steady state, saturated conditions range between 0.12 m/day to 0.16 m/day. The hydraulic properties of the column laboratory experiments suggest that the ash properties change over time as the process water moves through the ash. The hydraulic conductivity values are highly affected by the core texture, contact time with the process water, hence different ranges for the initial hydraulic conductivity and steady state hydraulic conductivities are observed.

Darcian velocities were calculated for only one core were 0.12 m/day and the center of mass calculated velocities of 0.78 m/day for both the column experiments. The effective porosity was calculated at 15 % for both the core experiment.

CHAPTER 5: ASH FIELD COMPONENT

5.1 Introduction

Hydraulic and tracer test experiments were conducted to assess the hydraulic and transport properties of the ash dump system on a field scale. Field experiments were conducted at the saturated part of the ash dump system and where most of the leaching of process water occurs. The physical environment (section 3.4) of the ash dump system indicated that saturated conditions and leaching of the process water occurs at the toe of the ash dump. It was therefore decided to perform the experiments at the toe of the ash dump and on the fractured Malmesbury aquifer representing the fractured aquifer underlying the ash dump.

Field methods applied on the ash dump included a slug test, single well dilution test and natural radial divergent tracer test. On the surrogate aquifer a forced gradient radial divergent tracer test was performed.

5.2 Ash Aquifer

5.2.1 Methods

Two duplicate experimental sites were developed at the toe of the ash dump for field experiments. Holes were hand augured to depths of 1.5m hereafter piezometers was installed. Piezometers were equipped with a 0.5m screen using a hacksaw and covering it with a filter sock (Figure 5.1). Each site had a total of seven piezometers that were installed at the same depths and distances from each other (Figure 5.2). Experiments were performed 24 hours after installation of the piezometers, to assess the natural flow and transport properties of the ash dump system.

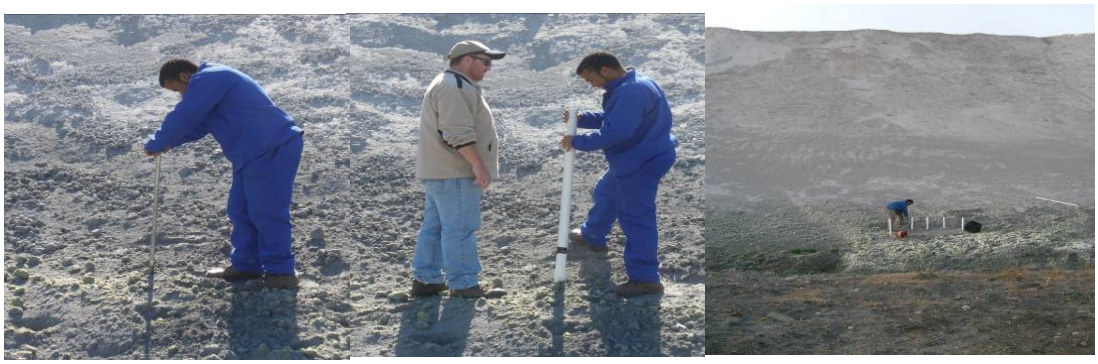

Figure 5.1 **Development of experimental site included installation of 7 boreholes each at the eastern edge of the ash dump.**

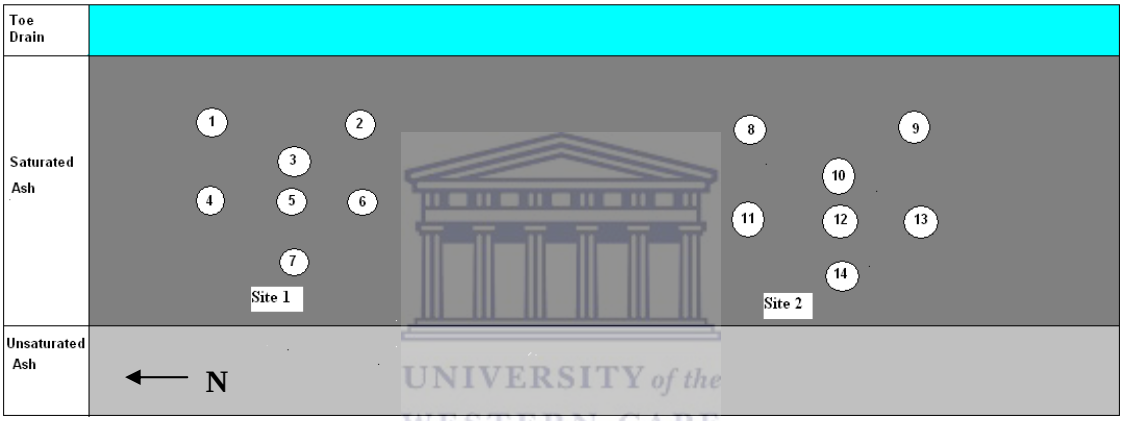

Figure 5.2 **Plan view of experimental site with the relative position of all the installed piezometers.**

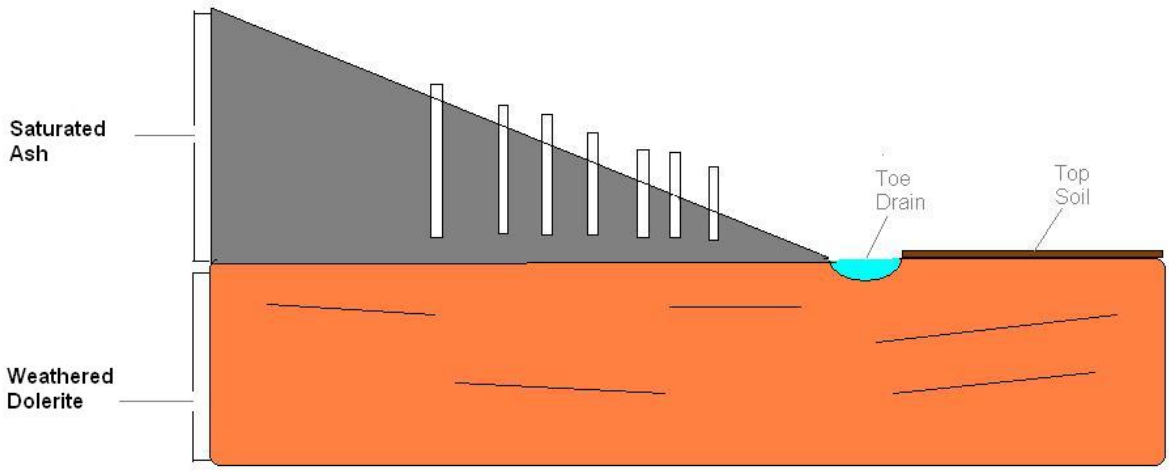

Figure 5.3 **Cross-section of the installed piezometers displaying the different physical mediums. The piezometers were installed at depths of 1.5m with screens of 0.5m. The piezometers were only installed in the saturated zone of the ash.**

Slug tests were performed by removing water through the use of a bailer from the piezometers to record the rise in water level to reach the initial water level. The water level recovery was measured by using an electrical contact meter. Measurements were taken at intervals of 30 seconds and increased to intervals of 60 seconds. The data was interpreted by using the Bouwer and Rice interpretation (Equation 2.10, Section 2.6.1) method that estimates hydraulic conductivity.

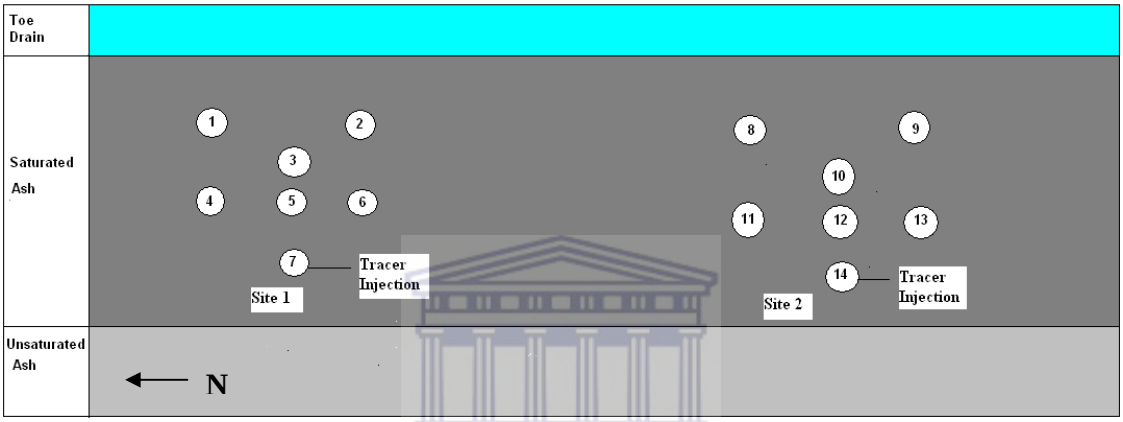

Figure 5.4 Plan view of tracer injection point for the tracer tests performed on the 2 sites.

Both natural gradient divergent and tracer dilution tests were performed on the two sites (Figure 5.5). Based on the hydraulic conductivity calculations it was decided to use TA 7 as a tracer injection borehole for site 1. The tracer dilution test was repeated at site two and it was decided to use TA 14 as a tracer injection borehole for site 2.

The procedure is as follows: 250g of salt is diluted into 500ml of water and injected over a time period of 5 minutes into the injection piezometer. The rate of tracer dilution in the injection piezometer is then measured over time in the screen zone with a Solinst TLC calibrated with standard calibration. The advective dilution of the tracer in the injection piezometers provides the platform for the Darcy velocity to be calculated (Equation 2.12, Section 2.8.2.).

The tracer dilution test served as the tracer injection point for the radial divergent tracer test. Observation piezometers were installed radially at 0.5m-1m away from the injection piezometer.

The radial spreading of the tracer away from the injection piezometers was monitored by electrical conductivity measurements at the observation piezometers. These measurements established whether the injection piezometers were connected with the observation piezometers. If the observation piezometers are well connected with the injection piezometers, a tracer breakthrough curve can be obtained from the observation piezometers to calculate the transport parameters and establish the transport behavior on the ash dump.

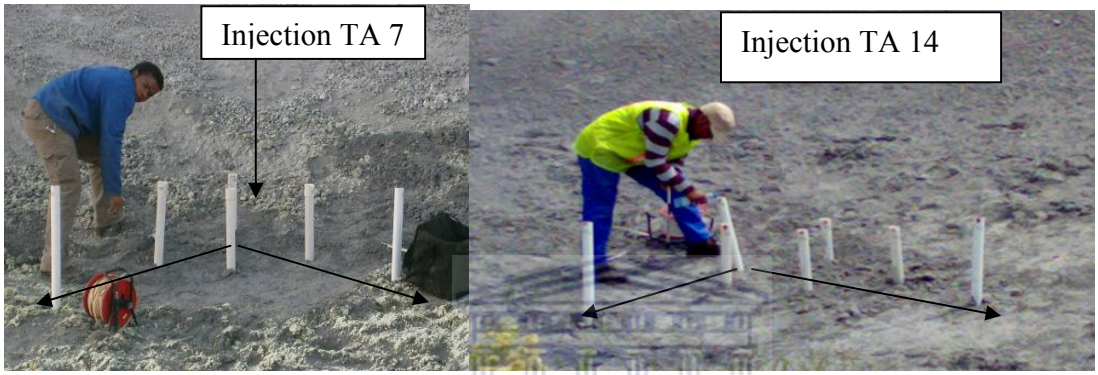

Figure 5.5 Injection of tracer for dilution and natural gradient radial divergent tracer test.

5.2.2 Hydraulic Data and Discussion

Hydraulic conductivity for site 1 and 2 for the different piezometers are displayed in (Figure 5.6 and Figure 5.7). Each piezometer is represented by a different colour that displays different hydraulic conductivity values.

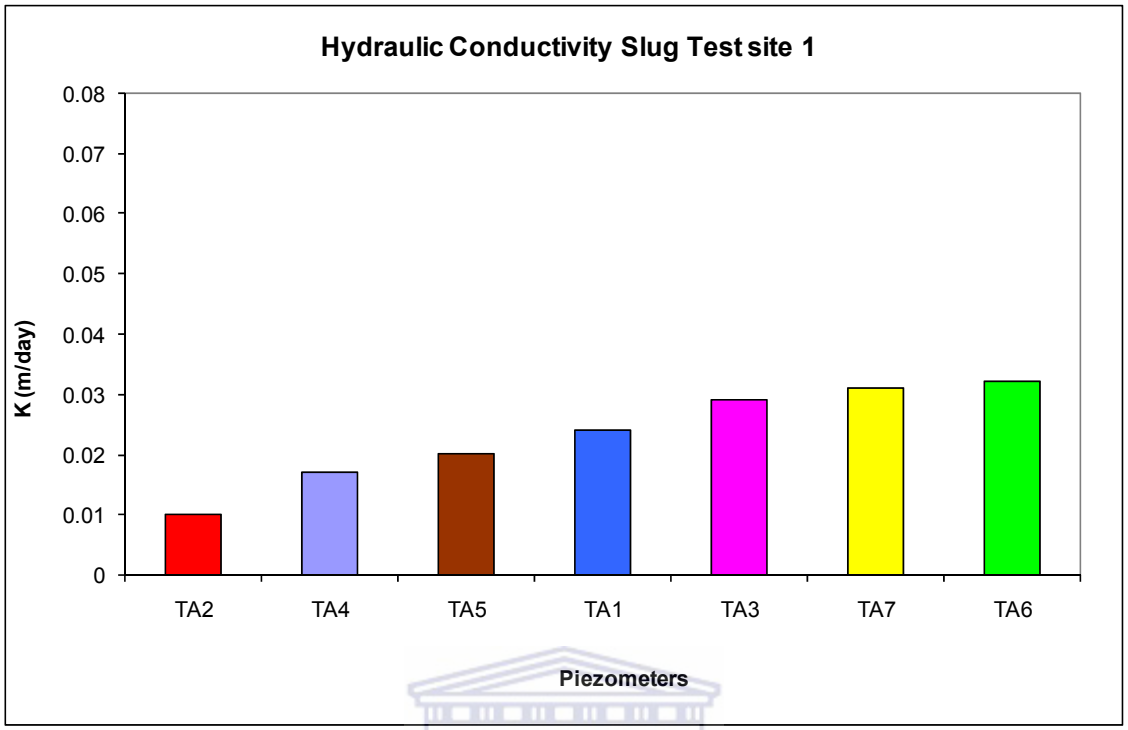

Figure 5.6 **Hydraulic conductivity for piezometers of site 1.**

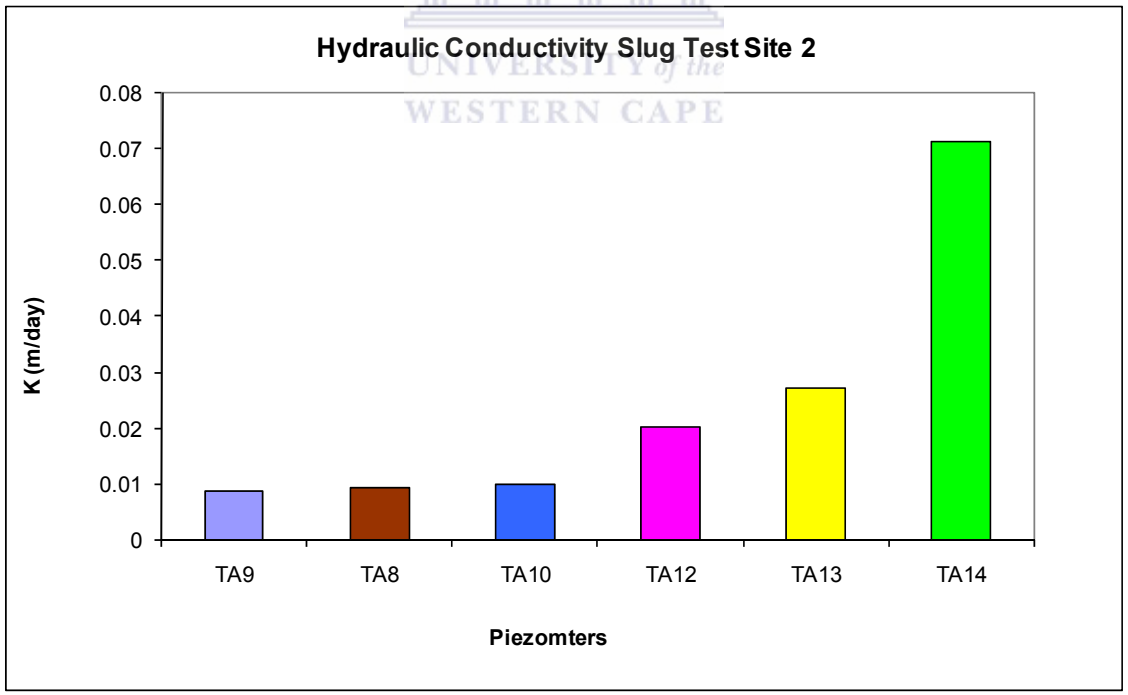

Figure 5.7 **Hydraulic conductivity of piezometers site 2.**

Hydraulic conductivity values ranges from a minimum of 0.008 a mean of 0.023 and a maximum of 0.071m/day at a thickness of 0.5m. The geometric mean of the hydraulic conductivities for both sites is 0.0245 m/day.

5.2.3 Transport Data and Discussion

The rate of tracer dilution over time for piezometer TA 7 is displayed in Figure 5.8. A straight line is fitted on the measured data to calculate the transport parameters. The rate of the tracer dilution for Site 1 yielded a Darcy flux of 0.06 m/day at a flow thickness of 0.5m under the natural flow conditions.

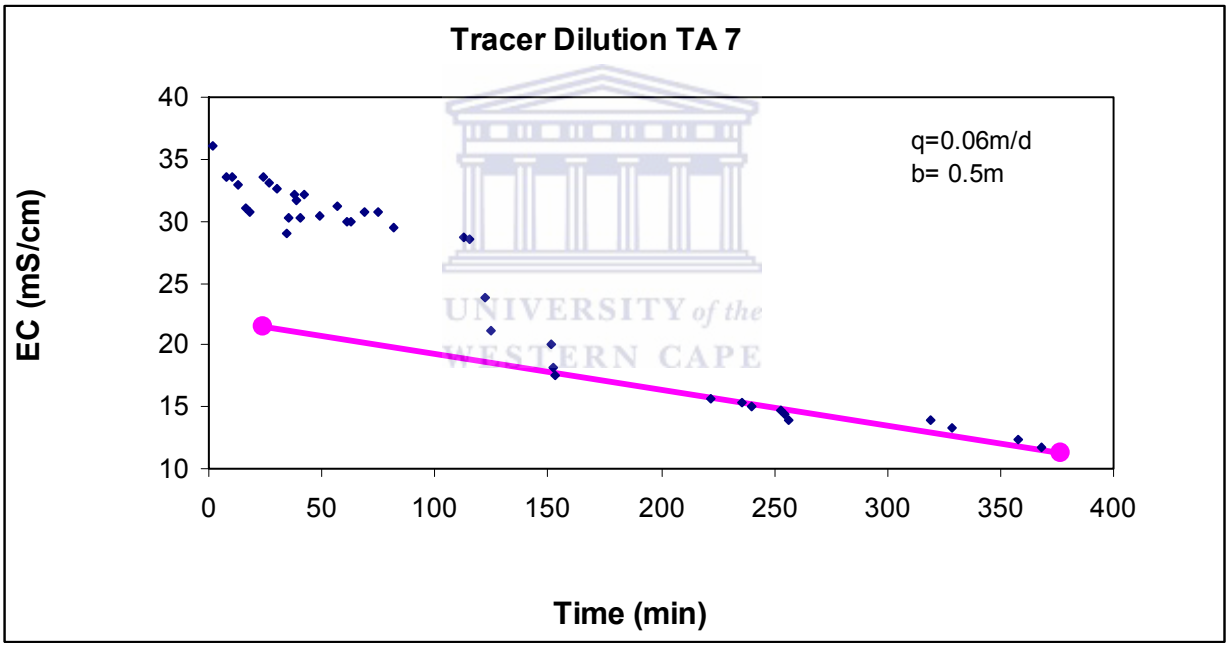

Figure 5.8 Tracer dilution data injected at piezometer TA 7

The rate of tracer dilution over time of piezometers TA 14 is displayed in Figure 5.9. The initial values are difficult to interpret caused by the fluctuation of the electrical conductivity. A sudden decline in the electrical conductivity is observed and could possibly be caused by a measurement error of the equipment. Therefore only the latter part of the graph - where the dilution rate is steadier – is interpreted. A straight line is fitted on the measured data to calculate the transport

parameters. The dilution rate of the tracer for site dilution yielded Darcy velocities of 0.10 m/day at a flow thickness of 0.5m Figure 5.9.

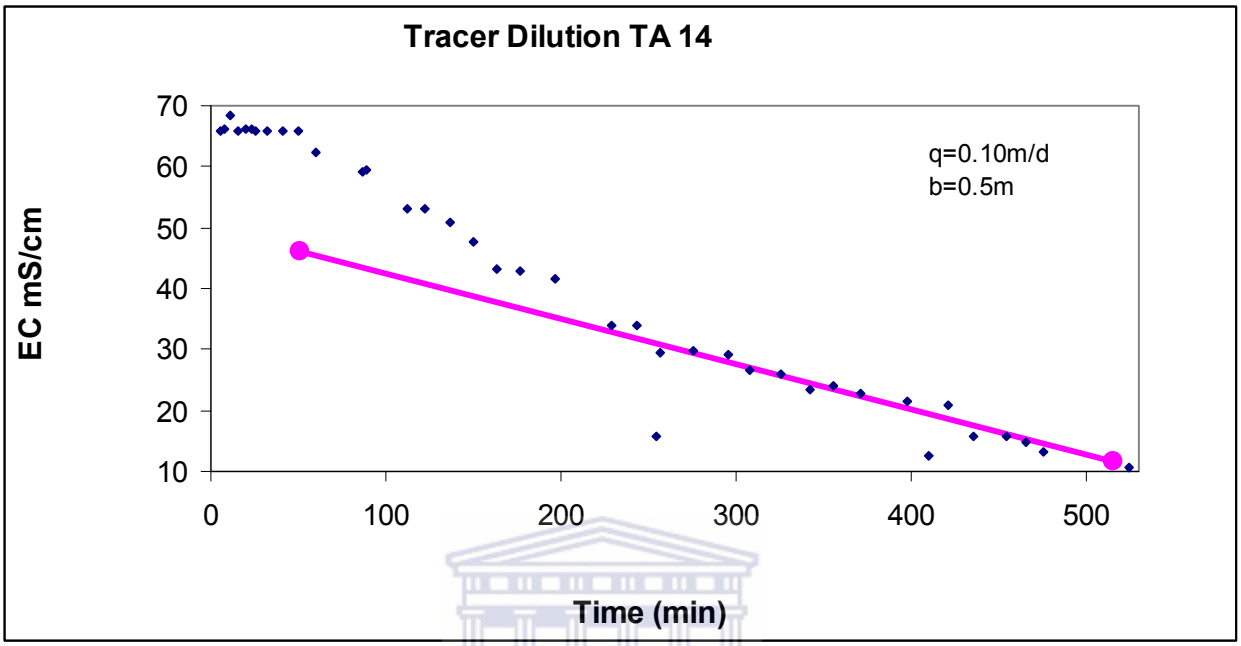

Figure 5.9 Tracer dilution data injected in piezometer TA 14.

Where the dilution is injected at the piezometers, the tracer followed the natural gradient flow path and was observed at the observation piezometers. The tracer breakthrough curve for observation piezometer TA 6 site 1 is displayed in Figure 5.10. The tracer breakthrough curve shows a bimodal shape, with a steep initial peak and long tail at the end. The center of mass of the tracer breakthrough curve was calculated for the breakthrough curve to establish the tracer velocity. Velocities and other transport parameters were also calculated using a breakthrough curve fit that is based on the advection dispersion equation (Equation 2.11, Section 2.6.5).

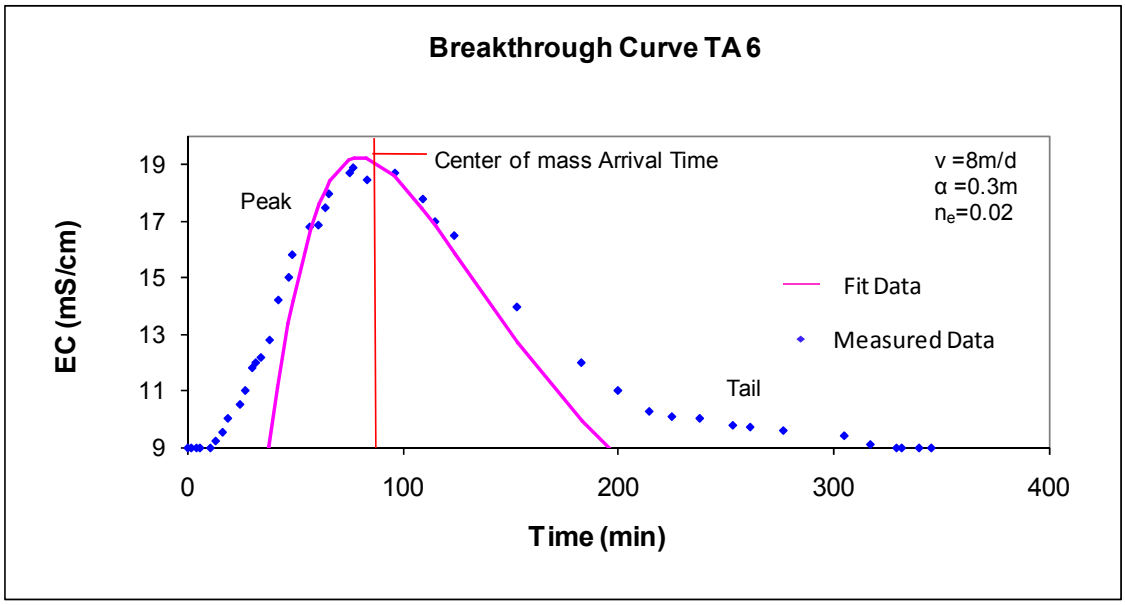

Figure 5.10 Breakthrough curve natural radial divergent test piezometer TA 6.

The center of mass for the tracer arrival time was calculated at 89 minutes and from this information the velocity was calculated at 8.3m/day using (equation 2.7, section 2.5.4) over a distance of 0.5m. The fitted curve was used to calculate a velocity of 8m/day at a flow thickness of 0.5m under the natural gradient and an effective porosity of 2%. The rate of dispersion of the tracer is calculated at 2.4m^2/day.

The tracer breakthrough curve for observation piezometers TA 13 site 2 is displayed in Figure 5.11. The tracer breakthrough curve also displays a bimodal shape, with a steep initial peak and long tail at the end.

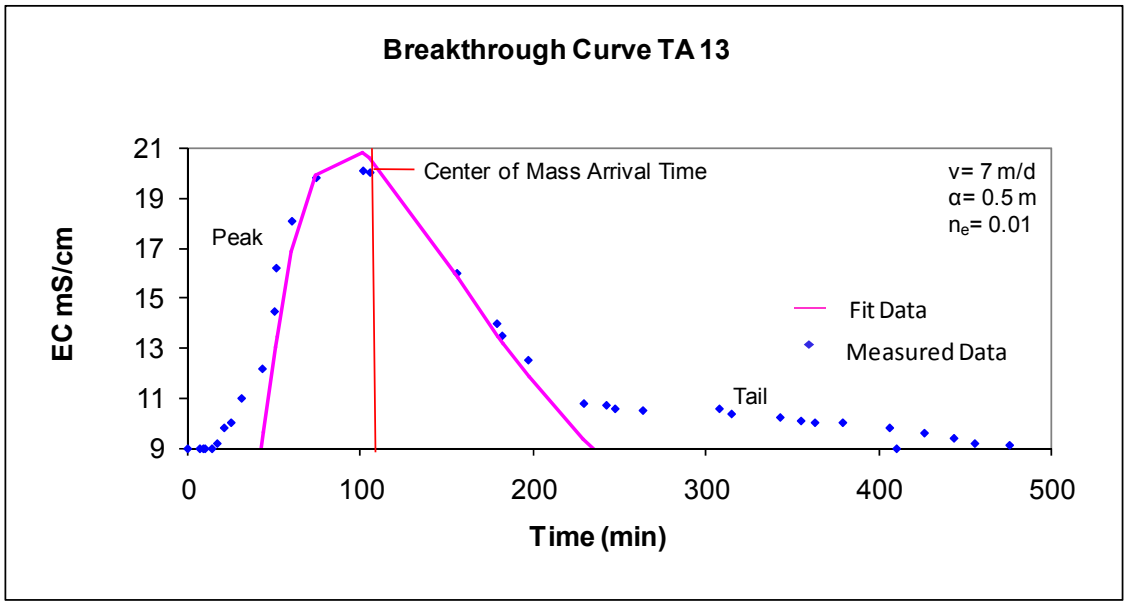

Figure 5.11 Breakthrough curve from natural gradient radial divergent tracer test TA 13.

The center of mass for the tracer arrival time was calculated at 103 minutes and from this information the velocity was calculated as 7.14m/day using (equation 2.7, section 2.5.4) over a distance of 0.5m. The fitted curve calculated velocities of 7m/day with a flow thickness of 0.5m under the natural flow gradient and effective porosity were calculated 0.01. The rate of dispersion of the tracer was calculated at 3.5m^2/day.

The initial steep peak in the first half of the tracer breakthrough curves can be accounted to advection of the tracer displacing water along the shorter flow paths. In the second half of the tracer breakthrough curve the peak starts to reduce resulting into a long tail. The tailing can possibly be as a result of the tracer spreading and moving along longer flow paths.

5.3 Surrogate Fractured Aquifer

The ash dump system, according to the physical environment, is underlain by a fractured aquifer. A surrogate approach was used to define the hydraulic and transport properties of another fractured aquifer. This was achieved by obtaining hydraulic and transport parameters of the Malmesbury fractured aquifer at the UWC research site (Figure 5.12). Two boreholes have been

drilled into the Malmesbury secondary aquifer and are situated 30m apart from each other. The boreholes were drilled at different depths of 80m (UWC 6) and 100m (UWC5), with screens of 12m deep for both boreholes. The major fracture zone are situated in the vicinity of the screen zones and this is where major flow and transport occurs

5.3.1 Methods

Both forced gradient radial divergent and tracer dilution test were performed on the surrogate aquifer (Figure 5.12). The tracer tests were performed by pumping UWC 6 at a rate of 0.8L/s until steady conditions were achieved. Hereafter 500g of NaCl and 100ug/l of Rhodamine was injected into UWC 5. The tracers were circulated consistently in the injection borehole between a depth of 105m and 93m to perform a tracer dilution test. The electrical conductivity was measured at a depth of 93m to observe the rate of tracer dilution over time (Figure 5.12). The concentrations were measured until the initial background of the aquifer concentration was achieved. The concentration of the tracer is plotted over time and a dilution curve can be obtained to calculate the transport parameters using Equation 2.12 (Section 2.6.5).

Rhodamine was sampled at the pumping borehole UWC 6, to perform the forced gradient radial divergent tracer test. The Rhodamine was sampled rather than the NaCl due to its low detection limit. The concentration of Rhodamine was plotted over time to obtain a tracer breakthrough curve. The flow velocity and transport parameters were calculated from the breakthrough using (Equation 2.10 Section 2.8.3.).

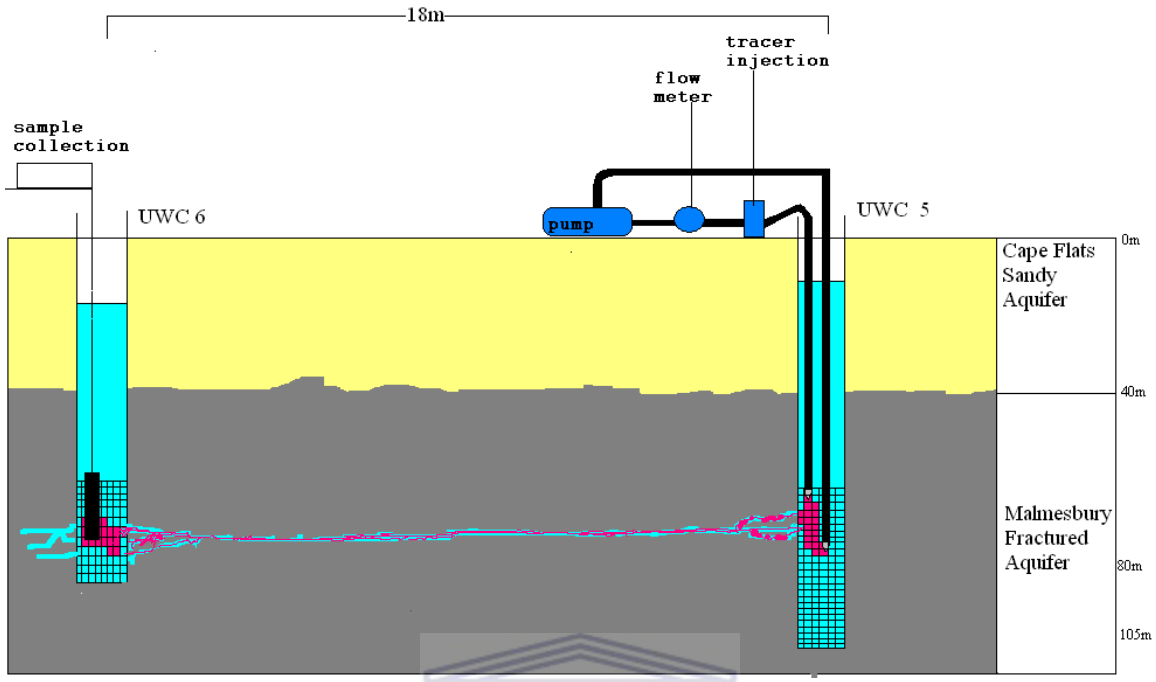

Figure 5.12 Experimental conceptual model for tracer test performed on the surrogate fractured aquifer.

5.3.2 Hydraulic Data and Discussion

During the tracer test a pumping test was also conducted and a Transmisivty of 20m/day was calculated. The transmisivity was multiplied by the thickness of the well and a hydraulic conductivity of 1m/day was calculated.

5.3.3 Transport Data and Discussion

The rate of tracer dilution over time of the injection borehole UWC 5 is displayed in Figure 5.13. The initial values are unsteady due to the injection; the data are therefore interpreted at the steady part of the graph where steady dilution conditions are present.

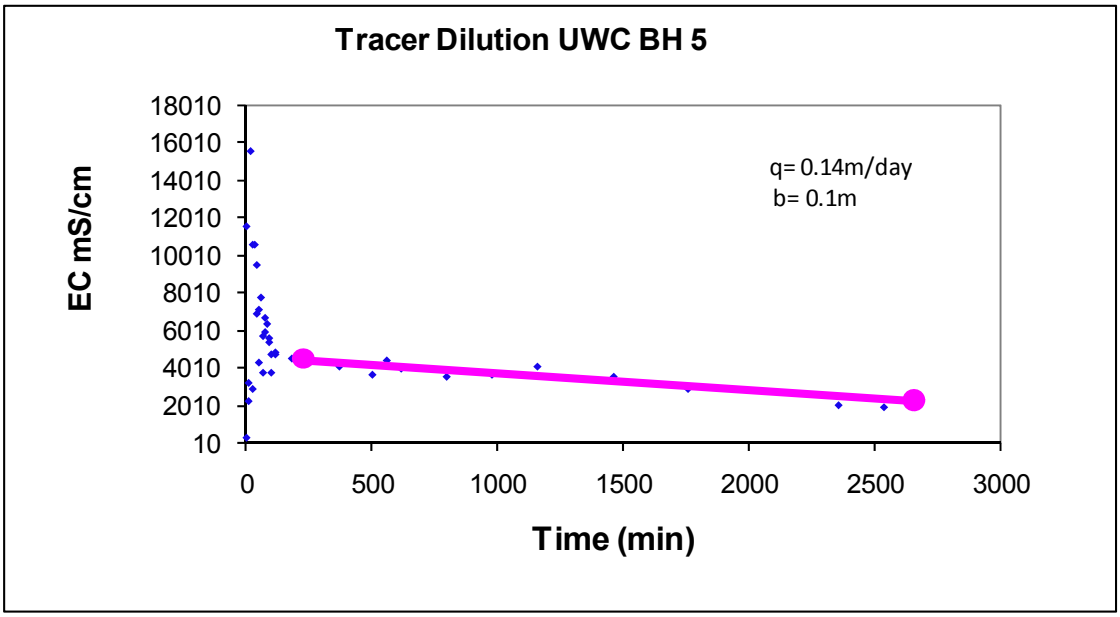

Figure 5.13 Tracer dilution curve for surrogate fractured aquifer of borehole 5.

A straight line was fitted on the measured data to calculate the transport parameters. The rate of the tracer dilution for UWC 5 resolved Darcy fluxes of 0.14 m/day at a fracture thickness 0.1m.

The tracer breakthrough curve for the pumping borehole UWC 6 is displayed in Figure 5.14. The tracer breakthrough curve displays a unimodal shape, with a fast initial peak and short tail at the end. The center of mass of the tracer breakthrough curve was calculated for the breakthrough curve to establish the tracer velocity. Velocities and other transport parameters were also calculated using a breakthrough curve fit that is based on the advection dispersion equation.

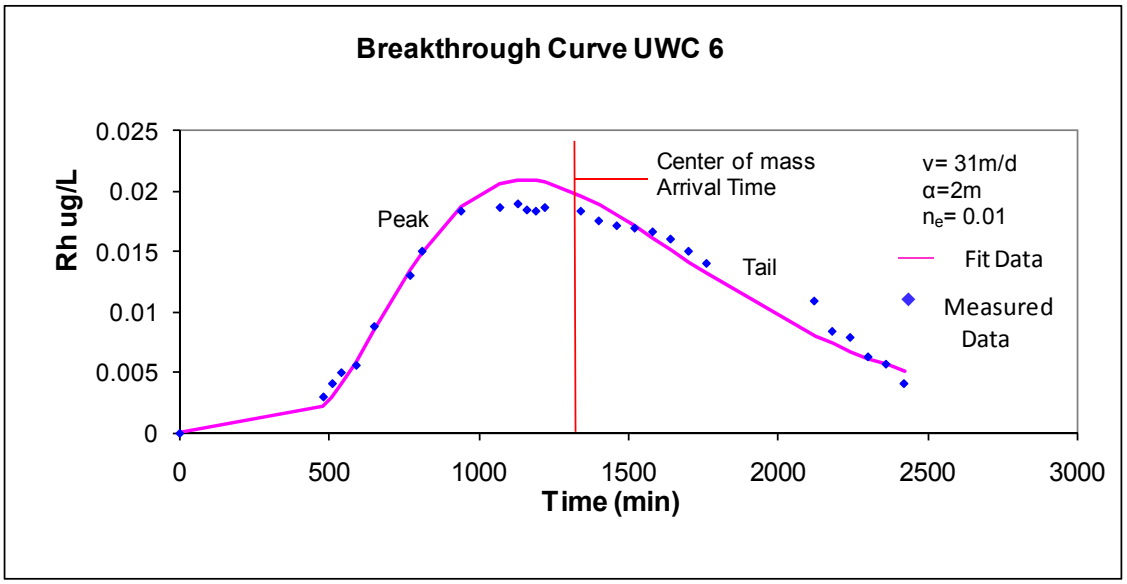

Figure 5.14 Breakthrough Curve surrogate fractured aquifer borehole 6.

The fast initial peak and short tail of the tracer breakthrough curve shows that the tracer moves rapidly through the fracture and is unaffected by dispersion. The center of mass arrival time for the breakthrough curve arrived at 1430 minutes the velocity was calculated at 29.9m/day. The velocities were also calculated using curve fit data, the curve fit data is based on the advection dispersion equation. Velocities were calculated at 31 m/d over a distance of 30m, at a flow thickness of 0.1m. Dispersivity was calculated at 2m and the effective porosity at 0.01 (Figure 5.14).

5.3.4 Ash Field Component Summary

Field experiments were conducted on the saturated part of the ash dump to obtain hydraulic and transport parameters. Field experiments were also performed on the surrogate Malmesbury aquifer to compare it with the underlying fractured aquifer at the actual ash dump system site.

Slug tests performed on the ash dump resulted in hydraulic conductivity values ranging between a minimum of 0.008, a mean of 0.023 and a maximum of 0.071m/day at a thickness of 0.5m. The geometric mean of the hydraulic conductivities for both sites is 0.0245 m/day at a thickness of 0.5m.

Tracer dilution test performed on TA7 and TA14 the ash dump calculated Darcian velocities to be 0.06m/day (site1) and 0.10m/day (site2). Breakthrough curves were obtained from the observation piezometers TA 6 and TA 13, situated in a south easterly direction from there injection piezometers. An increase in electrical conductivity was observed in the rest of the monitoring wells but not as prominent as TA6 (site 1) and TA 13(site2). Hence TA6 and TA13 were more connected to their injection piezometers.

The center of mass were calculated at 8.3m/day (site1) and 7.14m/day (site2), the modeled data fitted on a curve calculated velocities of 8m/day (site1) and 7m/day (site2) with dispersion rates of 0.3m^2/day and 0.5m^2/day. Effective porosities calculated for the ash ranged between 1-2%.

Breakthrough curves for the observation piezometers of both sites displayed a bimodal shape, suggesting a steep initial peak of the tracer with a long tail. The initial peak of the tracer breakthrough curve suggests that the initial movement of the tracer is through the shorter preferred pathways hence resulting in a shorter time span. The long tail of the tracer can be accounted dispersion of the tracer taking place over time and moving into longer preferred pathways. The longer preferred pathways can also allow desorption to take place due to the longer contact time of the tracer.

Darcian velocities were also calculated for the surrogate Malmesbury aquifer and velocities of 0.14m/day were obtained. The center of mass was calculated with velocities of 29.9m/day and the modeled data velocities of 31m/day. The effective porosity was calculated to be 1%. The tracer breakthrough curve displayed a short and fast initial peak and a short tail, suggesting that transport is mainly through the fractures and is unaffected by dispersion. Contamination from the ash dump would therefore occur rapidly through the fractured aquifer, once the leachate reached the bottom.

Darcian fluxes for the laboratory was more than a magnitude higher than the field calculated Darcian fluxes except for the core experiment that display values similar to that of the field. Velocities for the laboratory experiments were more than a magnitude lower than that of the field experiments, suggesting an underestimation of the velocities. The effective porosities were also more than a magnitude higher than that of the field calculated parameters.

The laboratory experiments were lightly over estimated or underestimated for both the hydraulic and transport properties compared to the field experiments. This could be due to the limiting conditions of the experiments performed in laboratory compared to the actual field conditions. The laboratory experiments still provide a good platform to perform field experiments.

CHAPTER 6: CONCEPTUAL MODEL AND MANAGEMENT

6.1 Introduction

This thesis developed a conceptual model for the ash dump system through data generated by numerous field and laboratory experiments. The physical environment is described based on literature review and research conducted during this study. Both laboratory and field experiments were conducted to estimate the hydraulic and transport properties under saturated flow conditions.

The site conceptual model predicts the flow and transport for the saturated ash dump system and the possible impact it might have on the underlying weathered dolerite aquifer. The conceptual model development for the ash dump system can now provide a platform to enhance site management of the ash dump system.

6.2 Physical Environment

Fly ash (10% moist) is deposited from a conveyer belt and serves as the main material for ash dump formation. The height of the ash dump ranges from between 26 to 30 meters high and are associated with steep slopes. The ash displays a fine to medium to coarse grain size and takes up silt to sandy appearance observed in ash cores.

The ash dump is underlain by a weathered dolerite aquifer (Figure 6.1). Patches of clay occur only in small amounts on the side of the ash dump. The clay patches are absent in the inner part of the ash dump because it is dug out for rehabilitation on top of the ash dump. The clay has no impact on the hydraulic and transport properties of the ash dump. Hence the ash dump and the weathered dolerite aquifer are directly connected.

Natural or fresh recharge occurs by natural precipitation primarily during the summer, whereas artificial or process water (90% NaCl) recharge via irrigation occurs on a daily basis. Irrigated process water infiltrates the ash dump system through the unsaturated ash (25m tick) and creates a saturated zone inside the ash dump of about 5m thick. The saturated zone contributes process water directly into the underlying weathered dolerite aquifer, or discharges out at the side of the ash dump. Some visible water and salts leaching from the dump is visible here. The ash dump system is surrounded by toe drains designed to capture the process water discharge.

6.3 Hydraulic Properties

The unsaturated part of the ash dump is heterogeneous and varies from fine ash to coarse grained ash this was observed in the core drilled ash. Process water percolates trough the unsaturated zone to the bottom of the ash dump where saturated conditions for the ash dump are established. The hydraulic conductivity of the saturated zone in the laboratory was calculated to between a minimum of 0.12 m/day, a mean of 0.34 m/day and a maximum of 0.92 m/day. The hydraulic conductivity in the saturated zone for the field experiments calculated a minimum of 0.008 m/day, a mean of 0.023 m/day and a maximum of 0.071 m/day.

The hydraulic properties are primarily controlled by the contact time of the process water with the ash. This is observed in the high initial hydraulic conductivities during the initial contact time and a decrease in hydraulic conductivity over time. The contact time of the process water with the ash in the field is much longer hence lower hydraulic conductivities are observed.

The surrogate fractured aquifer displays hydraulic conductivities of 1 m/day, higher than that of the ash dump.

6.4 Transport Properties

The flow paths on the ash dump are not all connected hence heterogeneity is observed on the ash dump. There are however flow paths that are connected and displayed effective porosities of between 1 and 2%. The average velocity for the process water trough the ash on a laboratory scale was calculated at a min of 0.12 and a maximum of 6.5m/day. The average velocity on the field scale was calculated at a min of 0.06m/day and a maximum of 0.1m/day. The flow velocity of the process water through the connected flow paths is between 7 and 8m /day (under natural hydraulic gradients). Transport occurs primarily through advection along both short and long flow paths. Transport along longer flow paths can result into desorption of the salts contained in the process water.

The groundwater velocity for the surrogate fractured aquifer display values of 31m/day with an effective porosity 1% under forced gradient conditions. The velocity for the underlying aquifer is therefore higher than that of the ash dump. The direct connection between the ash dump and the underlying aquifer suggest that seepage from the above process water would transport faster in the underlying aquifer.

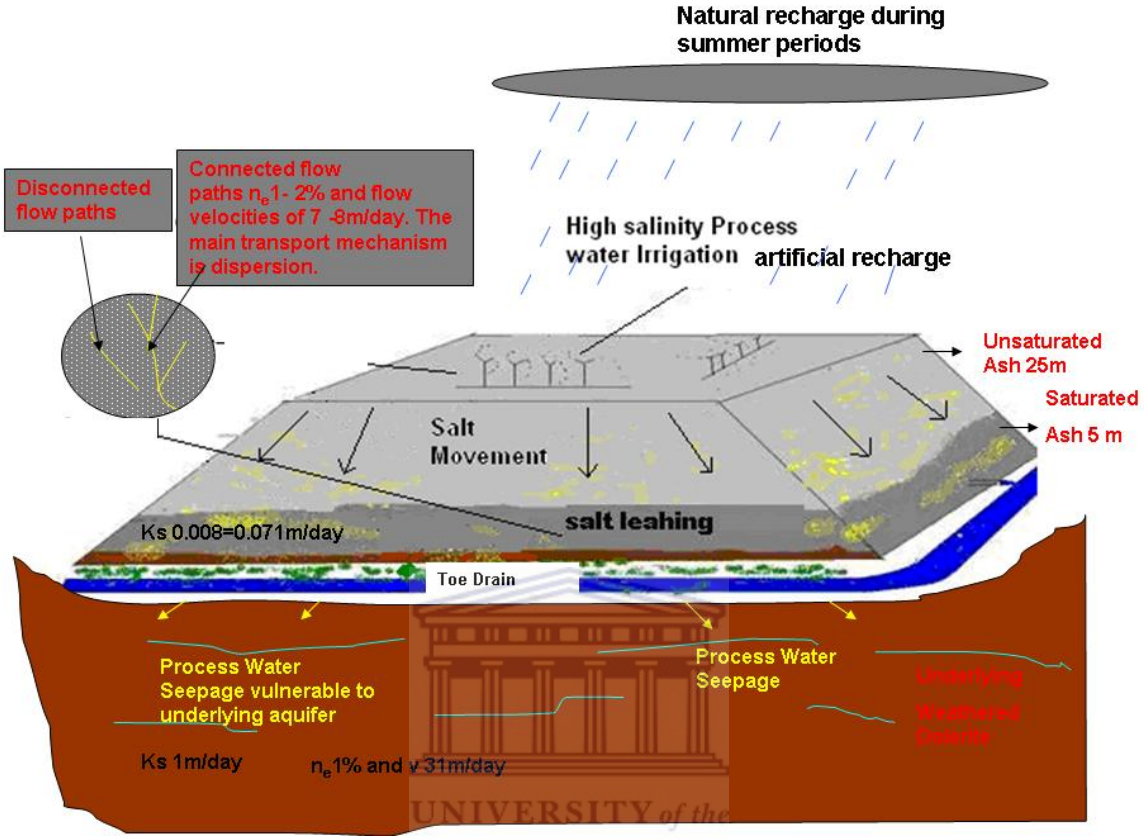

Figure 6.1 **Updated site conceptual model with parameters with calculated parameters. Distinct zones of flow such as unsaturated, saturated and underlying weathered dolerite. The process water transport is also visible in the updated conceptual model.**

Table 6.1 provides a summary of the calculated parameters for the conceptual model. The field hydraulic properties and transport measured display values a magnitude lower compared to the laboratory. Hence a slight over estimation of the hydraulic and transport properties was calculated in the laboratory.k

Table 6.1 Summary of calculated parameters of the conceptual model

Laboratory Experiments			
Ash Column Experiments		**Ash Core Experiments**	
K (m/day)	0.92	Kmin (m/day)	0.12
q (m/day)	6.5	Kmean(m/day)	0.14
v (m/day)	0.9	Kmax(m/day)	0.16
n_e (%)	13	q (m/day)	0.12
k	0.2	v (m/day)	0.78
		n_e (%)	15
Field Experiments			
Ash Slug Tests		**Ash Tracer Test**	
Kmin (m/day)	0.008	qmin (m/day)	0.06
Kavg (m/day)	0.023	qmax (m/day)	0.1
Kmax (m/day)	0.071	v min (m/day)	7
		v max(m/day)	8
		n_e (%) (min)	1
		n_e (%) (max)	2
		α(m^2/day)	0.3
Surrogate Pump Tests		**Surrogate Tracer Test**	
K (m/day)	1	q (m/day)	0.14
		v (m/day)	31
		n_e (%)	14
		α(m^2/day)	62

6.5 Benefit of Conceptual Model

The development of the conceptual model for the ash dump system has enhance the understanding of the hydraulic and transport properties of the process water trough the ash dump. It has been established that the ash dump has an unsaturated and saturated flow zones. The ash dump is directly connected to the underlying aquifer and the possibility exists of process water entering the underlying aquifer. The conceptual model shows that the hydraulic conductivities of the saturated as is dependent on the contact time of the ash with the process water and also the geology of the ash. It is therefore important to consider the management of the ash dump irrigation times.

The conceptual model has also made it clear that more information is required on some parts of the ash dump system that would further enhance the understanding and management of the ash dump system. The conceptual model has therefore optimized the monitoring of the ash dump system. (Figure 6.2) displays a diagram of newly proposed monitoring network that would further enhance the understanding and management of the ash dump system.

Monitoring of the surface and subsurface of the ash dump system (Figure 6.2) can be based on the conceptual model for the site. The monitoring on the surface should include water balance components by quantifying the high salinity process water irrigation input as well as the rainfall per annum. The toe drain of the ash dump can be sampled on a regular basis to contribute to the information from the outflow of the ash dump. Losses to the underlying aquifer can be estimated using Darcy's law and parameters obtained in this study.

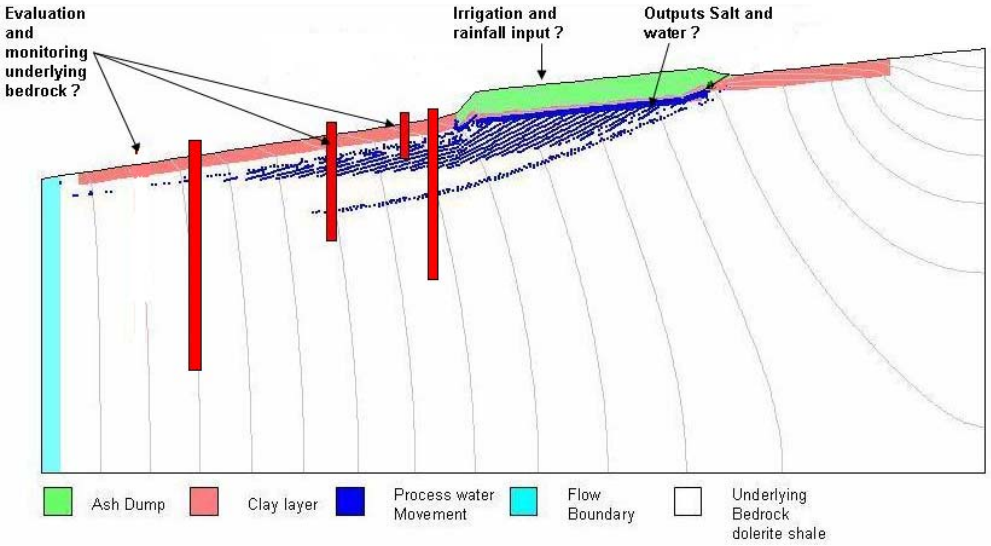

Figure 6.2 Monitoring network proposed for the ash dump system based on the information of the conceptual model one of the benefits of the conceptual model.

.

CHAPTER 7: CONCLUSIONS AND RECOMMENDATIONS

7.1 Conclusion

The burning of coal produces a large volume of ash that is disposed in the form of ash dump systems. In South Africa the hydraulic properties of ash dumps has been primarily studied for geotechnical purposes. The need to assess ash dumps from a hydrogeological perspective is therefore important to understand the high salinity process water movement through the ash dump and the possible impact it may have on the underlying aquifer. The main aim of this thesis was to establish the movement of process water trough the Tutuka ash dumps system, by developing a site conceptual model.

A thorough literature review has been completed on the components of a conceptual model and methods to investigate the components. According to the literature during the development of a conceptual model it is critical to understand the relevant components of the conceptual model. These components include the physical environment, hydraulic and transport properties that play a major role in the movement of high salinity process water through the ash dump. The appropriate investigative methods concerning the hydraulic and transport parameter estimation on both laboratory and field scale were summarized and established the platform for the laboratory and field experiments to be performed.

The physical environment of the ash dump has been described to provide an initial site conceptual model of the ash dump system. The initial site conceptual model suggested that the physical environment of the ash dump can be classified as an artificial environment. The ash dump system consists of three flow zones that of the unsaturated flow zone, saturated flow zone connected directly to a shallow underlying weathered dolerite aquifer

Both qualitative and quantitative hydraulic and transport methods have been applied in the study. The site description was based on previous studies, field observations, photos and sketches that were qualitative. The quantitative approaches were achieved by means of water level measurements, resistivity data, hydraulic and tracer test techniques. Hydraulic and transport methods was applied on both laboratory and field scale. The laboratory results included ash column and ash core experiments. Whereas the field experiments included slug test and tracer

test. Both hydraulic and transport properties were quantified for the ash dump system and surrogate aquifer.

The laboratory experiments for both ash column and ash core experiments exhibited unsteady and steady state hydraulic conductivities. High hydraulic conductivities is observed during the initial phase of both column and core experiments. This was proof not be caused by density driven flow suggested by the permeability results displaying similar values to that of the hydraulic conductivity. This is however explained by the contact time of the process water with ash (as observed in the experimental time frames of the column and core experiments) and the geology of the ash. The transport properties are more or less similar for both the core and column displaying effective porosities of more than 10%, with velocities of between 0.78m/day to 0.9m/day.

The field experiments conducted in the field displayed hydraulic conductivities with a magnitude difference between the different slug tests performed. The heterogeneity can therefore be observed on the ash dump. The hydraulic conductivity in the field was calculated to be lower than the laboratory experiments, this could be as a result of the longer contact time and higher moisture content of the field conditions. The transport properties suggest that not all of the flow paths on the ash dumps are connected. The flow path that is connected exhibit effective porosities of between 1% and 2 % with flow velocities of between 7m/day to 8m/day. The laboratory experiments were a slightly over estimated and underestimated for both the hydraulic and transport properties compared to the field experiments. This could be due to the limiting conditions of the experiments performed in laboratory compared to the actual field conditions.

Flow and transport within the surrogate bedrock aquifer display hydraulic conductivities and flow velocities higher than that of the saturated ash. The underlying shallow dolerite aquifer is therefore vulnerable to process water moving from the top of the dump into the aquifer.

The final updated ash dump conceptual model defines the ash dump system to be between 26m and thirty meters high. The ash dump system are exposed to different weather conditions straight trough the year. Both natural recharge (primarily during the summer) and artificial recharge (process water irrigation) occurs on the site. The ash dump system consist of three distinct flow zones that of an unsaturated , saturated and a weathered dolerite aquifer connected directly to the ash dump. The hydraulic properties of the ash dump are primarily controlled by the contact time

of the process water with the ash, moisture content of the ash and the geology of the ash. Not all the flow paths of the ash dump are connected and heterogeneity is observed on the ash dump. Some flow paths are however connected and display effective porosities less than 3%. Higher hydraulic conductivities of the underlying surrogate aquifer propose vulnerability of process water leaking.

The development of a site conceptual model enhanced the understanding of the flow and transport of the process water trough the ash dump. This also optimizes monitoring to enhance further understanding and management of the site.

7.2 Recommendations

It is recommended that a thorough understanding of the inflow and outflow of rain and process water is obtained to quantify the water balance and salt balance for the ash dump system. This will relate the flow and transport rates to actual volumes and would enhance the conceptual model.

. Laboratory experiments need to be conducted at longer time frames, to obtain the similar exposure time as the ash in the field.

The flow conceptualization of the ash dump system suggests that the underlying geology at the ash dump plays a significant role on the impact the saline water has on the underlying aquifer. It is therefore imperative to investigate the management of the clays and ash dump placement to evaluate the impact of the ash dump system. Evaluation of the physical properties, hydraulic properties and transport properties of the clay and geology are therefore recommended.

The installation of boreholes at different depths and different distances away from the ash dump system is recommended in the underlying aquifer based on the conceptualization of the contaminants leaching from the ash dump system.

CHAPTER 8: REFERENCES

ASTM D4874 95. (2006). Standard Test Method for Leaching Solid Material in a Column Apparatus.

Bear, J. (2008). *Modeling Groundwater Flow and Contaminant Transpor*t [electronic print] available at: http://www.cmdlet.com/demos/mgfc-course/mgfcaqtr.html [Accessed October 2009].

Boel, V., Audenaert K., De Schutter G., Heirman G., Vandewalle L., Desmet B. and Vantomme J. (2006). *Transport properties of self compacting concrete with limestone filler or fly ash*, Rilem.

Bouwer, H. (1978). *Groundwater Hydrology*, McGraw-Hill, New York.

Bouwer, H. and Rice, R.C. (1976). A slug test for determining hydraulic conductivity of unconfined aquifers with completely or partially penetrating wells. *Water Resources Research*, 12(3), pp 423-428.

Carter, M.R. and Gregorich, E.G. (2008). *Soil Sampling and Methods of Analysis*. 2nd ed. Danvers: Taylor and Francis Group.

Dann, R.L., Close, M.E., Pang, L., Flintoft, M.J., Hector., R.P. (2008). Complementary use of tracer and pumping tests to characterize a heterogeneous channelized aquifer system in New Zealand, *Hydrogeology Journal*, 16, pp 1177-1191.

Danquigny, C., Ackerer, P. and Carlier, J. (2004). Laboratory tracer tests on three-dimensional reconstructed heterogeneous porous media: *Journal of Hydrogeology*, 294, pp 196-212.

Darcy, H. (1856). *The Public Foundations of the City of Dijon*, Paris: Highways and Mines, Bookseller of the Imperial Corps of Bridges.

Davis, J.A., Coston, J.A., Kent, D.B., Hess, K.M., Joye, J.L., Brienen, P. and Campo, K.W. (2001). Multispicies Reactive Tracer in a Sand and Gravel Aquifer, Cape Cod, Massachusetts, *Environmental Protection Agency,* EPA/600/R-01/007b.

Domenico, P.A. and Swartz, F.W. (1998). *Physical and Chemical Hydrogeology*.2nd ed. New York: John Willey and Sons.

Eskom. (1993). Tutuka Ash Report. Eskom Internal Report.

Eskom.(2009) ESKOM Coal Power [electronic print] available at: www.eskom.co.za/live/content.php [Accessed November 2009].

Eskom. (2007). *Integrated Hydraulics Report for Tutuka and Secunda: Contribution to SASOL Eskom collaborative Project: Towards the Development of Sustainable Salt Sinks: Fundamental Studies on the Co-Disposal of Brines within Inland Ash Dams and Dumps*. Eskom Internal Report.

Fetter, C.W. (1994). Applied hydrogeology. 3rd ed. New Jersey: Prentice Hall.

Freeze, A.R and Cherry, J.A. (1979). *Groundwater.* Englewood: Prentice Hall.

Geo Hydro Technologies. (1998). *Brine irrigation and ash dump rehabilitation, Tutuka PowerStation. Report,* No. RVN143/195

Gierczak, R.F.D., Devlin, J.F. and Rudolph, D.L. (2005). Combined use of field and laboratory testing top predict flow paths in a heterogeneous aquifer, *Journal of Contaminant Hydrology*, 82, pp 75-98.

Goldscheider, N. (2008). A new quantitative interpretation of the long-tail and plateau-like breakthrough curves from tracer tests in the artesian karst aquifer of Stuttgart, Germany, *Hydrogeology Journal,* 16, pp 1311–1317.

Guven, O., Falta, R.W., Molz, F.J. and Mellville, J.G. (1985). Analysis and Interpretation Single Well Tracer Tests in Stratified Aquifers, *Water Resources Research*, 21(5), pp 676-684.

Hiscock, K. (2005). *Hydrogeology Principles and Practice*. Oxford: Blackwell Publishing.

Huang, K., Toride, N. and Van Genuchten, M.T.H. (1995). Experimental Investigation of solute Transport in Large, Homogeneous and Heterogeneous, Saturated Columns, *Transport in Porous Media*, 18, pp 283–302.

Irwin, N.C., Botz, M.M., and Greenkorn, R.A. (1996). Experimental investigation of characteristic length scale in periodic heterogeneous porous media. *Transport in Porous Media*, 25, pp 235–246.

James, J. and Butler, J.R. (1998). *The Design performance and analysis of slug Tests*. Florida: Lewis Publishers.

Johnson, M.R., Anhaeusser, C.R., Thomas, R.J. (2008). *The Geology of South Africa,* South Africa: Council for Geosciences.

Kass, W. (1998). *Tracing Technique in Geogydrology*. Rotterdam: A.A Balkema.

Khan, A.U.H. and Jury, W.A. (1990). A laboratory study of the dispersion scale effect in column outflow experiments, *Journal of Contaminant Hydrology*, 5, pp 119–131.

Klotz, D., Seiler, K.P., Moser, J. and Neumaier, F. (1980). Dispersivity and velocity relationship from laboratory and field experiments, *Journal of Hydrology,* 45, pp 169–184.

Konikow, L.F. (1996). Numerical Model of Groundwater Flow and Transport. Manual on Mathematical Models in Isotope Hydrogeology. *International Atomic Agency. Report.* IAEA TECDOC-910. Viena , pp 59-112.

Kostas, K., Georgios, .B. and Ioannis, P. (2005). *Hydraulic performance of laboratory PRBs for the decontamination of acidic mine waters*. International Mine Water Congress. September 5.

Kruseman, G.P. and De Ridder, N.A. (1994). *Analysis and Evaluation of Pumping Test Data* 2nd ed, Wageningen : International Institute for Land Reclamation and Improvement.

LeBlanc, D.R., Garabedian, S.P., Hess, K.M., Gelhar, L.W., Quadri, R.D., Stollenwerk., K.G., and Wood, W.W. (1991). Large-Scale Natural Gradient Tracer Test in Sand and Gravel, Cape Cod, Massachusetts 1. Experimental Design and Observed Tracer Movement, *Water Resources. Research*, 27(5), pp 895–910.

Leitão, T.E., Lobo-Ferreira., J.P. and Valochia. (1996). Application of a Reactive Transport Model for Interpreting Non -conservative Tracer Experiments, The Rio Maior Case-Study, *Journal of Contaminant Hydrology*, 24, pp 167-181.

Leitão, T.E., Smets, S., Van Beek, C. and Lobo-Ferreira, J.P.C. (2000). Risks of Contamination of Groundwater by Heavy Metals. Analysis of the Evolution of Contamination by Simulation in Laboratory Experiments. *Laboratório Nacional de Engenharia Civil*, Lisboa Final Report - GIAS/DH.

Maloszewski, P., and Zuber, A. (1993). Tracer experiments in fractured rocks: Matrix diffusion and the validity of models, *Water Resources. Research*, 29, pp 2723–2735.

Malozweski, P. and Zuber, A. (1990). *On the parameter estimation from Artificial Tracers Experiments, ModelCARE 90: Calibration and Reliability in Groundwater Modelling*: The Hague.

Mcworther, D.B. and Sunada, D.K. (1977). *Groundwater Hydraulics and Hydrology*, Colorado: Water Resource Publication.

Melby, J.T. (1989). A Comparison Study of Hydraulic Determination for a fine grained alluvium aquifer, Masters Thesis, Oklahoma: State University.

Monteith, J.L. (1985). Evaporation from land surfaces. In : Advances in Transpiration. Proc. of the National Conference of the ASAE, Chicago, ASAE Publications, pp 14-85.

O'Neill, M., Lombard, K., Onkin, B., Ulery, A. and Shukla, M. (2003). *Power Plant Combustion Byproducts for Improved Crop Productivity of Agricultural Soil*. Report 02-CBRS-W09. New Mexico, College of Agriculture and Home Economics, Navajo Agricultural Products Industry.

Pathan, S.M., Aylmore, L.A.G. and Colmer, T.D. (2002). Properties of Several Fly Ash Materials in Relation to Use as Soil Amendments, *Journal of Environmental Quality*, 32, pp 687-693.

Rashidi, M., Peurrung, L., Tompson, A.F.B. and Kulp, T.J. (1996). Experimental analysis of pore-scale flow and transport in porous media, *Advances in Water Resources,* 19, pp 163–180.

Rieman, K., van Tonder, G., Dzanga,P. (2002). Interpretation of single-well tracer tests using fractional-flow dimensions. Part 2: A case study, *Hydrogeology Journal*, 10, pp 357-367.

Rushton, K.R. (2003). *Groundwater Hydrology Conceptual and Computational Models*, Chichester: John Wiley & Sons Inc.

Sauty, J-P. (1980). An analysis of hydrodispersive transfer in aquifers. *Water Resources Research* 16(1), pp 145–158.

Shapiro, A.M. (2001). Effective matrix diffusion in kilometer-scale transport in fractured crystalline rock, *Water Resources Research*, 37, pp 507–522.

Sivapullaiah, P.V. and Laksmikamtha, H, (2004). Properties of Fly Ash as Hydraulic Barrier, *Soil and Sediment Contamination*, 13, pp 489-504.

Sternberg, S.P.K., Cushman, J.H. and Greenkorn, R.A. (1996). Laboratory observation of non-local dispersion. *Transport in Porous Media,* 23, pp 135–151.

Stevens, B. (1996). *Vadoze Zone Hydrology*, Florida: Lewis Publishers.

Stevens, B., Hsu, K., Prieskat, M.A., Akeney, M.D., Blandford, N., Roth, T.L., Kelsey., J.L. and Withworth., J.R. (1998). A Comparison of Estimated and Calculated Effective Porosity, *Hydrogeology Journal*, (6), pp 156-165.

Summers, S.K. (1983). *The hydraulic properties of the Pierre Shale: A Comparison of methods:* Private Distribution.

Taha, M.R. and Debnath, D.K. (1999). Interaction of cyanide with residual soil and kaolinite in batch adsorption tests. *Insitutitute of Engineering Malaysia* 60(3):pp 49–57.

Van Wyk. B., de Lange.F., Xu. Y., Van Tonder. G. and Chiang.W.H. (2001). *Utilization of Tracer Experiments for the Development of Rural Water Supply management Strategies for Secondary Aquifers,* Water Research Commission, No. 733/1/01.

Vandenbohede, A. and Lebbe, L. (2005). Double forced gradient test: Performance and interpretation of a field test using a new solute model*, Journal of Hydrology*, 317, pp 155-170.

Veith, J.A, Sposito G. (1977). On the use of the Langmuir equation in the interpretation of adsorption phenomena. *Soil Science Society of America* 41, pp 697–702

Viterito, A. (1987). The Köppen climate classification system, *Weatherwise*, 40(3), pp. 160-161.

Watson, S.J., Barry, D.A., Schotting. R.J. and Hassanizadeh, S.M. (2002). On the validity of Darcy's law for stable high concentration displacements in granular porous media. *Transport in Porous Media*, 47(2), pp 149–167.

Wolkersdofer C.H. & Hasche, A. (2001). Tracer Test in the abandoned Fluorspar Mine Straberg Harz Mountains, Germany, *Wissenschaftliche Mitteilungen*, (16): pp 57—67.

Xu, Y., Van Tonder, G.J., Van Wyk, B., Van Wyk, E.and Aleobua, B.O.Y. (1997). Borehole dilution experiment in a Karoo aquifer in Bloemfontein. *WaterSA*, 23 (2), pp. 141.

Yang, Y.S., Lin, X.Y., Elliot, T. and Kalin, R.M. (2001**).** A natural gradient field tracer test for evaluation of pollutant transport parameters in a porous medium aquifer*, Hydrogeology Journal*, 9, pp 313- 320

Yong Lee, J., Woo Kim., J., Yong Cheon, J. (2003). Combined performance of pumping and tracer tests: A case study, *Geosciences Journal*, 7(3), pp 237-241.

Younger, P.L. (2007). Groundwater in the Environment an Introduction, Victoria: Blackwell Publishers.

APPENDICES

APPENDIX A: ASH COLUMN LABORATORY DATA

ASH COLUMN Column Length (cm) 6.5
v (m/day) 0.0034
A (m2) 0.0063

EXPERIMENT 1

Time (min)	Vol (in) ml container	Vol (in) ml	Vol (out) ml	EC (mS/cm)	Q (m3/d) outflow	Q (m3/d) inflow	K (m/d)	q (m/d)
0	2700				Time			
9	2690				0.003472222			
14		70	52	11.9	0.014976		2.384713376	
19	2570	60	49	14.7	0.014112	0.01728	2.247133758	2.247133758
24	2500	45	48	13.5	0.013824	0.01296	2.201273885	2.201273885
		45	47	11.8	0.013536	0.01296	2.155414013	2.155414013
34	2480	30	45	11.3	0.01296	0.00864	2.063694268	2.063694268
39	2420	30	42	10.8	0.012096	0.00864	1.92611465	1.92611465
44	2390	30	42	11.8	0.012096	0.00864	1.92611465	1.92611465
49		45	39	13.6	0.011232	0.01296	1.788535032	1.788535032
54	2300	45	41	13.8	0.011808	0.01296	1.880254777	1.880254777
59	2280	40	38	12.8	0.010944	0.01152	1.742675159	1.742675159
64	2220	40	40	12.6	0.01152	0.01152	1.834394904	1.834394904
69		45	37	12.6	0.010656	0.01296	1.696815287	1.696815287
79	2130	45	29		0.008352	0.01296	1.329936306	1.329936306
84	2090	40	39	12.5	0.011232	0.01152	1.788535032	1.788535032
89		40	36.5		0.010512	0.01152		
94	2010	40	36.5	12.7	0.010512	0.01152	1.67388535	1.67388535
99		30	39.5		0.011376	0.00864		
104	1950	30	39.5	12.1	0.011376	0.00864	1.811464968	1.811464968
109			35		0.01008			
114			35	12.5	0.01008		1.605095541	1.605095541
124			28.5		0.008208			
134	1750		28.5	12.6	0.008208		1.307006369	1.307006369
144	1710	40	29	12.6	0.008352	0.01152	1.329936306	1.329936306
149		40	29		0.008352	0.01152		
154		36	30		0.00864	0.010368		
161	1600	34	31	13.7	0.008928	0.009792	1.421656051	1.421656051
166	1580	40	35	12.4	0.01008	0.01152	1.605095541	1.605095541
171	1500	40	32	12.5	0.009216	0.01152	1.467515924	1.467515924
176			33	12.6	0.009504		1.513375796	1.513375796
186	1460	40	32	12.5	0.009216	0.01152	1.467515924	1.467515924
191		35	32	12.9	0.009216	0.01008	1.467515924	1.467515924
196	1390	35	30	12.7	0.00864	0.01008	1.375796178	1.375796178
201	1310	40	30	12.5	0.00864	0.01152	1.375796178	1.375796178
211	1300	35	30	12.5	0.00864	0.01008	1.375796178	1.375796178
216	1280	35	29	12.7	0.008352	0.01008	1.329936306	1.329936306
221		35	29	12.7	0.008352	0.01008	1.329936306	1.329936306
226	1210	35	29	12.7	0.008352	0.01008	1.329936306	1.329936306
231			28	12.6	0.008064		1.284076433	1.284076433
236	1180	30	24	12.7	0.006912	0.00864	1.100636943	1.100636943
241	1120	30	23.5	12.6	0.006768	0.00864	1.077707006	1.077707006
246	1100	20	21	12.9	0.006048	0.00576	0.963057325	0.963057325
253		20	23	12.5	0.006624	0.00576	1.05477707	1.05477707
258	1040	20	21	12.6	0.006048	0.00576	0.963057325	0.963057325
263		20	20	12.5	0.00576	0.00576	0.917197452	0.917197452
268	1000	20	20	12.6	0.00576	0.00576	0.917197452	0.917197452
273		20	20	13.4	0.00576	0.00576	0.917197452	0.917197452
278	960	20	20	14.5	0.00576	0.00576	0.917197452	0.917197452
283		20	20	15.1	0.00576	0.00576	0.917197452	0.917197452
288	900	20	20	16.2	0.00576	0.00576	0.917197452	0.917197452
293		20	20	16.9	0.00576	0.00576	0.917197452	0.917197452
298	860	20	20	17.8	0.00576	0.00576	0.917197452	0.917197452
303		20	20	18.1	0.00576	0.00576	0.917197452	0.917197452
308	820	20	20	18.8	0.00576	0.00576	0.917197452	0.917197452
313		20	20	19.6	0.00576	0.00576	0.917197452	0.917197452
318	780	20	20	20.2	0.00576	0.00576	0.917197452	0.917197452
323		20	20	21.1	0.00576	0.00576	0.917197452	0.917197452
328	740	20	20	20	0.00576	0.00576	0.917197452	0.917197452
333		20	20	19.4	0.00576	0.00576	0.917197452	0.917197452
338	700	20	20	19	0.00576	0.00576	0.917197452	0.917197452
343		20	20	18.7	0.00576	0.00576	0.917197452	0.917197452
348	660	20	20	18.4	0.00576	0.00576	0.917197452	0.917197452
353		20	20	18.1	0.00576	0.00576	0.917197452	0.917197452
358	620	20	20	17.9	0.00576	0.00576	0.917197452	0.917197452
363		20	20	17.6	0.00576	0.00576	0.917197452	0.917197452
368	580	20	20	17.1	0.00576	0.00576	0.917197452	0.917197452
373		20	20	16.9	0.00576	0.00576	0.917197452	0.917197452
378	540	20	20	16.7	0.00576	0.00576	0.917197452	0.917197452
383		20	20	16.4	0.00576	0.00576	0.917197452	0.917197452
388	500	20	20	16.2	0.00576	0.00576	0.917197452	0.917197452
393		20	20	16	0.00576	0.00576	0.917197452	0.917197452
398	460	20	20	15.4	0.00576	0.00576	0.917197452	0.917197452
403		20	20	15	0.00576	0.00576	0.917197452	0.917197452
408	420	20	20	14.8	0.00576	0.00576	0.917197452	0.917197452
413		20	20	14.2	0.00576	0.00576	0.917197452	0.917197452
418	380	20	20	13.8	0.00576	0.00576	0.917197452	0.917197452
423		20	20	13.2	0.00576	0.00576	0.917197452	0.917197452
428	340	20	20	12.7	0.00576	0.00576	0.917197452	0.917197452

ASH COLUMN	Column Length (cm)	6.5
	v (m/day)	0.0034
	A (m^2)	0.006

EXPERIMENT 2

Time	Vol (in) ml container	Vol (in) ml	Vol (out) ml	EC mS/cm	Q (m3/d) outflow	Q (m3/d) inflow	K (m/d)	q (m/d)
0	2700	0			Time			
5	2650	50			0.003472222			
10	2610	40	37	21.9	0.010656	0.01152	1.696815287	1.696815287
15			41	22.1	0.011808		1.880254777	1.880254777
20	2580	30	49	24	0.014112	0.00864	2.247133758	2.247133758
25	2520	60	55	24.2	0.01584	0.01728	2.522292994	2.522292994
30	2500	20	56	24.2	0.016128	0.00576	2.568152866	2.568152866
35	2470	30	50	21.9	0.0144	0.00864	2.292993631	2.292993631
40	2440	30	47	21.9	0.013536	0.00864	2.155414013	2.155414013
45	2400	40	42	21.1	0.012096	0.01152	1.92611465	1.92611465
50	2370	30	39	21	0.011232	0.00864	1.788535032	1.788535032
55	2330	40	36	22	0.010368	0.01152	1.650955414	1.650955414
60	2300	30	33		0.009504	0.00864	1.513375796	1.513375796
65	2270	30	32	22	0.009216	0.00864	1.467515924	1.467515924
70	2220	50	34		0.009792	0.0144	1.559235669	1.559235669
75	2195	25	33	22	0.009504	0.0072	1.513375796	1.513375796
80	2170	25	33		0.009504	0.0072	1.513375796	1.513375796
85	2130	40	32		0.009216	0.01152	1.467515924	1.467515924
90	2100	30	32	22	0.009216	0.00864	1.467515924	1.467515924
95	2075	25	32		0.009216	0.0072	1.467515924	1.467515924
100	2040	35	31	22	0.008928	0.01008	1.421656051	1.421656051
105	2010	30	31		0.008928	0.00864	1.421656051	1.421656051
110	1980	30	30		0.00864	0.00864	1.375796178	1.375796178
115			33		0.009504		1.513375796	1.513375796
120	1950	30	34	22	0.009792	0.00864	1.559235669	1.559235669
125	1910	40	32		0.009216	0.01152	1.467515924	1.467515924
130	1880	30	33		0.009504	0.00864	1.513375796	1.513375796
135	1850	30	34		0.009792	0.00864	1.559235669	1.559235669
140	1810	40	33		0.009504	0.01152	1.513375796	1.513375796
145	1780	30	30		0.00864	0.00864	1.375796178	1.375796178
150	1750	30	31		0.008928	0.00864	1.421656051	1.421656051
155	1710	40	32	22	0.009216	0.01152	1.467515924	1.467515924
160	1680	30	31		0.008928	0.00864	1.421656051	1.421656051
165	1650	30	31		0.008928	0.00864	1.421656051	1.421656051
170		30				0.00864		
175	1590	30	31		0.008928	0.00864	1.421656051	1.421656051
180		55				0.00792		
185	1480	55	31		0.008928	0.00792	1.421656051	1.421656051
190		40				0.007632		
195	1400	40	31.5		0.009072	0.007488	1.444585987	1.444585987
200								
205	1360	40	30	22	0.00864	0.007632	1.375796178	1.375796178
210								
215								
220								
225	1230		29.5		0.008496		1.352866242	1.352866242
230								
235	1190	40	28.5		0.008208	0.007488	1.307006369	1.307006369
240		40				0.007632		
245	1110	40	28.5		0.008208	0.007488	1.307006369	1.307006369
250		25				0.0072		
255	1080	25	28	22	0.008064	0.0072	1.284076433	1.284076433
260		25				0.0072		
265	1000	25	28		0.008064	0.0072	1.284076433	1.284076433
270		25				0.0072		
275	950	25	26.5	22	0.007632	0.0072	1.215286624	1.215286624
280		25				0.0072		
285	900	25	24.5	21	0.007056	0.0072	1.123566879	1.123566879
290		20				0.00576		
295	860	20	24.5		0.007056	0.00576	1.123566879	1.123566879
300								
305								
310								
315	820	20	24		0.006912	0.00576	1.100636943	1.100636943
320								
325								
330								
335	800	20	22.5		0.00648	0.00576	1.031847134	1.031847134
340								
345	780	20	20	20.1	0.00576	0.00576	0.917197452	0.917197452
350			20	20.6	0.00576		0.917197452	0.917197452
355			20	21.1	0.00576		0.917197452	0.917197452
360			20	23.3	0.00576		0.917197452	0.917197452
365	620		20	23.1	0.00576		0.917197452	0.917197452
370	600	20	20	23.6	0.00576	0.00576	0.917197452	0.917197452
375		20	20	24.3	0.00576	0.00576	0.917197452	0.917197452
380		20	20	25.6	0.00576	0.00576	0.917197452	0.917197452
385		20	20	26.5	0.00576	0.00576	0.917197452	0.917197452
390	520	20	20	30.3	0.00576	0.00576	0.917197452	0.917197452
395		20	20	27.6	0.00576	0.00576	0.917197452	0.917197452
400	480	20	20	25.3	0.00576	0.00576	0.917197452	0.917197452
405		20	20	24.9	0.00576	0.00576	0.917197452	0.917197452
410	440	20	20	23.1	0.00576	0.00576	0.917197452	0.917197452
415	420	20	20	22.7	0.00576	0.00576	0.917197452	0.917197452
420	400	20	20	22	0.00576	0.00576	0.917197452	0.917197452
425	380	20	20	22.2	0.00576	0.00576	0.917197452	0.917197452
430	360	20	20	22.1	0.00576	0.00576	0.917197452	0.917197452
435	340	20	20	22.1	0.00576	0.00576	0.917197452	0.917197452
440		20	20	21	0.00576	0.00576	0.917197452	0.917197452
445		20	20	21	0.00576	0.00576	0.917197452	0.917197452
450		20	20	21	0.00576	0.00576	0.917197452	0.917197452
455	260	20	20	21	0.00576	0.00576	0.917197452	0.917197452
460	240	20	20	21	0.00576	0.00576	0.917197452	0.917197452
465	220	20	20	22	0.00576	0.00576	0.917197452	0.917197452
470	200	20	20	21	0.00576	0.00576	0.917197452	0.917197452

Time	Viscocity (cSt/min)	Liquid Density	Viscocity (cSt/s	k (m/d)
0				
9				
14	0.0164	1.01	0.984	0.244846353
19	0.0165	1.01	0.99	0.229322295
24	0.0166	1.01	0.996	
29				
34				
39				
44	0.0161	1.01	0.966	0.201445495
49				
54				
59				
64				
69				
79				
84				
94	0.0161	1.01	0.966	0.175065727
104				
114				
124	0.016	1.01	0.96	0.137549502
134				
144				
161	0.016	1.01	0.96	0.168920441
166				
171				
176				
186	0.016	1.01	0.96	0.154441546
191				
196				
201				
211	0.016	1.01	0.96	0.139962651
216				
226				
231				
236	0.016		0.96	
241		1.01		
246				
253	0.016			
258				
263	0.016	1.01	0.96	0.096525966
268				
273				
278				
283				
288				
293	0.016	1.01	0.96	0.096525966
298				
303				
308				
313				
318				
323				
328				
333				
338				
343				
348				
353	0.016	1.01	0.96	0.096525966
358				
363				
368	0.016	1.01	0.96	0.096525966
373				
378				
383				
388				
393				
398				
403	0.016	1.01	0.96	0.096525966

Time (min)	Viscocity (cSt/min)	Liquid Density	Viscocity (cSt/s	k (m/d)
15	0.0166	1.01	0.996	
20	0.0176	1.01	1.056	0.190726005
25	0.0166	1.01	0.996	0.214989652
30	0.0167	1.01	1.002	0.255851958
35	0.0165	1.01	0.99	0.258943909
40				0.234002342
45				
50				
55				
60				
65				
70	0.01648	1.01	0.9888	
75				0.159314701
80				
85				
90				
95				
100				
105				
110				
115				
120				
125	0.0164	1.01	0.984	
130				0.150674679
135				
140				
145				
150	0.0164	1.01	0.984	
155				0.145966095
160				
165				
170				
175				
180				
185				
190				
195	0.0164	1.01	0.984	
200				0.148320387
205				
275				
280	0.0163	1.01	0.978	
285				
360				
365	0.0163	1.01	0.978	
370				0.094749415
420				
425	0.0163	1.01	0.978	
430				0.094749415

APPENDIX B: ADSORPTION TEST DATA

NaCl **ASH**

Experiemnt 2 Sample

Time	Time		Mass (kg)	initial C (mS/cm)	mg/l	Final (mS/cm)	Final (mg)	Ce (mg)	**1/Ce**	Q (adsorbed amount)	**1/q**
30 min		30	10	0.1	18.47	9235	18	9000	235	0.004255319	211500
60min		60	10	0.1	18.47	9235	18.03	9015	220	0.004545455	198000
120min		120	10	0.1	18.47	9235	18.06	9030	205	0.004878049	184500
240min		240	10	0.1	18.47	9235	18.21	9105	130	0.007692308	117000
9 hrs mi		540	10	0.1	18.47	9235	18.35	9175	60	0.016666667	54000
10 hrs		600	10	0.1	18.47	9235	18.6	9300	-65	-0.015384615	-58500
11 hrs min		660	10	0.1	18.47	9235	18.65	9325	-90	-0.011111111	-81000
11hrs:30min		690	10	0.1	18.47	9235	18.69	9345	-110	-0.009090909	-99000

APPENDIX C: LABORATORY ASH CORE DATA

ASH CORE BH 81(4.5m)

Column Length	43 cm	0.43m
Head Diff	28 cm	0.28m
Gradient		0.651163
Radius	8 cm	0.020096 m
Texture (fine-medium)		

	ml/h		m3/d			
Time (min)	Q	EC	Q	K	A	q
60	52	None	0.001248	0.095371	0.02	0.0624
120	80	None	0.00192	0.146724	0.02	0.096
180	80	None	0.00192	0.146724	0.02	0.096
240	76	528	0.001824	0.139388	0.02	0.0912
300	75	508	0.0018	0.137554	0.02	0.09
360	70	447	0.00168	0.128384	0.02	0.084
420	70	428	0.00168	0.128384	0.02	0.084
480	60	381	0.00144	0.110043	0.02	0.072
540	60	356	0.00144	0.110043	0.02	0.072
600	60	337	0.00144	0.110043	0.02	0.072

ASH CORE BH: 80 (7m)

Column Length	38 cm	0.38
Head Diff	33 cm	0.33
Gradient		0.868421
Radius	8 cm	0.020096
Texture (very coarse)		

	ml/h		m3/d			
Time (min)	Q	EC	Q	K	A	q
60	158	921	0.003792	0.217284	0.02	0.1896
120	193	2275	0.004632	0.265417	0.02	0.2316
180	196	2364	0.004704	0.269543	0.02	0.2352
240	310	1804	0.00744	0.426317	0.02	0.372
300	180	1701	0.00432	0.247539	0.02	0.216
360	175	1620	0.0042	0.240663	0.02	0.21
420	154	1610	0.003696	0.211783	0.02	0.1848
480	136	1394	0.003264	0.18703	0.02	0.1632
540	136	1294	0.003264	0.18703	0.02	0.1632
600	145	1107	0.00348	0.199406	0.02	0.174
660	133	1097	0.003192	0.182904	0.02	0.1596
720	129	1018	0.003096	0.177403	0.02	0.1548
780	121	997	0.002904	0.166401	0.02	0.1452
840	122	994	0.002928	0.167776	0.02	0.1464
900	123	982	0.002952	0.169152	0.02	0.1476
960	120	954	0.00288	0.165026	0.02	0.144
1020	115	925	0.00276	0.15815	0.02	0.138
1080	109	920	0.002616	0.149899	0.02	0.1308
1140	110	915	0.00264	0.151274	0.02	0.132
1200	110	910	0.00264	0.151274	0.02	0.132
1260	108	901	0.002592	0.148523	0.02	0.1296
1320	102	898	0.002448	0.140272	0.02	0.1224
1380	100	888	0.0024	0.137522	0.02	0.12
1440	122	994	0.002928	0.167776	0.02	0.1464
1500	123	982	0.002952	0.169152	0.02	0.1476
1560	120	954	0.00288	0.165026	0.02	0.144
1620	115	925	0.00276	0.15815	0.02	0.138
1680	109	920	0.002616	0.149899	0.02	0.1308
1740	110	915	0.00264	0.151274	0.02	0.132
1800	110	910	0.00264	0.151274	0.02	0.132
1860	108	901	0.002592	0.148523	0.02	0.1296
1920	102	898	0.002448	0.140272	0.02	0.1224
1980	100	888	0.0024	0.137522	0.02	0.12

ASH CORE BH: 79 (11.9m)

Borehole Name	79 11m		
Column Length	37 cm	0.37	
Head Diff	30 cm	0.3	
Gradient		0.810811	
Radius	8 cm	0.020096	

Texture (medium)

	ml/h		m3/d	m/day		
Time (min)	Q	EC	Q	K	A	q
60	71	921	0.001704	0.104578	0.02	0.0852
120	78	2275	0.001872	0.114889	0.02	0.0936
180	70	2364	0.00168	0.103105	0.02	0.084
240	86	1804	0.002064	0.126672	0.02	0.1032
300	84	1701	0.002016	0.123726	0.02	0.1008
360	63	1620	0.001512	0.092795	0.02	0.0756
420	56	1610	0.001344	0.082484	0.02	0.0672
480	53	1394	0.001272	0.078065	0.02	0.0636
540	53	1294	0.001272	0.078065	0.02	0.0636
600	50	1107	0.0012	0.073646	0.02	0.06
660	50	1097	0.0012	0.073646	0.02	0.06
720	52	1018	0.001248	0.076592	0.02	0.0624
780	50	997	0.0012	0.073646	0.02	0.06
840	48	994	0.001152	0.070701	0.02	0.0576
900	50	982	0.0012	0.073646	0.02	0.06
960	49	954	0.001176	0.072174	0.02	0.0588
1020	49	925	0.001176	0.072174	0.02	0.0588
1080	50	920	0.0012	0.073646	0.02	0.06
1140	50	915	0.0012	0.073646	0.02	0.06
1200	47	910	0.001128	0.069228	0.02	0.0564
1260	47	901	0.001128	0.069228	0.02	0.0564
1320	47	898	0.001128	0.069228	0.02	0.0564
1380	47	888	0.001128	0.069228	0.02	0.0564
1440	47	994	0.001128	0.069228	0.02	0.0564
1500	47	982	0.001128	0.069228	0.02	0.0564
1560	47	954	0.001128	0.069228	0.02	0.0564

ASH CORE BH: 82 (4.5m)

Borehole Name	80 7m		
Coloumn Length	20 cm	0.1	
Head Diff	30 cm	0.3	
Gradient		3	
Radius	8 cm	0.020096	
Texture (Fine)			

	ml/h		m3/d			
Time (min)	Q	EC	Q	K	A	q
60	130	921	0.00312	0.051752	0.02	0.060287525
120	125	2275	0.003	0.049761	0.02	0.060288177
180	123	2364	0.002952	0.048965	0.02	0.060287961
240	124	1804	0.002976	0.049363	0.02	0.06028807
300	122	1701	0.002928	0.048567	0.02	0.06028785
360	121	1620	0.002904	0.048169	0.02	0.060287737
420	123	1610	0.002952	0.048965	0.02	0.060287961
480	120	1394	0.00288	0.047771	0.02	0.060287622
540	120	1294	0.00288	0.047771	0.02	0.060287622
600	116	1107	0.002784	0.046178	0.02	0.060288449
660	114	1097	0.002736	0.045382	0.02	0.06028822
720	110	1018	0.00264	0.04379	0.02	0.060287737
780	108	997	0.002592	0.042994	0.02	0.060287482
840	100	994	0.0024	0.039809	0.02	0.060287875
900	95	982	0.00228	0.037818	0.02	0.060288751
960	92	954	0.002208	0.036624	0.02	0.060288336
1020	92	925	0.002208	0.036624	0.02	0.060288336
1080	92	920	0.002208	0.036624	0.02	0.060288336
1140	91	915	0.002184	0.036226	0.02	0.060288191

ASH CORE BH: 81 (12m)

Column Length	30 cm		0.3
Head Diff	28 cm		0.28
Gradient			0.933333
Radius	8		0.020096
Texture(Coarse)			

Time (min)	EC	Q	K	A	q
5	NONE	0.0043	0.231603	0.02	0.2172
10	NONE	0.0044	0.234162	0.02	0.2196
15	NONE	0.0044	0.232882	0.02	0.2184
20	NONE	0.0044	0.235441	0.02	0.2208
25	NONE	0.0044	0.236721	0.02	0.222
30	NONE	0.0045	0.23928	0.02	0.2244
35	NONE	0.0046	0.243119	0.02	0.228
40	NONE	0.0046	0.244398	0.02	0.2292
45	NONE	0.0046	0.245678	0.02	0.2304
50	NONE	0.0047	0.248237	0.02	0.2328
55	NONE	0.0047	0.250796	0.02	0.2352
60	NONE	0.0048	0.255914	0.02	0.24
120		0.0049	0.262312	0.02	0.246
180		0.0048	0.257194	0.02	0.2412
240		0.0047	0.252076	0.02	0.2364
300		0.0046	0.246957	0.02	0.2316
360		0.0046	0.243119	0.02	0.228
420		0.0048	0.253355	0.02	0.2376
480		0.0045	0.238	0.02	0.2232
540		0.0043	0.231603	0.02	0.2172
600		0.0042	0.226484	0.02	0.2124
660		0.0042	0.222646	0.02	0.2088
720		0.0041	0.218807	0.02	0.2052
780		0.004	0.214968	0.02	0.2016
840		0.004	0.211129	0.02	0.198
900	2200	0.0039	0.207291	0.02	0.1944
960	2109	0.0038	0.203452	0.02	0.1908
1020	1987	0.0037	0.199613	0.02	0.1872
1080	1867	0.0037	0.195775	0.02	0.1836
1140	1771	0.0036	0.191936	0.02	0.18
1200	1678	0.0035	0.185538	0.02	0.174
1260	1500	0.0034	0.181699	0.02	0.1704
1320	1432	0.0033	0.176581	0.02	0.1656
1380	1345	0.0032	0.170183	0.02	0.1596
1440	1234	0.0031	0.167624	0.02	0.1572
1500	1193	0.0031	0.166344	0.02	0.156
1560	1039	0.0031	0.165065	0.02	0.1548
1620	991	0.0031	0.163785	0.02	0.1536
1680	875	0.003	0.162506	0.02	0.1524

TRACER CORE

ASH CORE BH: 80 (7m)

Time	EC (out)	EC (in)	Vol	Km/day	n_e	v m/day	q	
0	150	69	25	0.0000926		0.02	4.9	0.12
210	151	69	300	0.001111				
390	316	69	900	0.003333				
450	270	69	922	0.003415				
570	417	68	450	0.001667				
630	503	68	271	0.001004				
750	669	69	542	0.002007				
810	590	68	270	0.001				
870	585	68	280	0.001037				
930	580	68	285	0.001056				
990	578	68	285	0.001056				
1290	570	69	2200	0.008148				
1350	501	69	600	0.002222				
1410	436	68	500	0.001852				
1470	409	69	500	0.001852				
1530	407	69	550	0.002037				
1590	405	68	600	0.002222				
1650	399	69	590	0.002185				
1710	385	68	550	0.002037				
1770	385	69	425	0.001574				
1830	384	68	425	0.001574				
1890	380	69	520	0.001926				
2070	371	68	1600	0.005926				

APPENDIX D: FIELD DATA SLUG TESTS

SLUG TEST ASH	Site 1						
Piezometer Depths	1.5m						
Screen length	0.5m						
Time (min)	**TA 1**	**TA 2**	**TA 3**	**TA 4**	**TA 5**	**TA 6**	**TA 7**
0	129	137.5	102	138	141	135.5	114
30	127.5	135	140	136	139.5	133.5	113.5
60	127	130.1	138	133	138.5	133	112.5
90	126.5	128	136	130.5	136.5	133	112
120	125.5	127	134.5	130	135	132	111.5
150	124	124	134	129	132	132	111
180	124	124	133	127.5	130.5	131.5	110.5
210	123	122	132	125.5	129.5	131	109.5
240	122	121.5	130.5	124.5	129	130	109
270	121.5	121	130	123.5	128	130	108
300	121	120.5	129	123	126.5	130	108
330	121	120	126.5	122	126	130	107
360	120	119.5	126	122	125.5	129.5	107
390	120	119	125.5	122	124	129	106.5
420	120	118.5	124.5	120.5	122	129	106
450	120	118.5	123.5	120	122	128.5	105.5
480	119.5	118	123	119.5	121	128.5	105
510	119		123	118.5	120	128	105
540	118.5		122.5	118	119	128	104
570	118		122	117	118	128	104
600	117.5		121	116.5	116	127.5	104
630	117.5		120	116	116.5	127.5	
660	117.5		119	116	116	127	
690	117		119	115	114.5	126.5	
720	117		117	115	113.5	126	
750	117		116.5	114.5	113	126	
780	116.5		115.5	113.5	113	125	
810	116		115	113.5	112	125	
840	116		114	111.3	111.5	125	
870	116		114	111.2	111.5	124.5	
900	116		113	111.2	111	124.5	
930	116		113	111.2	111	124	
960	115.5		111	110.5	110	124	
990	115.5		111	110.5	110	124	
1020	115.5		110.5	110	110	123.5	
1050	115.5		110.5	110	110	123	
1080	115.5		110	109	109.5	123	
1110	115.5		110	109	109		
1140	115.5		110	109	109		
1170	115.5		110	108	108.5		
1200	115.5		109.5	107.5			
1230	115		109.5	107.5			
1260	115		109	107.5			
1290	115		108.5	107			
1320	114.5		108.5	107			
1350	114.5		108	107			
1380	114.5		107.5	106.5			
1410	114.5		107.5	106			
1440	114.5		107.5	106			
1470	114.5		107	105.5			
1500	114		107	105.5			
1530	114		106.5	105			
1560	114		106	105			
1590			106	105			
1620			105.5	104.5			
1650			105.5	104.5			
1680			105.5	104			
1710			105	104			

SLUG TEST ASH Site 2
Piezometer Depths 1.5m
Screen Length 0.5m

Time	TA 8	Time	TA 9	TA 10	TA 11	TA 13	TA 14
0	116.5	0	151.5	113	162	147	140
30	112	15	147.5	111.5	161.5	147	139
60	112	30	147	110.5	161.5	146	138
100	97	45	146.5	109.5	160.5	145.5	136.5
110	95	60	145	108	160.5	145	135.5
128	94	66	144	107.5	160	144.7	134.5
146	92.5	90	143	107	160	144.5	133
141	91.5	109	142.5	106	159.9	144	132.5
160	90	130	141.5	106	159	143.7	132
191	89.5	150	141.5	105.5	159	143.5	131.7
225	88	180	141	105.5	158.7	143.5	131.5
235	87	196	140.5	105	158	142.5	130.5
266	86.5	240	139.5	105	157.5	142.5	130
280	85.5	266	139.5	105	157.5	142	129.5
300	85	300	139	105	157.2	141.5	129.5
340	84	312	139	104	156.8	141	129
370	83.5	350	139	104	156.5	141	129
412	83	354	138.5	104	156.4	139.5	129
422	82.5	360	138.5	104	156	139	128.5
470	82.2	432	138.5	103.5	156	139	128
480	81.7	480	138.5	103.5	155.5	139	128
524	81.5	531	138.5	103.5	154.5	138.5	127.5
620	81.5	570	138.5	103.5	154.5	138.5	127.5
670	80	620	138.5	103	154	138.5	127.3
		660		102.5	153.5	138	127
		720		102.5	153	138	127
		780		102	152.7	137	127
		495		102	152	137	127
		900		102	152	136.5	127
		960		102	151.5	136.5	127
		1095		102	150.8	136	127
		1149		101.5	150.5	136	127
		1200		101.5	150.5	136	127
		1252		101.5	150	136	127
		1326		101	150	136	
		1340		101	149.8		
		1360		101	149.5		
		1410		101	149.5		
		1470		101	149.5		
		1472		101	149		
		1602		101	148.7		
		1668		101	148.5		
		1740		101	148.5		
		1800		100.5	148		
		1815		100.5	148.5		
		1860		100.5	148.3		
		1968		100.5	148.3		
		2040		100.5	148		
		2070		100.5	148		
		2108		100.5	147.5		
		2192		100.5	147.5		
		2266			147.5		
		2280			147.5		

APPENDIX E: TRACER TEST DATA ON ASH

FIELD TRACER
ASH SITE 1

INJECTION PIEZ TA 6
INITIAL TRACER CON. 45 mS/cm
Tracer NaCl

Time	TA 7	TA 5	TA 4	TA 3	TA 2	TA 1	TA 6
0	10.2	8.973	8.632	7.073	8.646	9.449	9.073
2	12.5	10.5	10.7	11.2	11		45
4		10.4	10.8	11.1	10.8	10.5	43.3
6	12.2	12.4	10.8	10.9	10.7	12.1	
8	12.7				10.7		42.6
10						11.2	42.5
11		13	11.1				
12	12.1			11.2	10.7		
13		13.4	11.9			10.8	41.9
14	11.6			10.9			
15				10.7	10.5	10.6	
16		13.8	12				40
17	11.1			10.1			
18					11.9	10.9	39.7
19		14	12.2				
20	11			10	10.8		
24		14.5					42.5
25	10.9		12.3	9.866			
26					10.6	10.8	
27		14.1	11.9	10.6	9.913		42.1
28							
29	10.8			9.713	10.7		
30		13.8			10.6	10.1	41.6
31			11.6				
32		13.4		10.3			
33	10.6				10.6		
34		13				10.4	38
35			11.2	10.4			39.2
36	10.5				11.9	10.8	
38	10.4	12.1	11	10.2			41.2
39					10		40.6
40							39.2
42		12.2	10.6	10	10.7		41.2
43							
44	10.3						
45					11.6	11.5	
47		12.1	10.5				
48	9.55			10			
49		11.5					39.4
50							
51	9.46		11.3				
52				11.6	11.4	10.7	
57	9.044	11.73	10.7				40.2
58							
59					11.4	11	
60	9.032						
61		11.7	10.8	11.4			38.9
62					11.3	11.3	
63							38.9
64	8.923	11.6	10.7	10.3			
65					10.2	11.5	
66		11.7					
69	9.096		10.6	10.2	11.5		39.7
70						11.3	
71							
72	9.053						
74							

FIELD TRACER
ASH SITE 2

INJECTION PIEZ TA 14
INITIAL TRACER CON. 75.2 mS/cm
Tracer NaCl

Time (min)	TA 8	TA 9	TA 10	TA 11	TA 12	TA 13	TA 14
0						9	
6				12.3	12.2		75
7	11.4		10.7	12.3		10.2	
8							75.1
9				12.4			
10			10.9			12.9	
11	11.5						77.5
13					12.3		
14				12.6		13.2	
15			10.7	12.3			75
16	11.5						
17					12.3	13.9	
18				12.2			
19			10.6	12.3			
20	11.2						75.1
21					12.4	14.1	
22				12.2	12.1		
23	11.4						75.1
24							
25				12	12.4	15	
26	11.3		10.5	11.5			75
30				11.8	12.8		
31	11.3		10.2	11.6		15.6	
32							75
33							
41							74.9
42					12.5		
43				11.7	11.7	16	
44			10.2				
50	11.9					17	74.9
51					12.2	18.2	
52				11.7			
53	11.4		10.9	11.8			
60						20	71.2
63				12	12.2		
64	11.9		10.3	11.7			
72					12.1		
73				11.8	11.8		
74	11		10.1			18.6	
87							68.3
88							
89			10.1	11.7	11.2	12.1	68.4
90	10.9						
100							
101				11.5	12	17.5	
103				11.9			
104			10.5				
105	10.7				11.3	16.4	
112							62.2
114				11.7	11.7		
116	10.8		10.9				
122							62.2
124				11.6	11.6		
125							
126	10.8		10.9	11.6			
127			10.1				
128	10.8		11.6	10.1	11.5	11.5	
137							59.7
150							56.7
151					11.4		
152				11.2			
153				11.5			
154			9.8				
156	10.6					15.2	
163					11.7		52.3
168							
169	10.6						

APPENDIX F: FIELD DATA SURROGATE AQUIFER

SURROGATE FRACTURED AQUIFER TRACER DILUTION TEST
PUMPING RATE 0.8 L/s

TIME (min)	EC uS/cm
5	12000
10	3649
15	2723
20	16000
25	11000
30	3378
35	11000
40	10000
45	7324
50	4720
55	7616
60	8206
65	6157
70	4244
75	7147
80	6366
85	6841
90	5855
95	6049
100	5170
105	4203
115	5213
120	5256
125	4111
130	4912
135	4433
140	4025
145	4140
150	4485
160	2435
165	2384
170	2347
175	2243
180	2222
185	2158
190	2150
195	2095
200	2024
205	2003
210	1974
215	1907
220	1885
225	1874
230	1852
235	1807
240	1706
245	1715
250	1715
255	1714

SURROGATE FRACTURED AQUIFER PUMPING RATE	RADIAL DIVERGENT 0.8L/s
Time (min)	Rh (ug/l)
0	0
480	3
510	4.1
540	5
590	5.6
650	8.8
770	9.7
810	11.3
940	18.3
1070	18.6
1130	18.9
1160	18.4
1190	19.3
1220	21.1
1340	20
1400	19.4
1460	20.1
1520	17.5
1580	17.6
1640	16.3
1700	16.3
1760	16.2
2120	16.1
2180	15.7
2240	15.3
2300	15.6
2360	15.1
2420	14.6
2480	14.1
2440	14.3
2500	15.3
2560	16.1
2620	15
2680	15.3
2740	15.1
2800	16.3
2860	16
2920	15.4
2980	14.1
3040	14.3
3640	13.9
3820	13.4
4300	12.4
4360	12.1
4540	12
4720	11.7
4900	11.3
5080	10.7
5560	10.4
5800	10.1
6520	9.8
7000	9.4
7180	9
7360	8.6
8080	8.1
8440	7.3
8880	5.7
9100	4.1